The Dissertation Committee for Matthew James Pinnow
certifies that this is the approved version of the following dissertation:

DESIGN AND SYNTHESIS OF MATERIALS FOR 157nm PHOTORESISTS APPLICATIONS

Committee:

_____
C. Grant Willson, Supervisor

_____
Eric V. Ansyln

_____
Brent L. Iverson

_____
Alan Campion

_____
William D. Hinsberg

DESIGN AND SYNTHESIS OF MATERIALS FOR 157 nm PHOTORESISTS APPLICATIONS

by

Matthew James Pinnow, B.S.

Dissertation

Presented to the Faculty of the Graduate School of

the University of Texas at Austin

in Partial Fulfillment

of the Requirements

for the Degree of

Doctor of Philosophy

The University of Texas at Austin
May 2005

Dedicated to *BLR*

Acknowledgements

First I would like to thank Professor Willson for allowing me to conduct my thesis work in his laboratories. I have learned many things above and beyond chemistry in my stay here. Many of these lessons I am sure will prove to be worth as much as the technical knowledge gained.

I would like to thank Brian Trinque for an excellent sense of humor as well as some fun times making acrylates for the early 157 nm polymers. Jordan Owens, Andrew Jamieson and Brian Osborn were extremely helpful in imaging experiments. Andrew was a great collaborator on the TSI project as well. Many others that I have had daily interaction with and whose help was greatly needed include Dr. Ryan Callahan, Charles Chambers, Takashi Chiba, Dr. Peter Tattersall, Dr. H. V. Tran, Dr. Les Carpenter, Dr. Scott Grayson, Bill Heath, Stefan Caporale, and Yukio Nishimora.

During my stay I have had the unique opportunity to work and collaborate with several undergraduates. Ben Noyes was a tremendous help in working on the beta lactone project. Mikey Lin was helpful in the synthesis of TSI materials as well as gaining understanding of the HFA:ether separations problem. Jerred Chute has been very competent and productive during his time working on the negative tone resist project. Overall my thesis would have had a different feel if not for the help provided by these undergraduates.

Of course I have to give a big thanks to Kathleen Sparks. She has been a tremendous help over the past 5 years. Without her things would have been much more difficult.

DESIGN AND SYNTHESIS OF MATERIALS FOR 157 nm PHOTORESISTS APPLICATIONS

Publication No._____

Matthew James Pinnow, Ph.D.

The University of Texas at Austin, 2005

Supervisor: C. Grant Willson

The move towards 157 nm as the next generation of photolithography has presented many challenges. One of the more challenging aspects of 157 nm photolithography is the development of a suitable photoresist. Two of the issues faced when designing a suitable resist for 157 nm applications are transparency requirements and outgassing from the photoresist.

Designing a resist to not intentionally outgass upon exposure to acid and heat employed the screening of several new potential solubility switches. Several lactones were synthesized and NMR was used as a spectroscopic method to monitor whether the desired solubility switch occurred in model compounds. Successful model compounds were incorporated into polymers to form a photoresist. Subsequent imaging experiments gave insight into the desired copolymer ratios needed for imaging applications.

The formation of base insoluble lactones from base soluble precursors were also investigated for use as a non-outgassing negative tone photoresist. Successful model compounds were incorporated into copolymers. Imaging experiments gave insight on the terpolymer ratios needed for to obtain imaging.

Transparency of the polymer resin has been a major hurdle in the development of a 157 nm photoresist. Efforts to use top surface imaging (TSI), an alternative lithographic patterning technique have been explored. TSI, unlike traditional photolithographic schemes, does not require a transparent resin. However, line edge roughness (LER) has always hampered the feasibility of TSI. Efforts to reduce the LER of TSI through manipulation of the T_g of the polymer resin were investigated.

Table of Contents

List of Figures

Chapter 1 - Introduction to Photolithography

Invention of the Transistor and Integrated Circuit

The first electronic computation devices were built using vacuum tubes. One of the first such computers was called the Electronic Numerical Integrator and Computer (ENIAC) (Fig. 1.1). ENIAC[1] built in 1946 at the University of Pennsylvania, was constructed using vacuum tube technology.

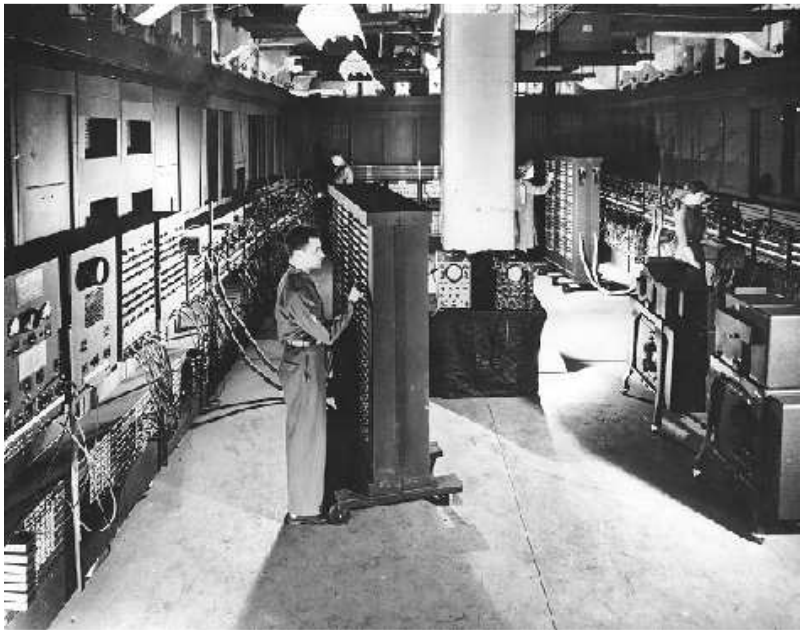

Figure 1.1: ENIAC Computer: example of computer built using vacuum tube technology.

ENIAC demonstrated powerful digital computing that would not have been possible without vacuum tube technology. The sheer complexity of the computer, and the number of vacuum tubes required (approx. 18,000), brought to light limitations of

using vacuum tubes in the design and construction of computers. Due to the size of the vacuum tubes used, the ENIAC computer took up an entire room and required several people to maintain it as the vacuum tubes frequently burned out. While ENIAC clearly demonstrated the potential power of a computer, it was clear that improved technology that could replace the vacuum tube was necessary to generate more complex computers, ones that could perform faster and more efficiently.

The invention of the transistor in 1947 provided a means to replace the vacuum tube with a smaller and more reliable electrical switch. This transition away from the vacuum tube to the transistor allowed for smaller and more powerful electronic devices to be designed and built. Once again though engineers reached a limit as they soon found that even with the smaller and more reliable transistor it was difficult to produce very complex electronic devices for several reasons. One reason was that it was very hard and time consuming to solder together an entire electronic device without having any bad connections. This proved to be very important as one bad connection would ruin the device. Secondly, as the design continued to grow in complexity and the number of transistors increased, the physical length of the wires used to connect the transistors began to adversely affect the speed of the device. To enable more advanced circuit designs another technological breakthrough was needed.

These issues were soon laid to rest with the invention of the integrated circuit (IC). In 1959, the integrated circuit was co-invented by Jack Kilby at Texas Instruments and by Robert Noyce at Fairchild Semiconductor. The integrated circuit combines many transistors into a single piece of semiconducting material which allows for both the

conducting and passive parts of the transistor to be constructed on the same piece of material, silicon. This design allows for devices to be made much smaller and also allows for automation to be used in the manufacturing of circuits. The benefits of smaller device designs as well as automation of device manufacturing set off a race between semiconductor companies to create increasingly complicated devices.

Moore's Law

In 1965, then CEO of Intel,[2] Gordon Moore, noted that the transistor count of semiconductor devices double about every 18 months.

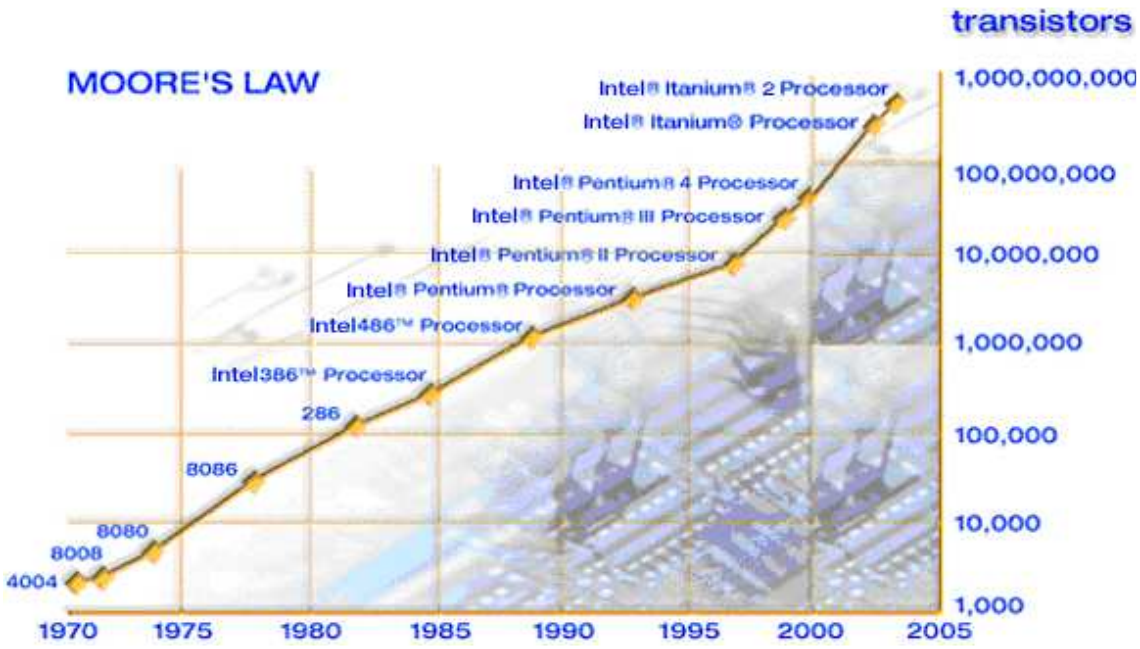

Figure 1.2: Moore's Law plot showing transistor count versus year.

While Gordon Moore's observation that the transistor count doubles is not a law, it has provided a benchmark that industry to this day has strived to maintain. The invention of

the integrated circuit has provided a platform from which to build compact devices but other technological advances were also needed to maintain the exponential growth as displayed by Moore's Law (**Fig 1.2**).

Photolithography

Photolithography is the key process used in the manufacturing of integrated circuits. The term photolithography can be broken into two components; *photo* and *lithography*. The *photo* component is derived from the use of light to pattern the desired features for the integrated circuit. *Lithography* was first invented in 1798 by Alois Seneflder when he discovered he could pattern images on stone using a greasy mixture, water and ink. The first example of lithography is not radically different then photolithographic techniques used in the manufacturing of integrated circuits today.[3] In place of grease on stone what is called a photoresist is used on a silicon wafer. The photoresist is a polymer that when exposed with light undergoes a solubility change such that selected areas of the film can be washed away. This allows for selective patterning to ultimately produce an IC. The photolithographic process can be divided into five different steps; coating, exposure, development, etch transfer and resist stripping.

Photoresist Tone Schemes

There are two schemes, negative and positive tone, which describes the solubility switch that takes place in the photoresist film. In the positive tone system the bulk resin is not soluble in the developer (usually aqueous tetramethylammonium hydroxide

(TMAH)). Upon exposure to acid, the resin becomes soluble in developer. In a negative tone system, the bulk resin is soluble in the developer and after exposure to acid, becomes far less soluble in the developer (**Fig. 1.3**).

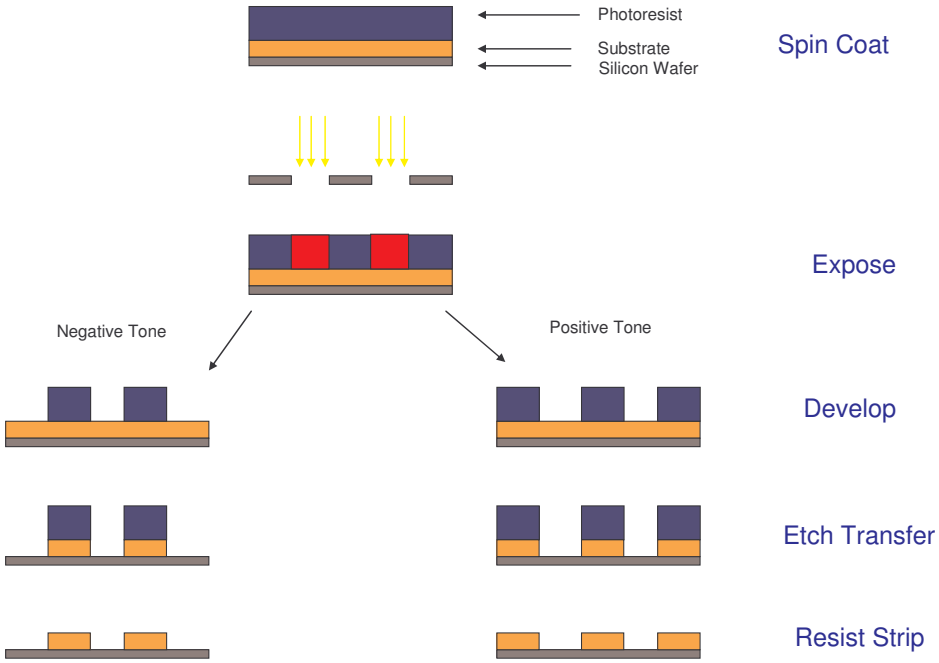

Figure 1.3: The photolithographic process for negative and positive tone resist schemes.

Most resist systems used in industry are positive tone resist systems, although negative tone resists do have benefits that led to their use in certain applications. The benefit of negative tone resists over positive tone resists in certain applications will be discussed in chapter 3.

Spin Coating

The first step in the lithographic patterning process is coating the substrate with photoresist. After the resist is spin coated onto the substrate, the wafer is baked to remove solvent used in the spin coating process. This baking step is referred to as the post apply bake (PAB). Spin coating and baking steps produce a very uniform film, which is important for high resolution imaging.

Exposure

During the exposure step a circuit pattern is transferred onto the photoresist by irradiation through a mask. The mask is typically made of quartz and chromium. The areas of the mask without chromium allow light to pass through the quartz and irradiate the photoresist. The exposure of the resist film generates acid from the photoacid generator (PAG), which is used to switch the solubility of the film. After exposure the wafer is baked again. This is termed the post-exposure bake (PEB). This final bake drives the resist solubility switch to completion. The mechanism of this solubility switch will be discussed shortly.

Development

The next step is to develop the wafer to produce a 3-D image. The wafer is immersed in a developer which selective washes away parts of the film. In the case of the positive tone system, the area of the film that was exposed to light is now soluble in the developer and is subsequently washed away. In the case of the negative tone system,

the area exposed to light is rendered insoluble and the area not exposed to light is washed away. In both the positive and negative tone resist schemes the result is there now exists exposed substrate where the resist was washed away while resist remains in other areas covering the substrate.

Etch Transfer and Resist Stripping

The next step is to transfer the three dimensional image left after the development step into the substrate. This is accomplished with an etch process. The wafer is exposed to an etch chemistry which is selective towards the exposed substrate. The substrate is etched away while the remaining photoresist that covers some of the substrate "resists" the etch process and does not allow for the substrate in those areas to be etched. The final step is to strip the remaining photoresist off which leaves the desired three dimensional image in the original substrate. This process is continued many times in the course of making an integrated circuit to build the necessary three dimensional architecture for the final device.

Photoresist Chemistry and Relation to Exposure Wavelength

To keep up with the demands of Moore's Law the semiconductor industry continues to shrink the feature size used in the construction of the integrated circuit. This increase in transistor count and decrease in feature size is directly related to the resolution limits of projection photolithography. The resolution ($\boldsymbol{F}$ = feature size) of a given

lithographic system is directly proportional to the exposure wavelength divided by the numerical aperture of the lens system (**Fig. 1.4**).

$$F = k\frac{\lambda}{NA}$$

Figure 1.4: Rayleigh equation, feature size is proportional to wavelength.

While much work is done by optics researchers to increase the NA of the lenses used in the current lithography tools, materials research is often looked upon to allow the use of a smaller exposure wavelength (λ), which results in smaller features.

To continually produce smaller transistors lithographers use shorter wavelengths of light. This is best illustrated by looking at what wavelengths of light that were used to produce dynamic random access memory (DRAM) in the past (**Fig 1.5**).

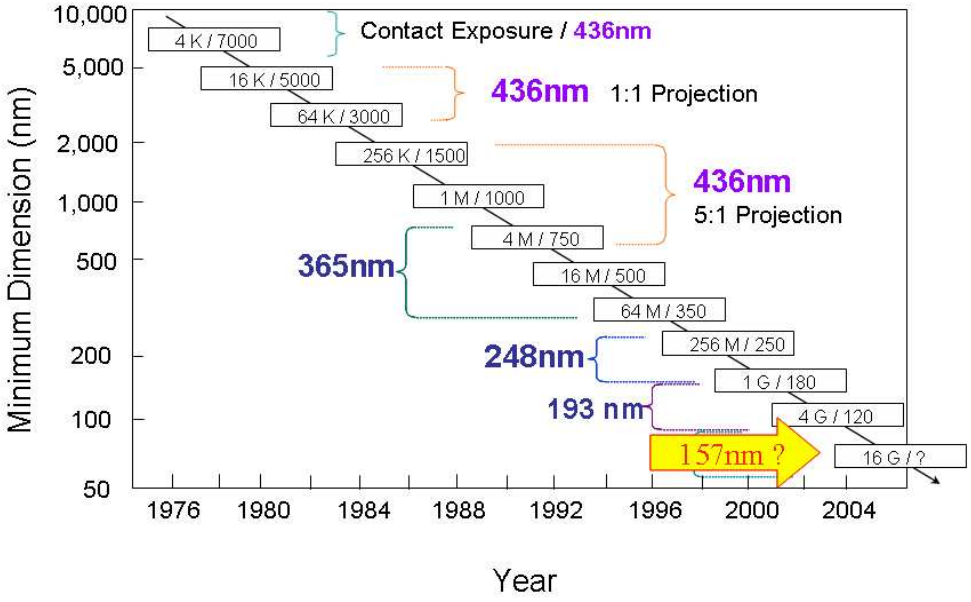

Figure 1.5: DRAM dimension versus year.

The numbers in the graph indicate the memory size and minimum feature size (*i.e.* 4K DRAM with 7000 nm feature size). The graph indicates as the features size decreases the wavelength used to print the same features also decreases. To move from one wavelength (i.e. generation) of lithography to the next often requires a completely new set of materials, specifically developed for the new wavelength of exposure.

g-line (436 nm) and *i*-line (365 nm) Photoresists

Photoresist materials used for 436 and 365 nm exposure rely on the same general chemistry. The base resin is novolac which is produced by the condensation of *meta*-cresol and formaldehyde (**Fig 1.6**).

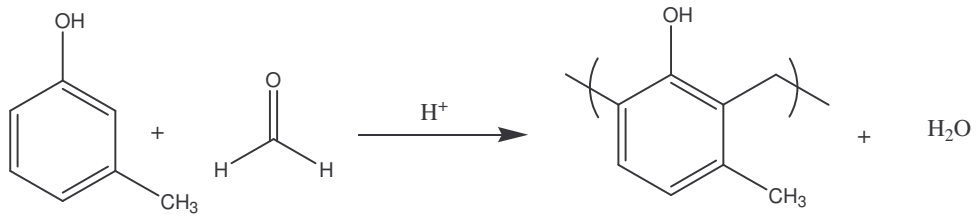

Figure 1.6: Acid catalyzed synthesis of novolac from *para*-cresol and formaldehyde.

To the novolac resin is added substance that inhibits the dissolution of novolac in aqueous base developer. This additive is usually a diazonapthoquinone (DNQ) and it interacts with the novolac resin via hydrogen bonding interactions such that the dissolution of the base resin is retarded.

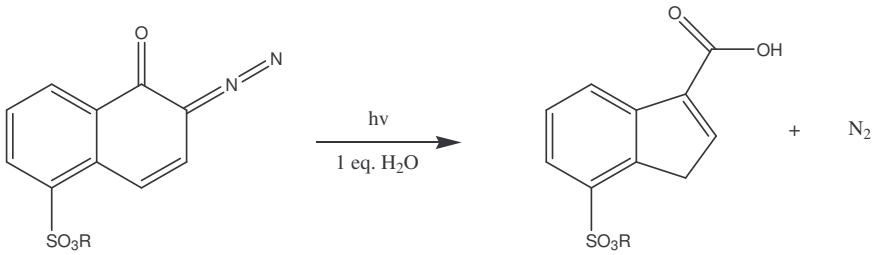

Figure 1.7: DNQ Reacting with Light to Form Indene Carboxylic Acid.

To affect a solubility switch the DNQ upon exposure to light undergoes a photochemical reaction that produces an indene-3-carboxylic acid (**Fig 1.7**). This not only removes the dissolution inhibition it supplied but actually functions as a dissolution promoter due to the presence of a highly base-soluble carboxylic acid group. The DNQ / novolac photoresist system has been used for over 20 years and continues in production today. While this system worked for two different exposure wavelengths the material design of future generations would prove more difficult.

248 nm Photoresists – The Birth of Chemically Amplified Resists

The move to 248 nm as the exposure wavelength was confronted by several challenges. The main issue was that the novolac resin that worked so well at 436 and 365 nm exposure was opaque at 248 nm. To solve the absorbance issue with novolac a new resin needed to be designed. Another issue with 248 nm photolithography is the output of a Hg arc lamp, which was used as the light source at the time, at 248 nm is very low (**Fig 1.8**).

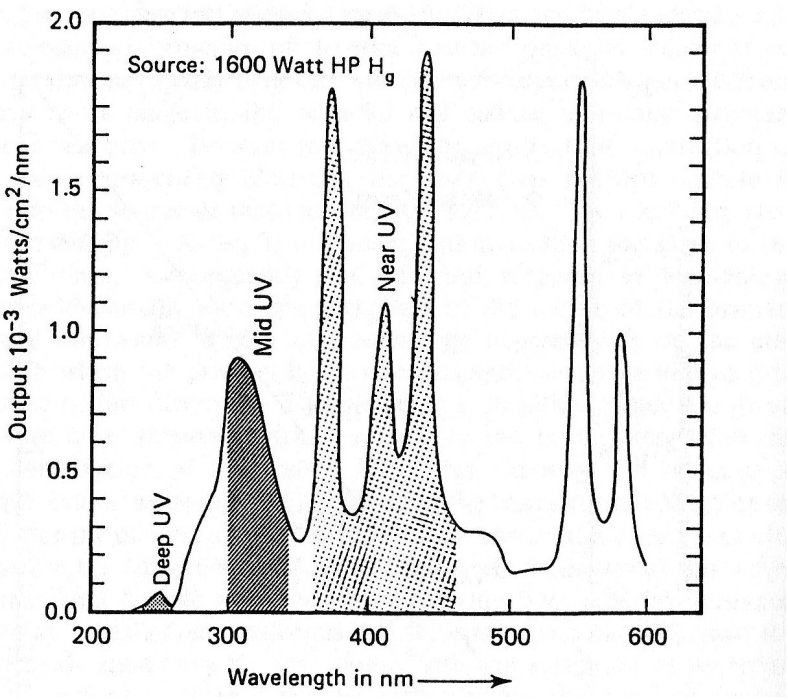

Figure 1.8: Output of Hg arc lamp versus wavelength.

Even though the DNQ / novolac system has a relatively slow photospeed (100-200 mJ/cm^2), imaging was still possible due to the high output of a Hg arc lamp at 436 and

365 nm wavelengths.[4] To resolve this problem a resist system needed to be developed that would more photosensitive.

Chemical Amplification

The solution to the low output of light at 248 nm was addressed by developing a new solubility switch. Since the novolac / DNQ type photoresists required at least one photon to make one molecule undergo the desired solubility switch they had slow photospeed. The solution to this was to have a catalytic deprotection scheme, in which one photon could enable several solubility (deprotection reactions) switches. The availability of photo acid generators (PAG) and the knowledge that many protecting groups in organic chemistry can be removed with catalytic acid, led to the birth of chemically amplified resists (CAR). Chemically amplified resists were developed in the early 80's at IBM[5]. A recent article[6] written by a co-inventor discusses the invention from his perspective as well as current uses of chemically amplified resists. The first catalytic solubility switch was a *t*-boc protected alcohol (**Fig 1.9**).

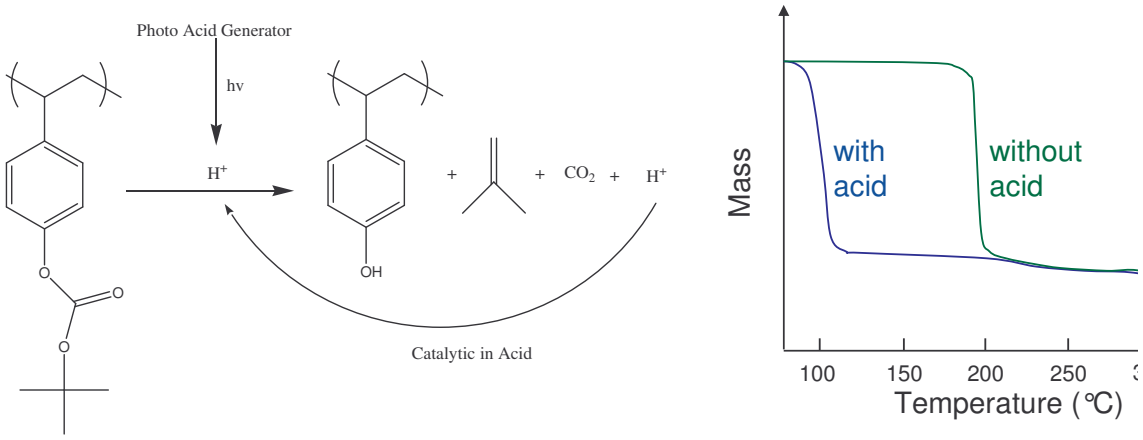

Figure 1.9: Chemically amplified photoresist system, t-boc protected PHOST shown with a TGA of with and without acid catalyzed thermal deprotection of t-boc.

The *t*-boc is removed via acid catalysis. The thermo gravimetric analysis (TGA) plot (**Fig. 1.9**) indicates the decomposition temperature of *t*-boc protected PHOST with and without acid. This difference in decomposition temperature allows for the selective deprotection (solubility switch) in the exposed areas of the photoresist films.

Since novolac is not transparent at 248 nm exposure, a new resin was also needed. Surprisingly *p*-hydroxystyrene (PHOST) which is a structural isomer of novolac is transparent enough at 248 nm exposure to be used as a photoresist.

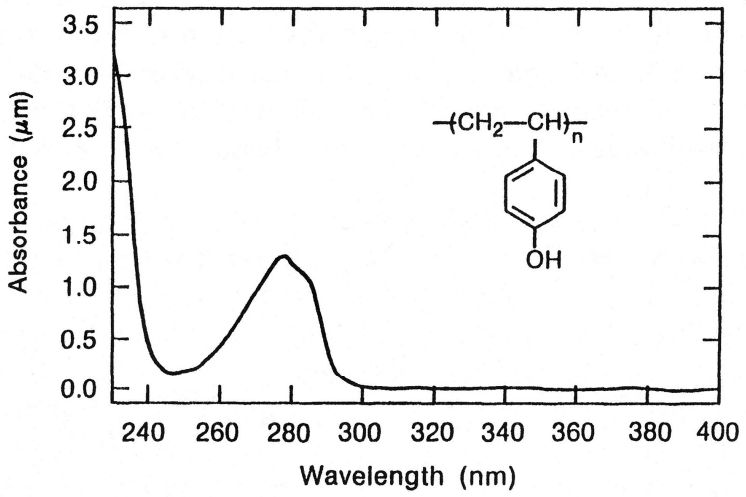

Figure 1.10: Absorbance of PHOST resin versus wavelength.

The use of *t*-boc protected PHOST in combination with a PAG was the first version of a chemically amplified resist. These systems proved to be very useful as a small amount of light would produce acid that could in turn deprotect many sites on the polymer chains rendering them soluble in developer. Chemical amplification has been so successful that nearly all current photoresists produced are variations of the original chemical amplified scheme.

193 nm Photoresists

Photoresists designed for use at 193 nm exposure continued on with the chemical amplified scheme that was developed for 248 nm photolithography. The main problem in moving from 248 nm to 193nm lithography was the absorbance of aromatic rings at 193nm. This precluded any use of styrene based photoresists and shifted focus on two main platforms: acrylates and norbornanes.

The norbornane platform showed some early promise, but failed to find a prominent place in manufacturing. One norbornane system that was auditioned was obtained by the copolymerization of a functionalized norbornane monomer and maleic anhydride, which became know as the COMA (Cyclic Olefin Maleic Anhydride) system[7] (**Fig. 1.11**).

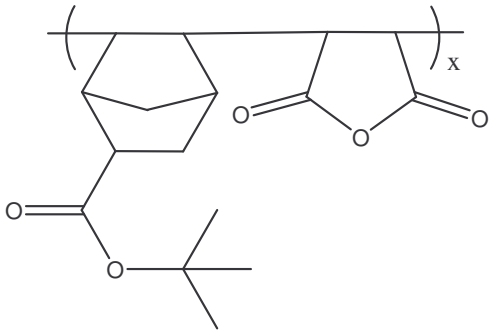

Figure 1.11: Cyclic Olefin Maleic Anhydride (COMA) 193nm photoresist system.

The acrylate platform was also extensively investigated for use at 193 nm lithography. Most acrylate polymers used are terpolymers. The three monomers used are typically free acrylic acid, *t*-butyl ester protected acrylic acid and another substituted acrylate in which the substitution (R group) provides etch resistance[8].

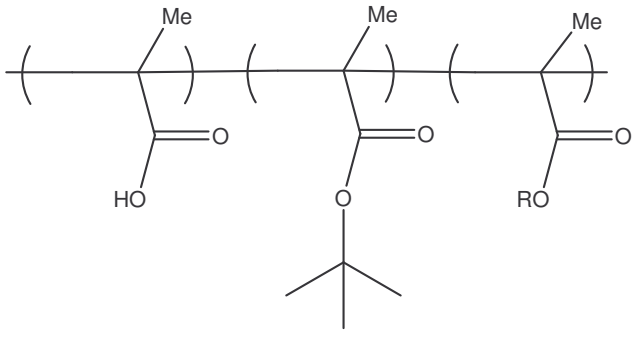

Figure 1.12: Typical 193 nm acrylate based photoresist.

While acrylate based 193nm photoresists are currently used in manufacturing the semiconductor industry always looks toward the next generation wavelength. The next wavelength on the roadmap is 157 nm lithography.

157nm Photoresist

The push towards 157nm lithography again brought about a host of new material requirements. The major requirement for 157nm lithography was the search for a transparent resin. Transparency of the photoresist at the exposure wavelength is crucial to obtain good imaging. If the resist is opaque the light will not penetrate the entire film and will only generate acid in the top part of the film. This will only cause the top of the film to undergo a solubility switch thereby leaving much of the film in place after development (**Fig. 1.13**). If a transparent resin is used the PAG is irradiated through out the thickness of the film, which will result the entire film in the exposed areas switching solubility and subsequently being developed away.

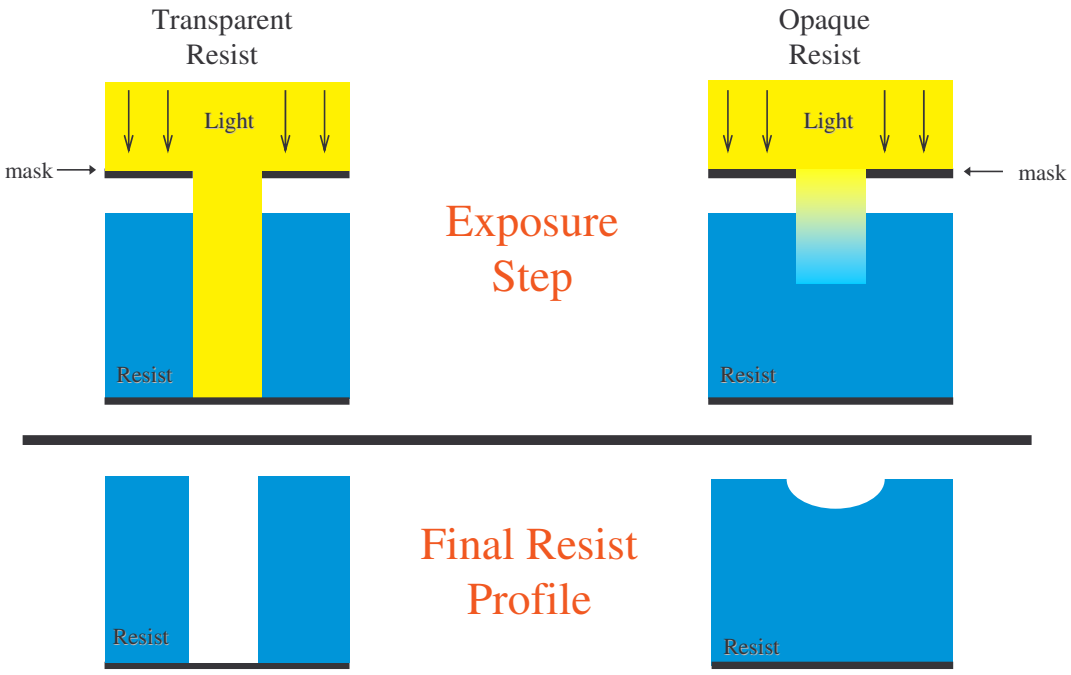

Figure 1.13: Transparent versus opaque photoresist and final image profile.

Early experiments[9] indicate that two classes of material are relatively transparent at 157nm exposure: fluorinated hydrocarbons and siloxanes. This put a major design constraint on the types of polymers that could potentially be used for 157nm lithography.

Another concern that started to arise with 193 nm lithography and increased in importance with 157 is outgassing from the photoresist. During the deprotection reaction the byproducts of the solubility switching reaction volatilize from the resist film. This becomes an issue when outgassing occurs inside the exposure tool as the outgassing

components contaminate the final lens element of the exposure tool. Given the high cost of a lens system and the sensitivity of the lens systems to contamination, a low outgassing resist is desired. This led to research into so-called "mass persistent" photoresists. Or photoresists that are designed not to outgass upon exposure to acid. The work in this thesis will be directed toward producing a "mass persistent" photoresist, one designed to reduce the outgassing found in current photoresists. Development of both a positive tone (chapter 2) and a negative tone (chapter 3) mass persistent photoresist will be discussed.

An alternative imaging technique called Top Surface Imaging (TSI) allows for the use of opaque resins. As a result TSI is being investigated as a potential solution for 157 nm lithography. Chapter 4 of this thesis will describe efforts directed towards the development of a TSI platform for use at 157 nm exposure.

---

[1] http://www.library.upenn.edu/exhibits/rbm/mauchly/jwmintro.html

[2] http://www.intel.com/research/silicon/mooreslaw.htm

[3] Willson, C.G.; Bowden, M. J., Eds. "Introduction to Microlithography," 2nd Edition, American Chemical Society, Washington, D.C., **1994**, Chapter 3.

[4] Wallraff, G. M; Hinsberg, W. D. *Chem. Rev.* **1999**, *99*, 1801-1821.

[5] MacDonald, S. A.; Willson, C. G.; Frechet, J. M. J. *Acc. Chem. Res.,* **1994**, *27*, 151-158.

[6] Ito, H. *J. Polym. Sci. Part A: Polym. Chem.* **2003**, *41*, 3863-3870.

[7] Patterson, K.; Okoroanyanwu, U.; Shimokawa, T.; Cho, S.; Byers, J.; Willson, C. G. *Proc. SPEI-Int. Soc. Opt. Eng.* **1998**, *3333*, 425-437.

[8] Ho, B.; Chang, J.; Liu, T.; Chen, J. *Proc. SPEI-Int. Soc. Opt. Eng.* **1998**, *3333*, 448-453.

[9] Kunz, R.R. *et al*., Proc. SPIE 3678, 13 (1999).

Chapter 2 - Mass Persistent Resists

During the lithographic process several expensive tools are used to produce the desired image. The most important tool in photolithography is the exposure tool. The exposure tool projects light from the laser through the photomask, through a series of lenses to collect and focus the light and onto the photoresist-coated wafer (**Fig. 2.1**).

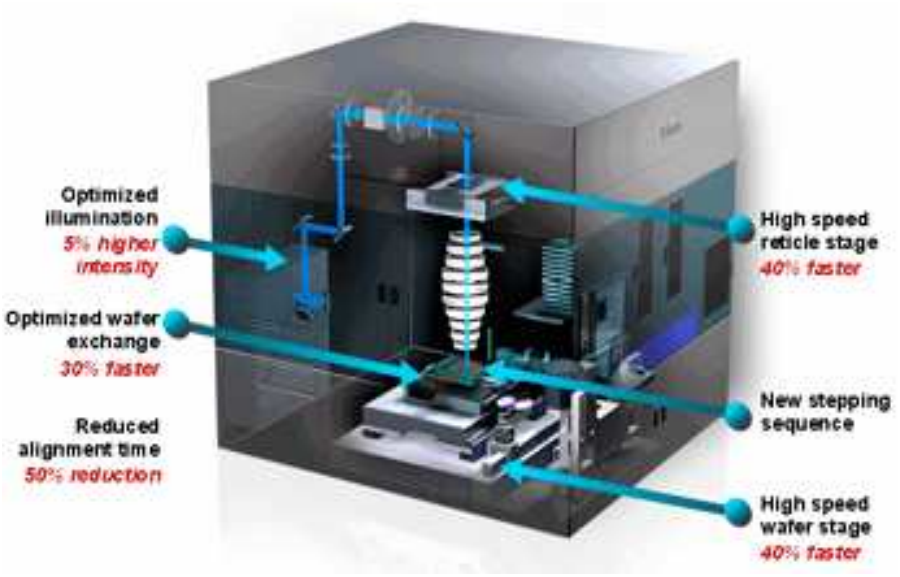

Figure 2.1: Diagram of an exposure tool showing laser path.

In the lens, system the light is focused and the projected pattern reduced in size (typically a 4X reduction) before it reaches the wafer surface. The wafer is often only 1-10 mm from the final lens element. The close proximity of the bottom lens element to the wafer makes that lens element susceptible to contamination from the photoresist. The photochemistry that takes place in the film often results in volatile organic species that

can coat onto the surface, contaminating the lens system. Such contamination results in diminished transmission through the lens system, as well as reduced imaging performance.

Outgassing from the Photoresist

Outgassing of volatile resist components was a problem for 193 nm lithography but became a critical issue when work on 157 nm photoresist began, as every experiment quickly and irreversibly contaminated very expensive lens elements.[10,11] Work published by Hien and co-workers in 2001 quantified the outgassing for an experimental 157 nm photoresist.[12] The method used to quantify the outgassing from a resist was developed by Roderick Kunz at MIT Lincoln Labs. In Kunz's process a photoresist formulation is coated onto a wafer. The wafer is placed into a chamber and the chamber is purged with inert gas. The wafer is exposed with an appropriate dose required by the specific photoresist. The headspace of the chamber is immediately emptied into a cryostat after exposure. The cryostat is warmed and the gasses fed into a gas chromatograph mass spectrometer (GC-MS) which allows for quantitative characterization of the volatile materials.

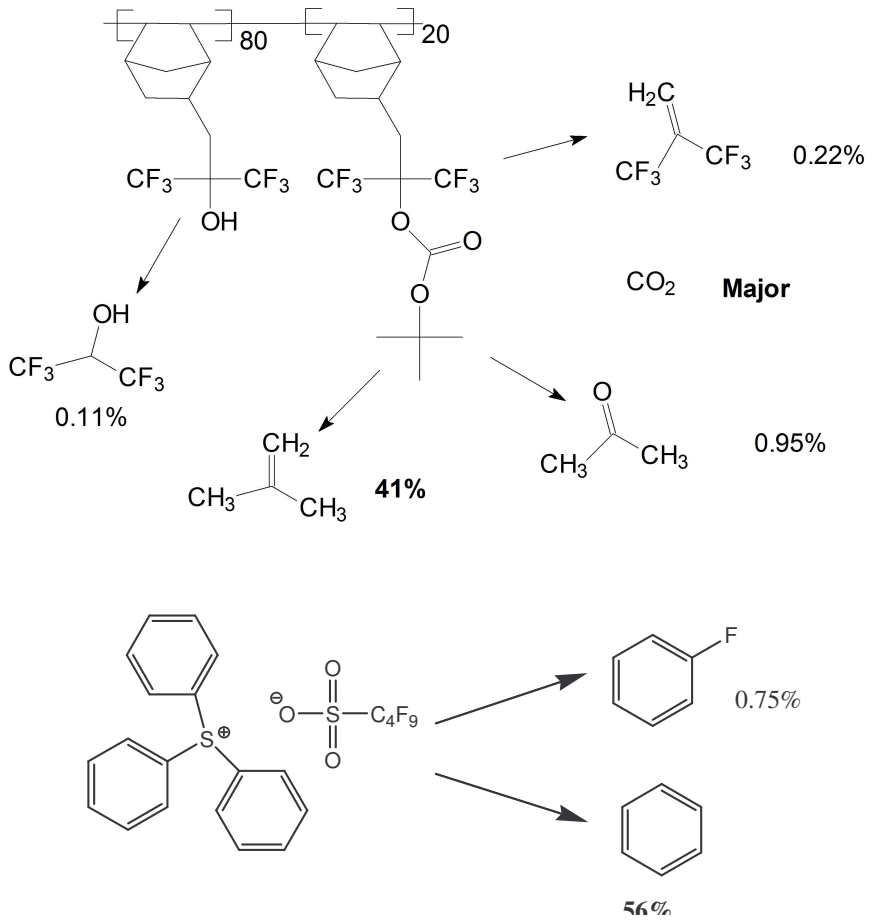

Figure 2.2: Outgassing observed from typical 157 nm photoresist as reported by Hein and co-workers.

The data revealed that the protecting group of the polymer and the photoacid generator (PAG) are the major sources of outgassing components from the photoresist (**Fig. 2.2**). Since lens elements are highly sensitive to contamination and expensive, outgassing is a serious concern for lithographic engineers. Kunz reported that a lens system has to withstand approximately 53 million exposures per year and should last at least 5 years to make the investment worthwhile. Although in most cases a contaminated lens systems

can be cleaned, and lenses do require periodic cleaning, it is in the best interest of the company to keep the tool running continuously as long as possible and at 157 nm, some components resisted cleaning. Any downtime has negative ramifications on the profitability of the fab. Outgassing from the resist will at least increase the tool downtime, and in some cases may permanently damage the lens system.

Mechanism for Formation of Outgassing Components

It has been determined that the outgassing material from a typical photoresist stems from two sources: the protecting group (solubility switch) on the polymer and the photoacid generator (PAG). The outgassing associated with the PAG is the result of an undesirable reaction that forms benzene.[13] During the photolysis of the PAG, a phenyl radical can react with a solvent molecule (R) to form benzene, which is volatile (**Fig. 2.3**).

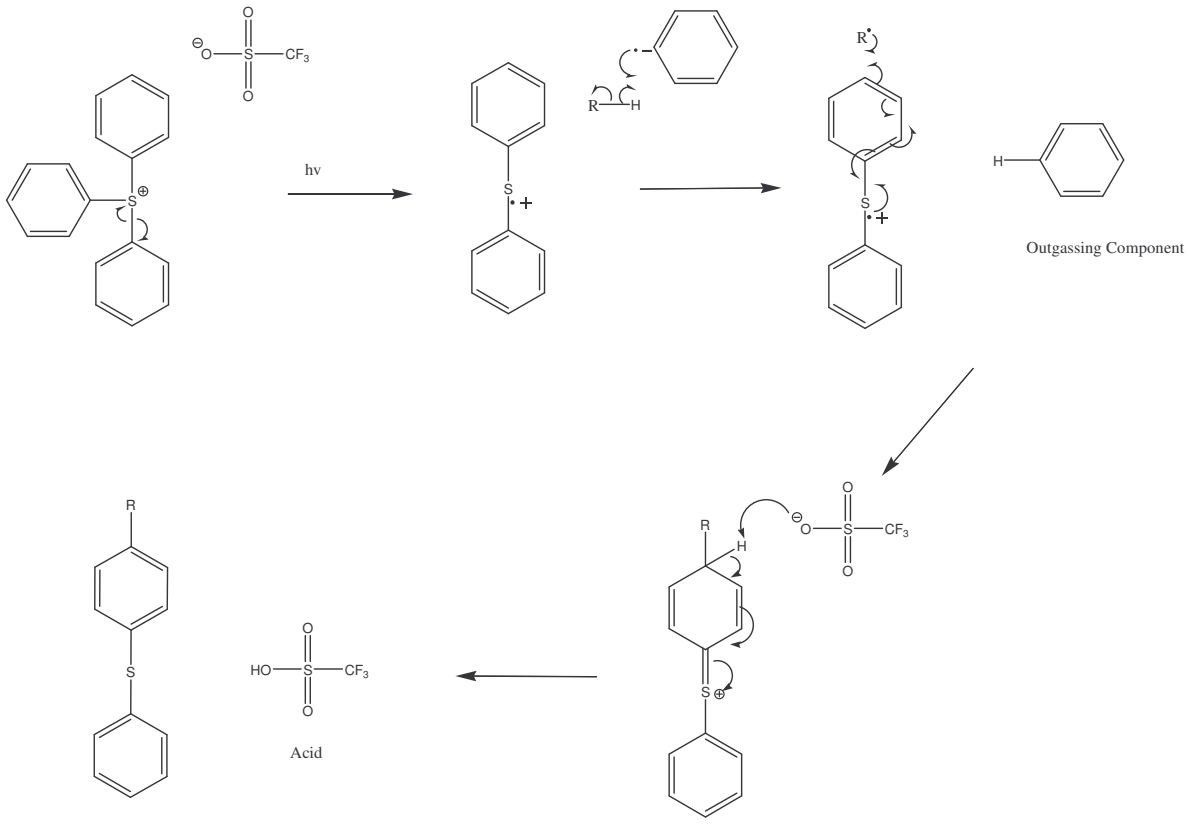

Figure 2.3: Mechanism of photolysis of PAG to produce acid and volatile byproduct benzene.

The photolysis of the PAG can also proceed through a mechanism that forms non-volatile by-products.

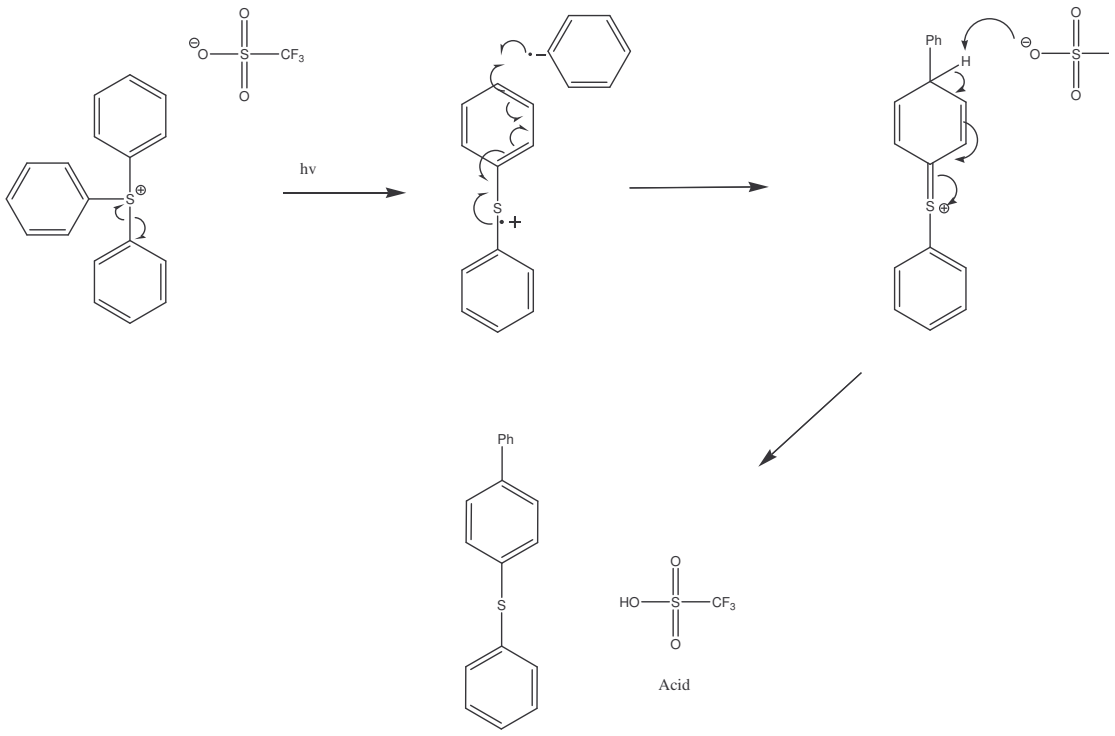

Figure 2.4: Photolysis of PAG to produce acid along with non-volatile by-products.

Here the phenyl radical formed upon photolysis reacts with the diphenylsulfonium to form a non-volatile byproduct along with the desired triflic acid (**Fig. 2.4**).

Outgassing from the polymer protecting group, however, is purposely designed to form volatile components upon exposure to acid. The three most commonly used protecting groups (carbonates, acetals and tertiary esters) all outgas upon acid catalyzed deprotection (**Fig. 2.5**).

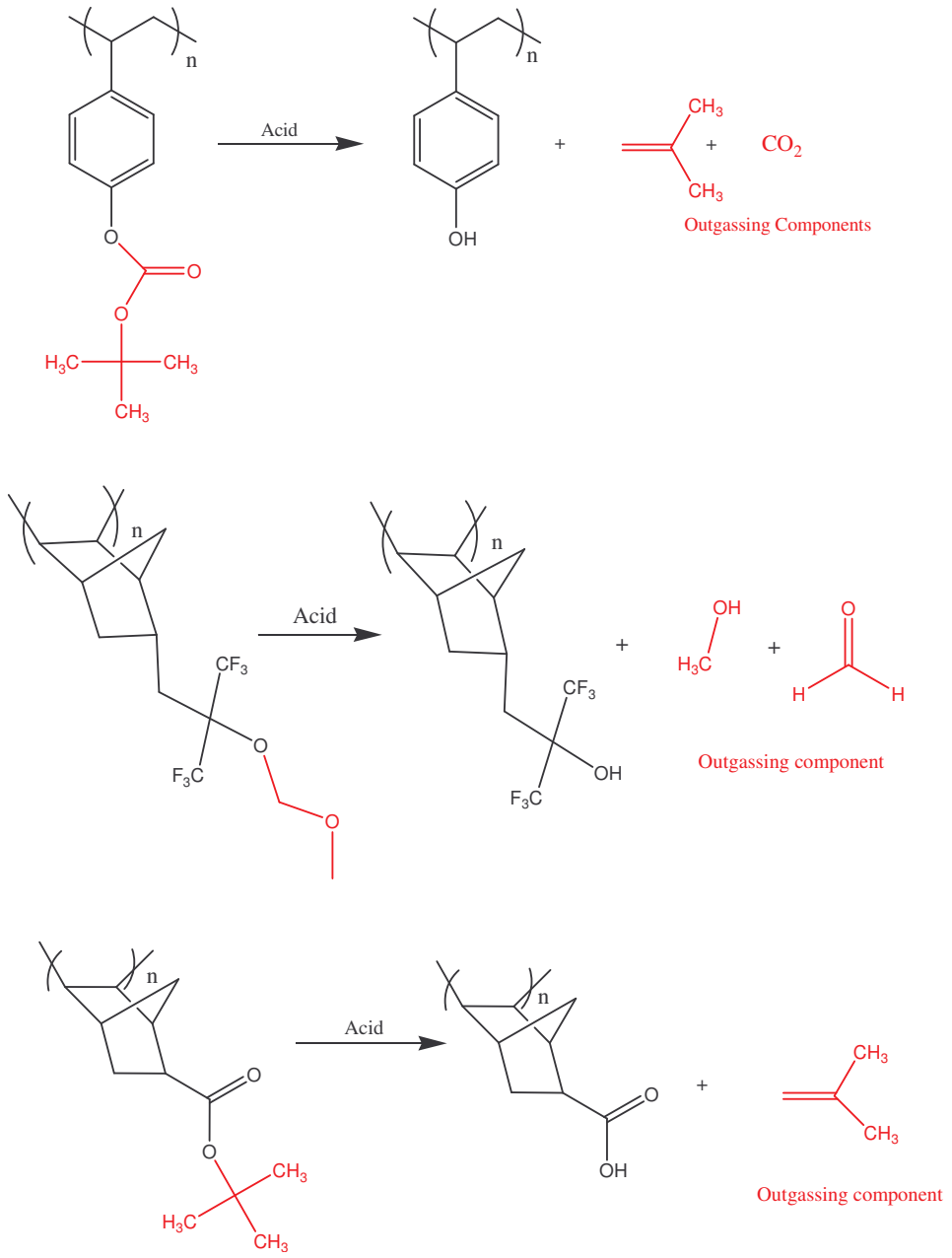

Figure 2.5: Deprotection of three most common protecting groups used in photoresist, *t*-boc, acetal and *t*-butyl ester. The corresponding outgassing components are shown.

The deprotection of the carbonate protecting group results in loss of benign carbon dioxide as well as undesirable isobutene by-products. Acetal protecting groups require one equivalent of water for the deprotection and result in the formation of an aldehyde and an alcohol. The deprotection of a *t*-butyl ester is similar to the *t*-boc deprotection, and gives off isobutene as a volatile deprotection fragment. In all cases, the formation of volatile byproducts ensures the deprotection reaction is irreversible and proceeds to completion during the post exposure bake.

Since the outgassing PAG fragments are the result of unintended side reactions and vary depending on the specific PAG, this thesis will focus on eliminating the intentional outgassing associated with the protecting group of the polymer. To design a resist that does not outgas, a functional group must be used that switches solubility without the loss of volatile byproducts. We have termed such non-outgassing resists, "mass persistent resists."

Designing a Mass Persistent Resist

To design a mass persistent resist, the project was divided into three parts: design, synthesis and testing of model mass persistent solubility switches; polymer synthesis; and the lithographic evaluation of promising polymer systems. Making model compounds allowed for easier characterization when determining whether the desired chemistry (solubility switch) was occurring. After finding model compounds with the desired

chemistry, polymers based on these compounds were synthesized and later lithographically evaluated.

Mass Persistent Concept and Model Compounds

As was shown in **Fig. 2.2**, the deprotection of the polymer to produce a base soluble polymer causes a significant amount of outgassing. To prevent outgassing, the protecting groups would have to be appended to the polymer backbone. Five different model compounds were synthesized to determine whether appending the deprotection fragment to the polymer backbone was feasible. Current photoresists utilize the volatility of the deprotection fragments to ensure that no equilibrium exists between the protected and deprotected forms of the polymer. So it was not immediately obvious that tethering the product to the polymer backbone would be successful.

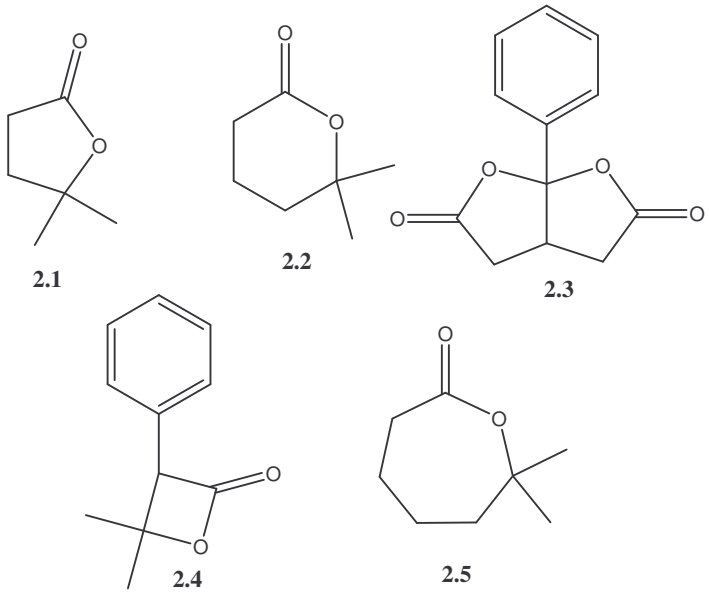

Figure 2.6: Structure of model compounds for a mass persistent solubility switch.

The model compounds (**Fig. 2.6**) were designed to mimic functional groups already employed in photoresist chemistry today. Four of the compounds (**2.1**, **2.2**, **2.4**, **2.5**) are lactones with ω-geminal methyl substitution which mimics a *t*-butyl ester solubility switch. Upon cleavage of the ester bond the resulting isobutene moiety is still appended to the polymer backbone (**Fig. 2.7**).

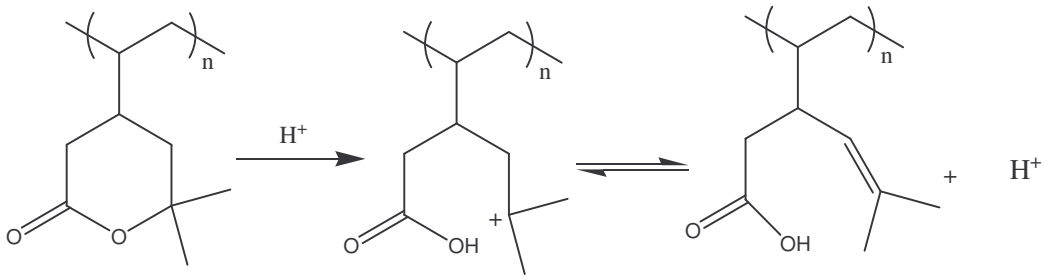

Figure 2.7: Proposed mechanism for a lactone ring-opening that forms a base soluble product without a loss in mass.

Compound **2.3**, while still a lactone, would conceivably proceed through a hydrolysis of the acetal functionality, mimicking acetal protecting group chemistry already used in current photoresists (**Fig. 2.8**).

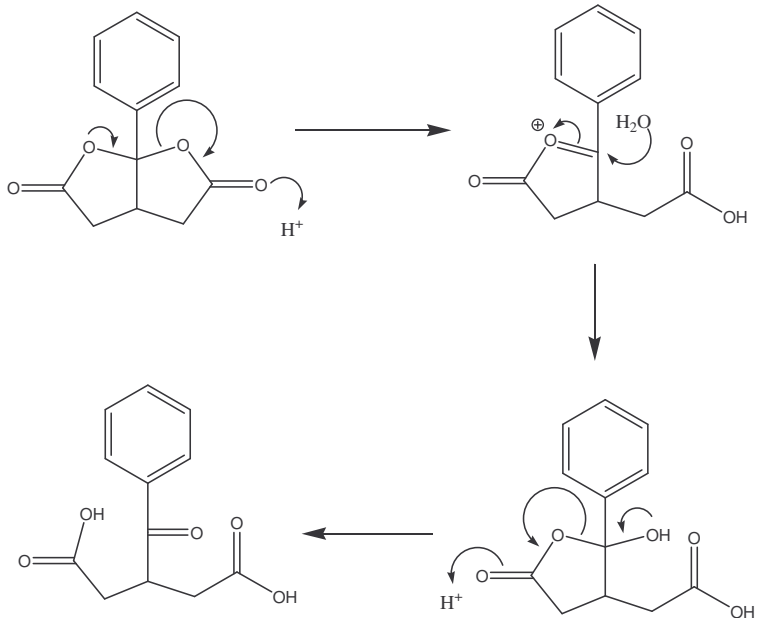

Figure 2.8: Proposed mechanism for hydrolysis of Fittig bis-lactone to base soluble product.

Model Compound Synthesis

The first lactone synthesized was the five member ring lactone (**2.1**).

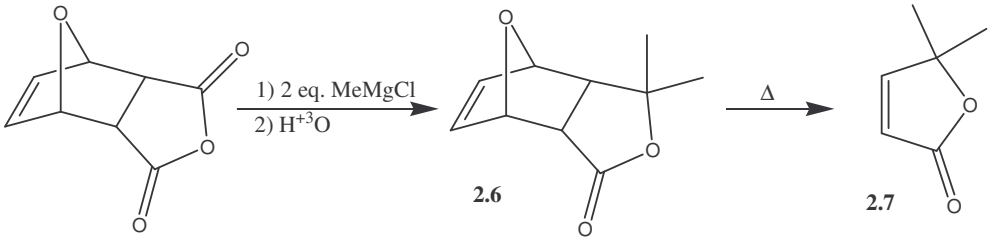

Figure 2.9: Synthesis of model lactone (2.1).

The commercially available Diels-Alder adduct of maleic anhydride and furan was reacted with two equivalents of methyl magnesium chloride, followed by an aqueous acid

workup to produce **2.6**. A retro Diels-Alder reaction afforded the α,β-unsaturated lactone **2.7**. Hydrogenation with palladium on carbon produced the desired model compound **2.1**.

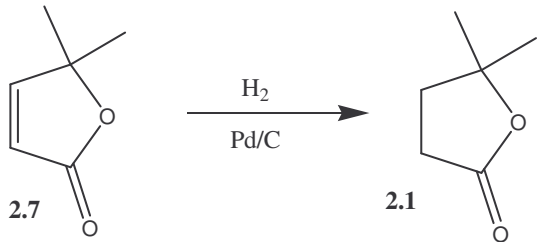

Figure 2.10: Synthesis of model lactone (2.1) continued.

The six member lactone was synthesized via a simpler route. Commercially available 2,2-dimethylcyclopentanone was oxidized to the corresponding lactone (**2.2**) via a Baeyer-Villiger oxidation with *m*-chloroperoxybenzoic acid (MCPBA) (**Fig. 2.11**).[14]

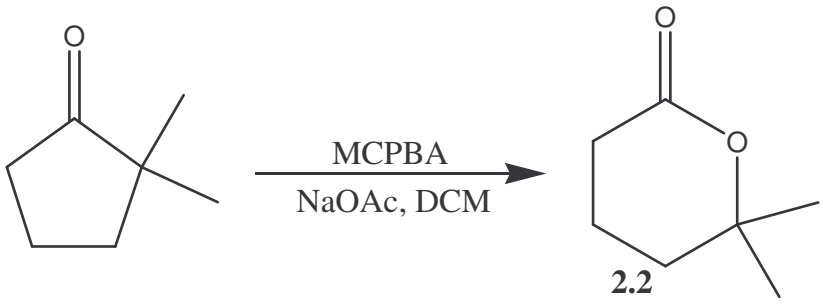

Figure 2.11: Baeyer-Villiger oxidation of 2,2-dimethylcyclopentanone with MCPBA to synthesize model compound 2.2.

Likewise, for the seven member lactone, a Baeyer-Villiger oxidation of 2,2-dimethylcyclohexanone furnished the desired lactone (**2.5**) (**Fig. 2.12**).

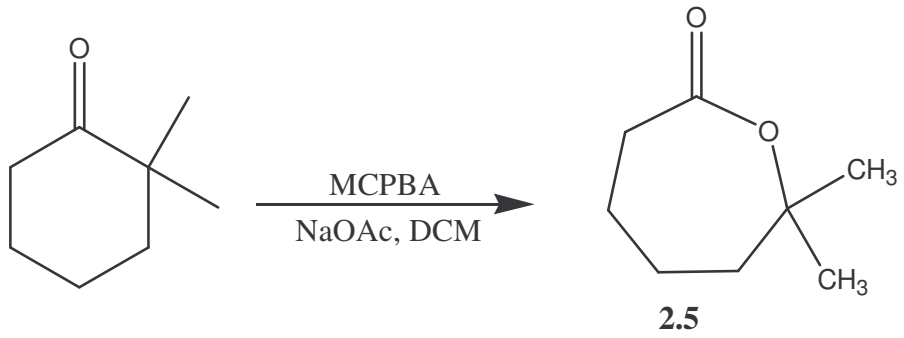

Figure 2.12: Synthesis of model compound 2.5 via Baeyer Villiger oxidation of 2,2-dimethylcyclohexanone.

The synthesis of the four-membered lactone (**2.4**) was accomplished in a two step synthesis following literature precedence.[15,16] The dianion of phenylacetic acid was made with two equivalents isopropyl magnesium chloride and condensed with acetone to form the β-hydroxy acid **2.8**.

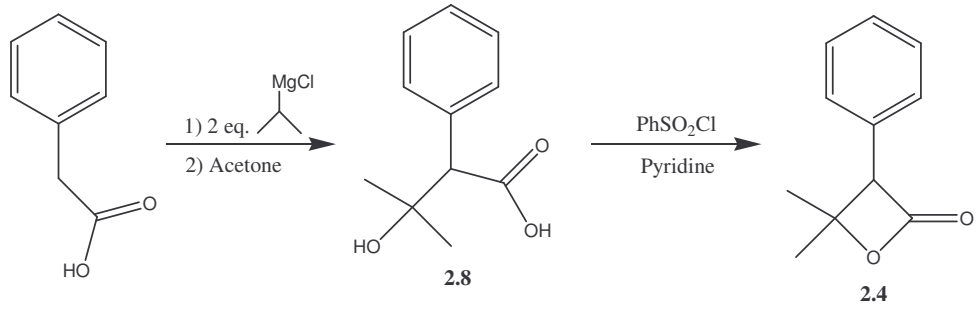

Figure 2.13: Synthesis of beta-lactone (2.4) model compound.

Cyclization of **2.8** in pyridine with phenylsulfonyl chloride produced the desired model compound **2.4** (**Fig. 2.13**).

Model compound **2.3** belongs in a class of lactones called Fittig bis-lactones, that are commonly used for anionic ring-opening polymerizations.[17] The synthesis of **2.3** is reported by Strunz and co-workers (**Fig. 2.14**).[18]

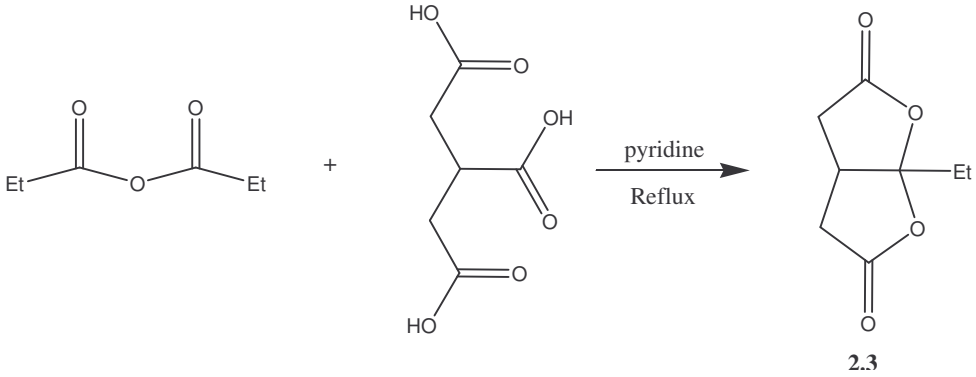

Figure 2.14: Synthesis of Fittig bis-lactone (2.3) model compound.

Tricarballyic acid was heated in propionic anyhydride as the solvent with a catalytic amount of pyridine to produce the corresponding Fittig bis-lactone **2.3**. With the prepared model compounds, the next step was testing for ring-opening when exposed to acid.

Model Compound Testing

Testing of the model compounds was conducted via proton NMR. This allowed the reaction to be monitored over time to determine reaction progress. The NMR spectra were taken in deuterated chloroform, with triflic acid used as the acid catalyst. This acid was chosen because it is a common acid produced by PAGs used in the photolithography.

Model compound **2.1** and **2.2** were both treated with 5% triflic acid in Chloroform and heated to 50° C. After heating for 30 minutes no reaction was observed in either compound.

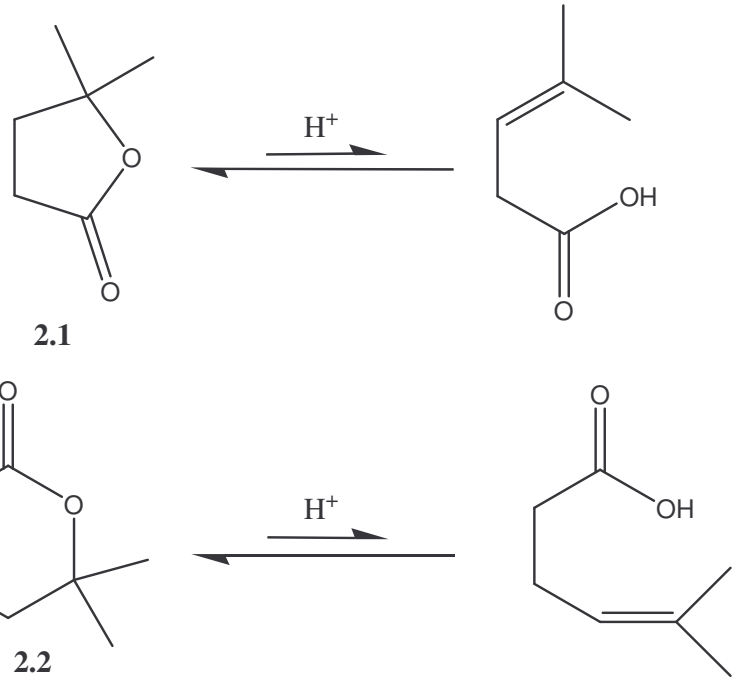

Figure 2.15: NMR test of model compounds 2.1 and 2.2 did not show any ring opened product.

These results are not so surprising given the lack of ring strain typically found in five and six member rings. Two papers report on the thermodynamics of ring-closing lactone formation.[19,20] The reported rate for the formation of lactones from ω-bromoalkane-carboxylate ions is fastest for formation of a five member lactone (n=1), with six member ring (n=2) being second fastest (**Fig. 2.16**).

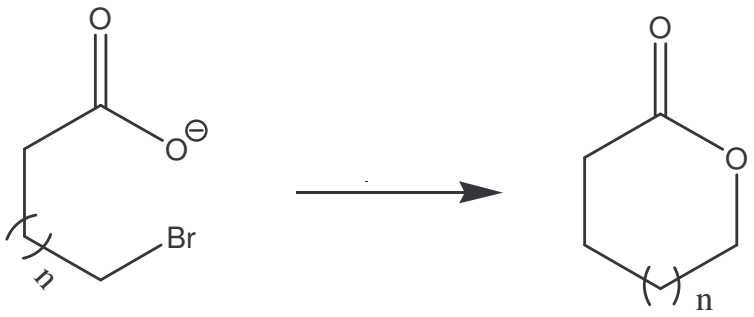

Figure 2.16: Literature Model compounds used in ring-closing kinetic experiments of lactones.

The proposed acid catalyzed ring-opening of the model lactones (**2.1**, **2.2**, **2.4**, **2.5**) would be an equilibrium between the ring opened and ring closed forms. Given the fact that the five and six member rings do not have much ring strain, it is proposed the equilibrium lies in the direction of the ring closed product.[21,22]

To push the equilibrium to the ring-opened product the use of ring strain was employed. Four-membered rings have high inherent ring strain and β-lactones are no exception. β-Lactones are well known to undergo facile ring opening polymerization due to their ring strain.[23] To determine if model compound (**2.4**) is strained enough to ring-open with acid catalyst to form the corresponding base soluble carboxylic acid and olefin, the lactone was heated with triflic acid for 1 min at 90° C. NMR spectra taken before and after heating indicate complete conversion of the starting lactone into two products (**Fig. 2.17**).

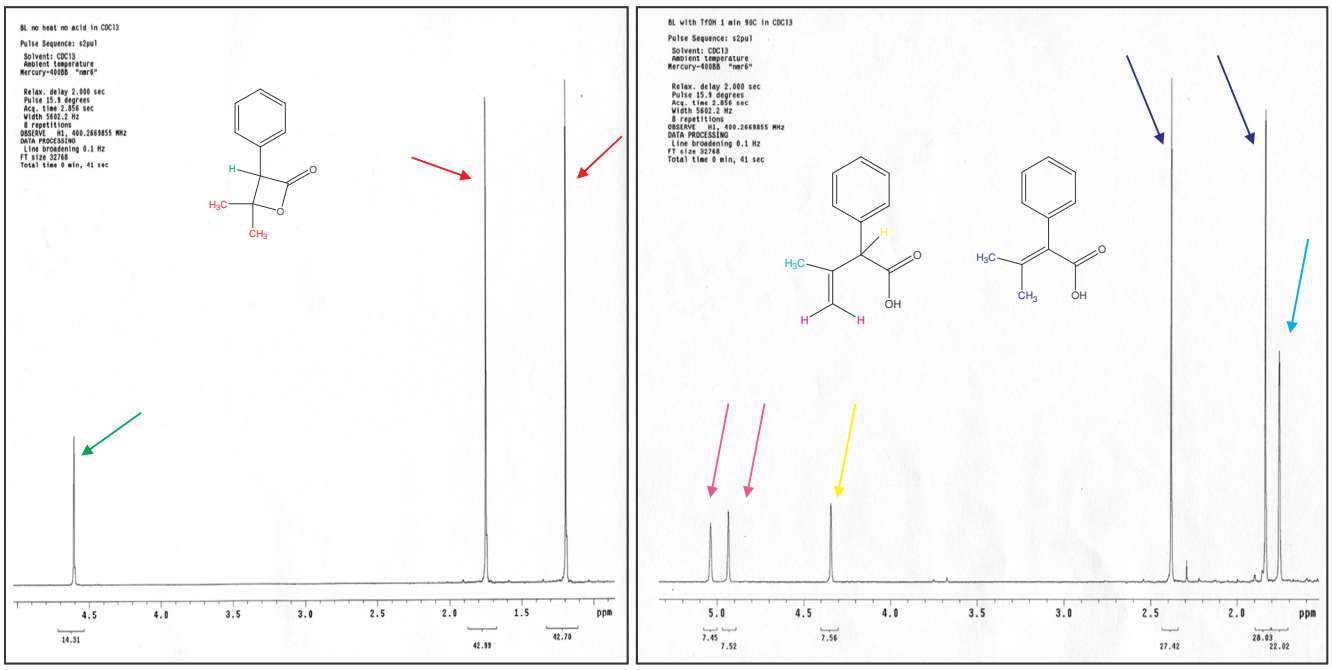

Figure 2.17: NMR showing ring-opening of beta lactone with triflic acid after heating for 1 min at 90° C.

The two products are structural isomers, and neither loses mass upon ring-opening to the base soluble carboxylic acid.

NMR Kinetics of β-Lactone Ring Opening

The successful ring opening of the β-lactone to two base soluble isomers invited further investigation of the ring opening reaction. Proton NMR was an ideal spectroscopic method as the starting lactone (**2.4**) and the two products (**2.10**, **2.11**) all have unique NMR peaks. The use of NMR allows for the concentrations of all species to be determined at different time intervals.

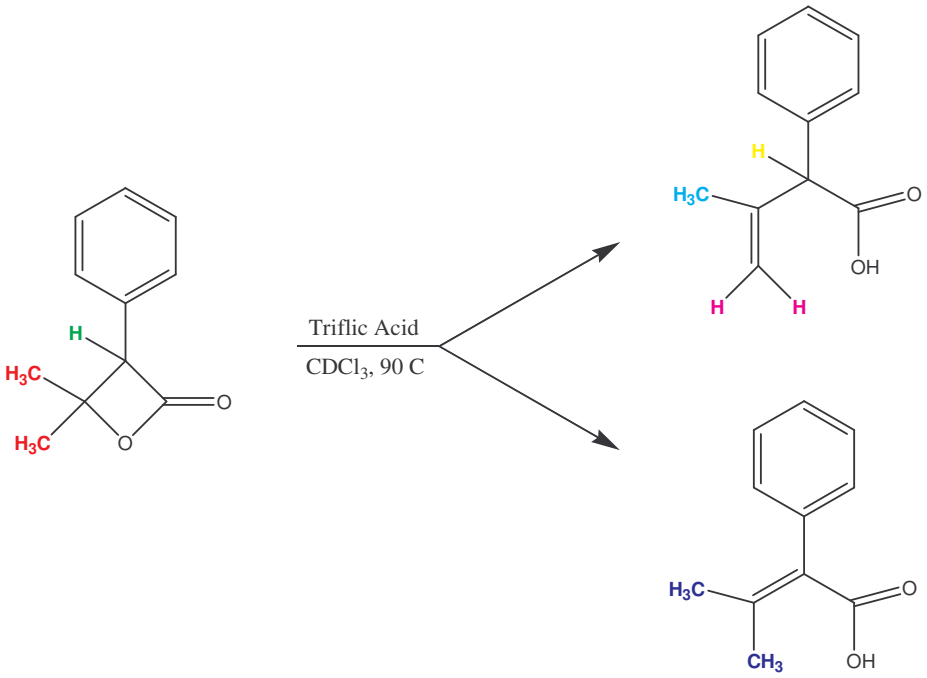

Figure 2.18: Acid catalyzed ring-opening reaction of β-lactone (2.4) to form two isomeric products.

The starting material was easily tracked by its benzylic proton marked in green (~4.6 ppm). Product A was tracked by integrating one of the vinyl hydrogens marked in pink (4.9 or 5.1 ppm) and product B was followed by one of the allylic methyl groups (2.4 or 1.8 ppm) (**Fig. 2.18**). A series of three NMR experiments were run at three different temperatures (50° C, 27° C and 0° C). A known concentration (0.55 M) of lactone (**2.4**) in $CDCl_3$ with 5.0 mol % triflic acid was added into a NMR tube. The NMR tube was immediately placed in the NMR probe and shimmed. Spectra were taken a set interval (114 seconds) apart. After collection of the spectra the peaks of interest for

the three compounds were integrated and the concentration of starting material and products were determined.

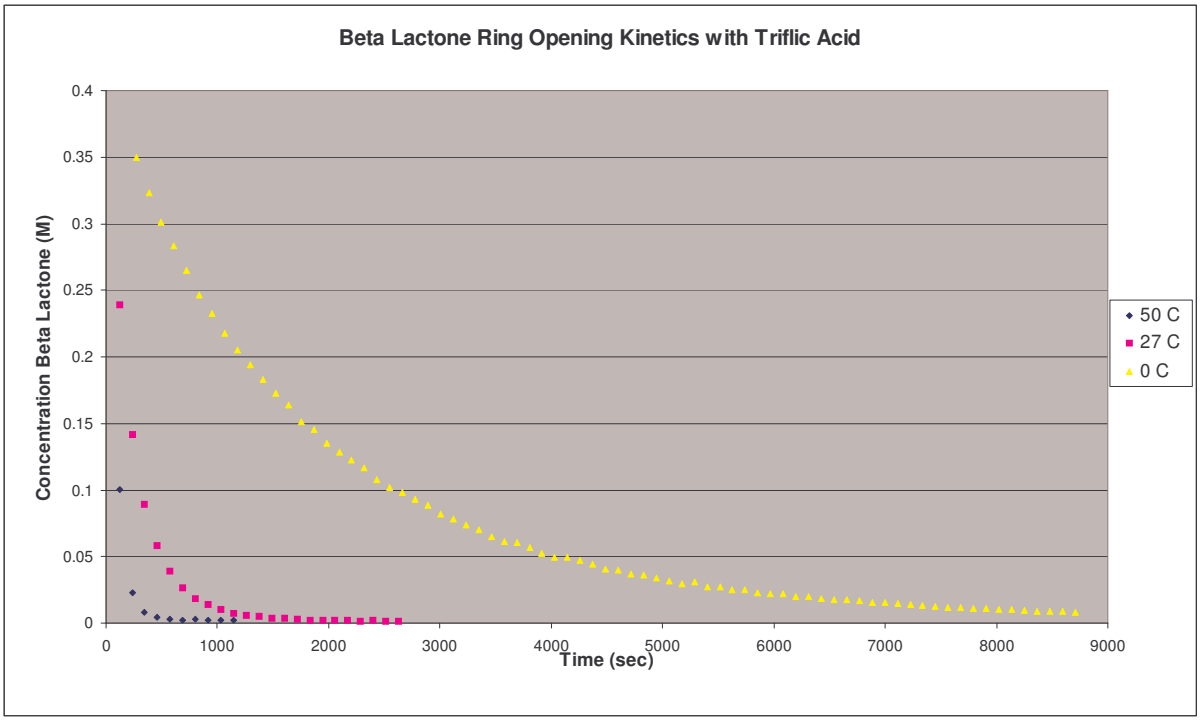

Figure 2.19: Kinetics plot showing disappearance of beta lactone during ring opening reaction.

Plotting the concentration of lactone versus time (**Fig. 2.19**) suggests first order kinetics. A plot (**Fig. 2.20**) of natural log of lactone concentration versus time reveals that the reaction is first order with respect to lactone.

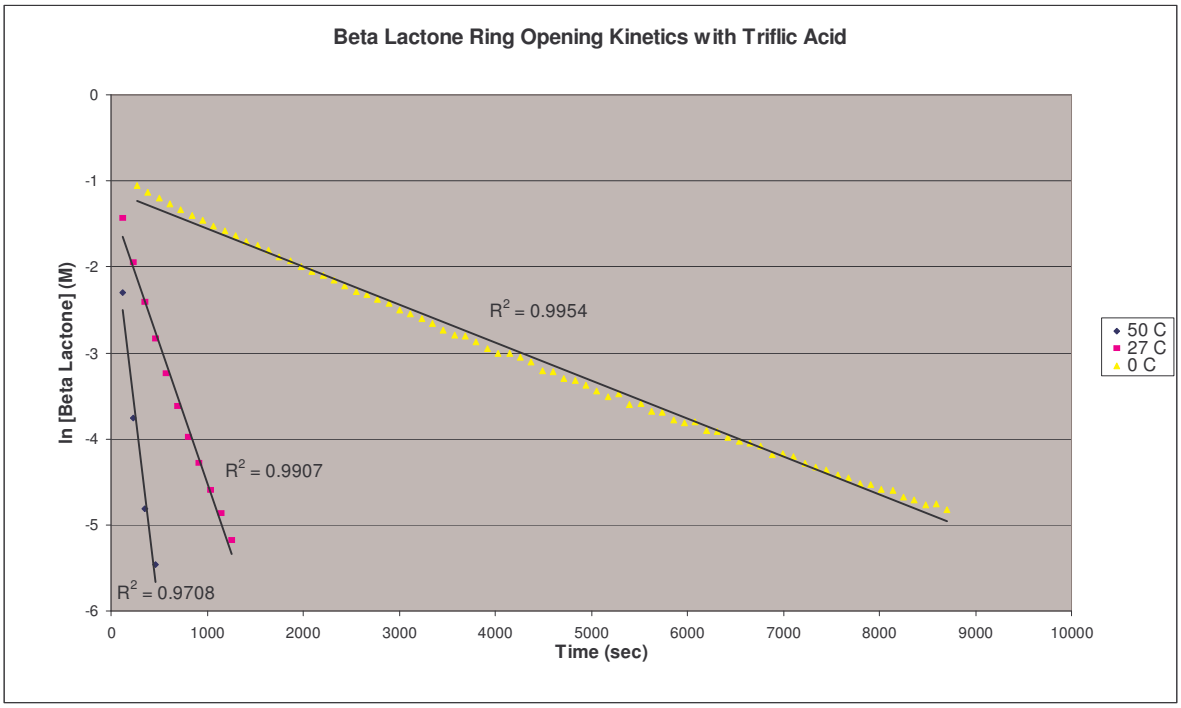

Figure 2.20: Kinetics plot showing that β-lactone ring-opening reaction is first order with respect to lactone.

More importantly the NMR data gives information that allows determination of the ratio of the two isomers formed. Data collected from the NMR experiments suggests one isomer is the kinetic product and one isomer is the thermodynamic product from the ring opening reaction. The data taken at 0 °C shows that product A (**2.10**) is formed much faster than product B (**2.11**).

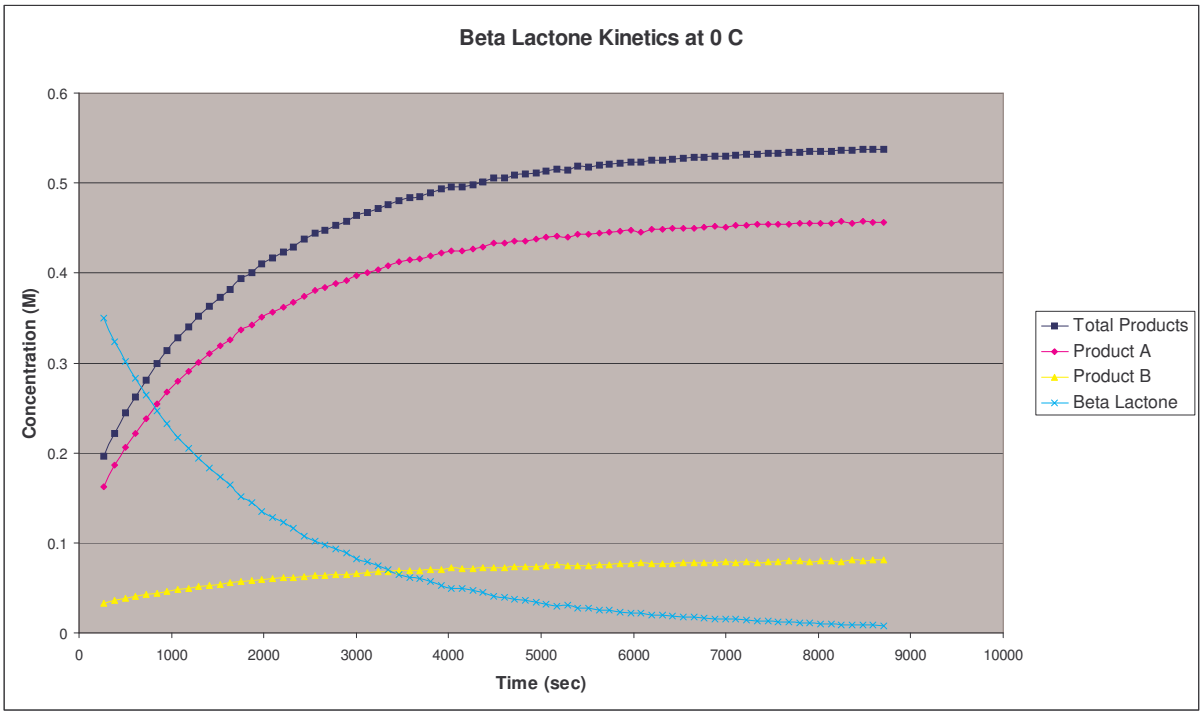

Figure 2.21: Plot showing kinetics of products formed at 0 °C of β-lactone reacting with triflic acid.

At the first data point taken, product A (**2.10**) was almost five times as abundant as product B (**2.11**). This suggests that product A (**2.10**) is kinetically favored over product B (**2.11**). Data taken at 27 °C shows a similar trend. Product A (**2.10**) increases in concentration very quickly compared to product B (**2.11**).

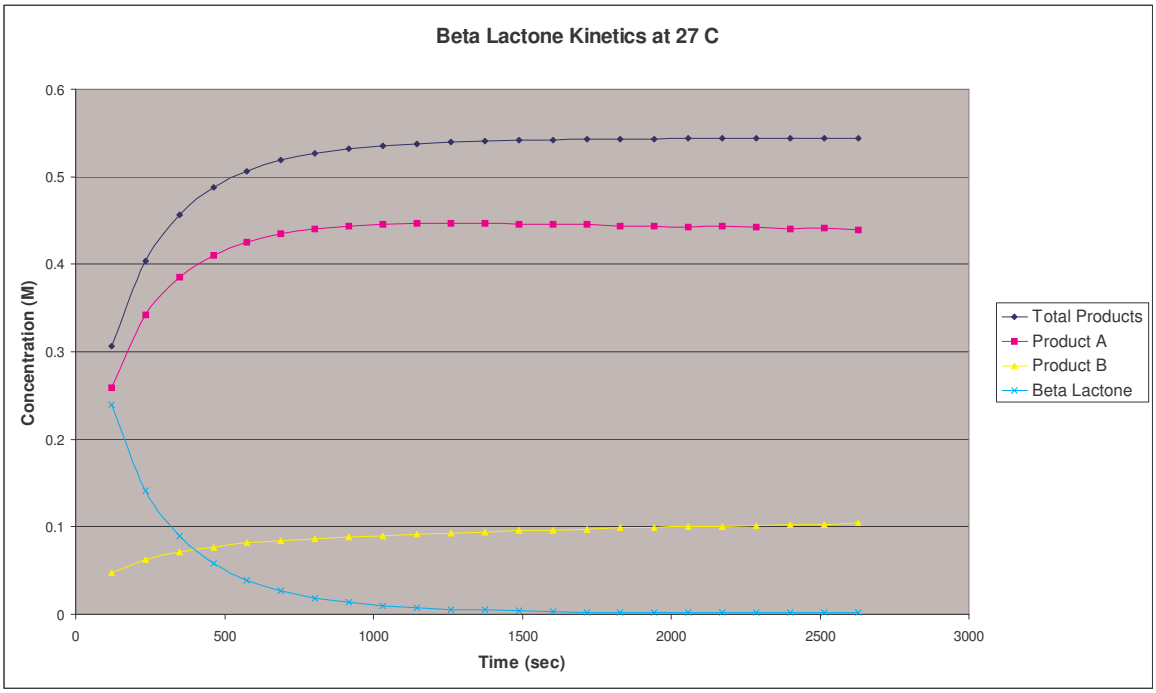

Figure 2.22: Plot showing kinetics of β-lactone-opening to form two products at 27 °C.

Even more importantly, after all the β-lactone has been consumed (~2000 secs) the concentration of product A (**2.10**) starts to decrease while the concentration of product B (**2.11**) increases. This indicates that product A (**2.10**), the kinetic product, slowly isomerizes to product B (**2.11**) which is the thermodynamic product. Data taken at 50 °C shows this same behavior (**Fig. 2.23**).

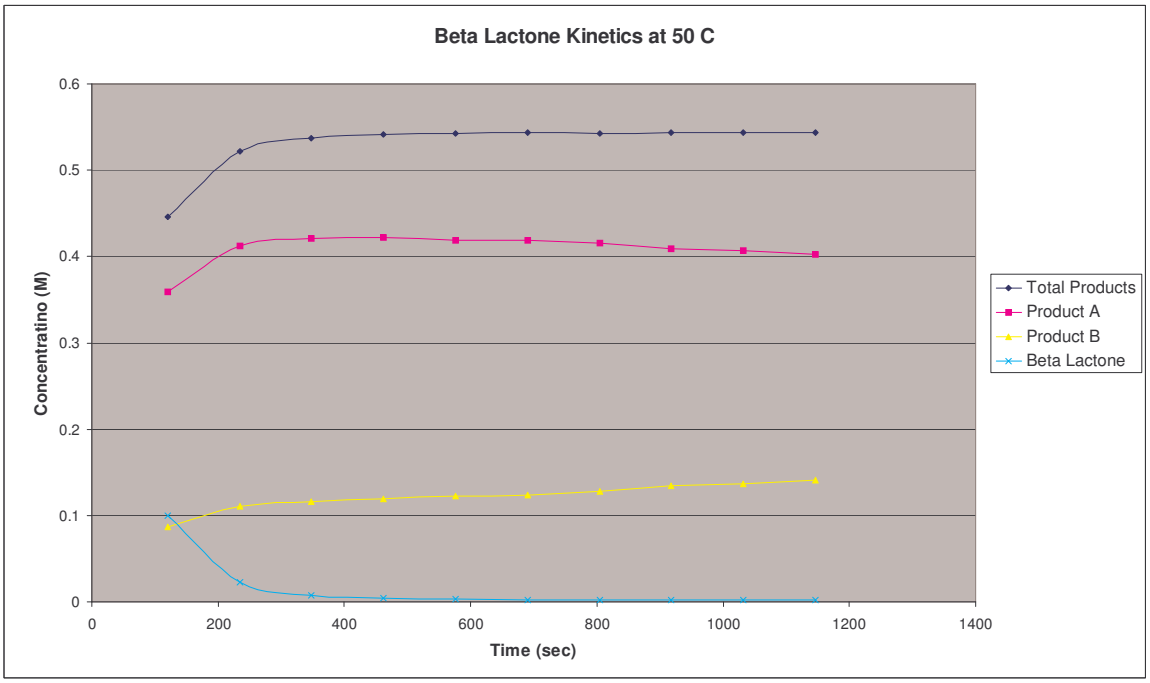

Figure 2.23: Plot showing kinetics of beta lactone ring opening reaction at 50 C.

This behavior is easily explained upon looking at the structure of both **2.10** and **2.11**. The kinetic product (**2.10**) forms faster due to the presence of six hydrogens available for elimination to form the corresponding olefin (**Fig. 2.24**).

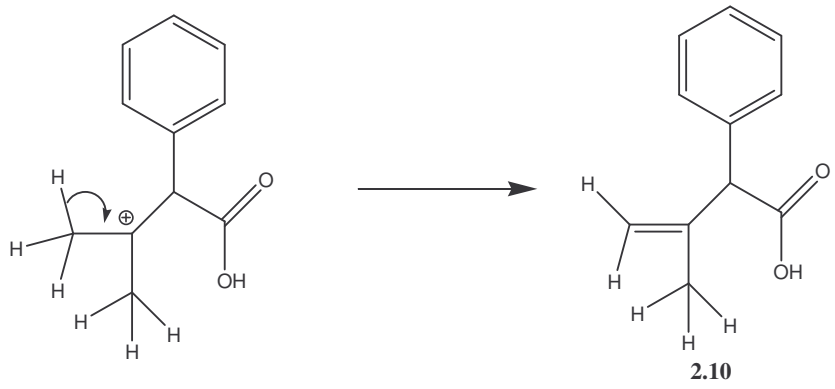

2.10

Figure 2.24: Elimination to form the kinetic product resulting from treatment of β-lactone (2.4) with acid.

The formation of the thermodynamic product (**2.11**) happens slower due to the presence of only one hydrogen available for elimination (**Fig. 2.25**).

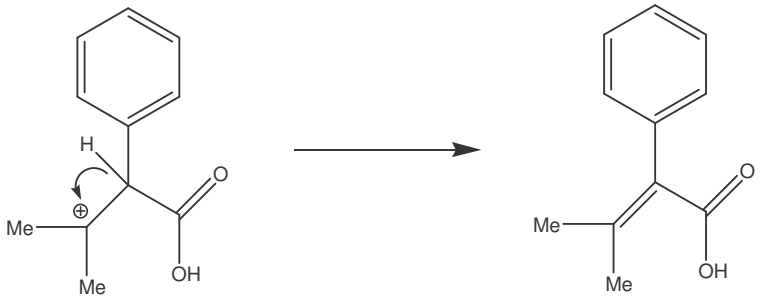

2.11

Figure 2.25: Elimination to form thermodyanmic product resulting from treatment of beta-lactone (2.4) with acid.

However, the acid catalyst isomerizes the kinetic product to the thermodynamic product. Product **2.11** is thermodynamically stable relative to **2.10** due the increase in conjugation of the olefin with both the aromatic ring and the carbonyl of the carboxylic acid.

Even with the success of the β-lactone two other molecules were synthesized and tested. To mimic acetal chemistry that is used in current chemically amplified resists a Fittig bis-lactone was synthesized (**Fig. 2.26**).[24]

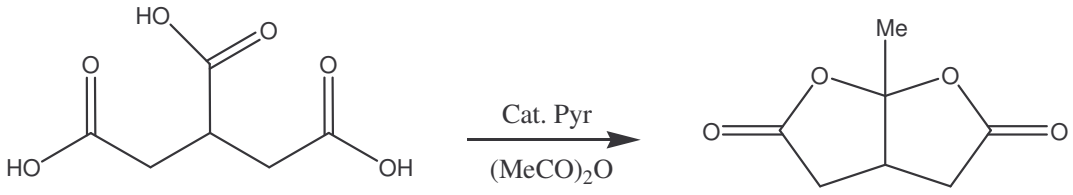

Figure 2.26: Synthesis of Fittig bis-lactone from tricarballyic acid and propionic anhydride.

The proposed mechanism for the ring opening of **2.3** in acidic conditions is through hydrolysis (**Fig. 2.8**). To test whether the Fittig bis-lactone would hydrolysis, a sample of **2.3** was heated at 90 °C with 12.5% tosic acid monohydrate along with 3 eq of water in deutereated acetonitrile. After 35 minutes of heating only starting material was present. No noticeable hydrolysis to the ring opened product was observed. It appears that the the Fittig bis-lactone is too stable towards hydrolysis to serve as a mass persistent analog of an acetal based photoresist.

It is well know that ε-caprolactone possesses enough ring strain to undergo ring opening polymerizations.[25,26] To determine whether ω-gem-dimethyl ε-caprolactone (**2.5**) would ring open with acid catalysis, compound **2.5** was treated with catalytic acid (**Fig. 2.27**).

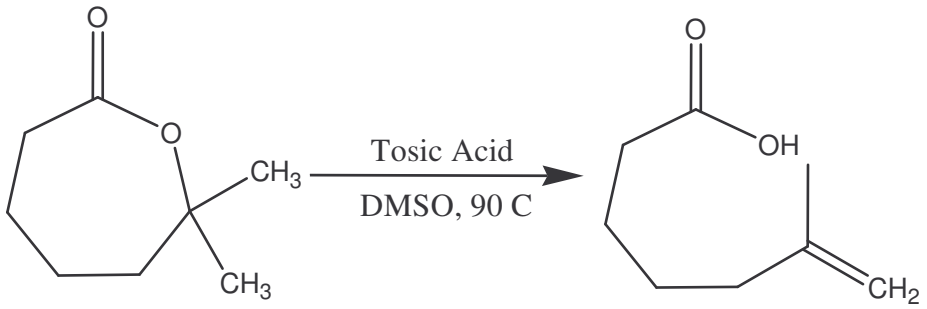

Figure 2.27: Ring-opening of caprolactone with tosic acid.

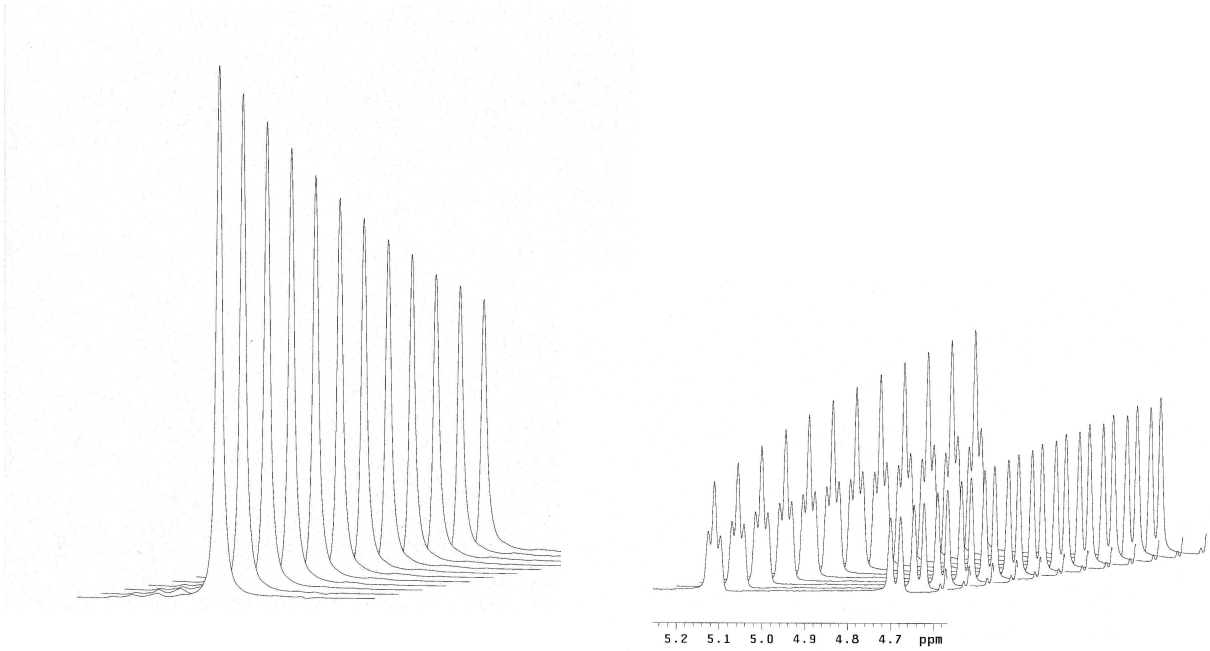

Figure 2.28: Time resolved NMR of caprolactone ring opening with tosic acid catalyst in DMSO at 90 °C. First NMR taken after 13 min, each subsequent NMR is another 114 sec of reaction time.

The lactone was heated with catalytic tosic acid in DMSO at 90 °C. Each NMR was taken 5 minutes apart (**Fig. 2.28**). The top NMR is the initial NMR taken and the bottom NMR indicates 30 minutes of reaction time. In the presence of tosic acid at 90 °C **2.5** is converted to the ring opened product in about 20 minutes. While work progressed

toward the development of mass persistent resists, another group published their work using **2.5** as a solubility switching group in a chemically amplified photoresist. [27,28,29]

The synthesis and subsequent testing of the model lactones shows that only strained ring systems will ring-open. The five and six-membered rings lack sufficient driving force to ring open. The Fittig bis-lactone was also too stable to hydrolyze in a timely enough fashion to be of use in lithographic applications. However, with two compounds that showed promise as positive tone, mass persistent resists, efforts to incorporate one of them into a polymer for lithographic evaluations were begun. Since another group had begun working on the seven-membered lactone, the development of a mass persistent resist based on the β-lactone was chosen as the next step.

Beta Lactone Monomer Synthesis

To incorporate the β-lactone into a polymer a polymerizable functional group would have to be added. The easiest way to envision this would be to replace the phenyl group of the model compound with a styrene moiety (**Fig. 2.29**).

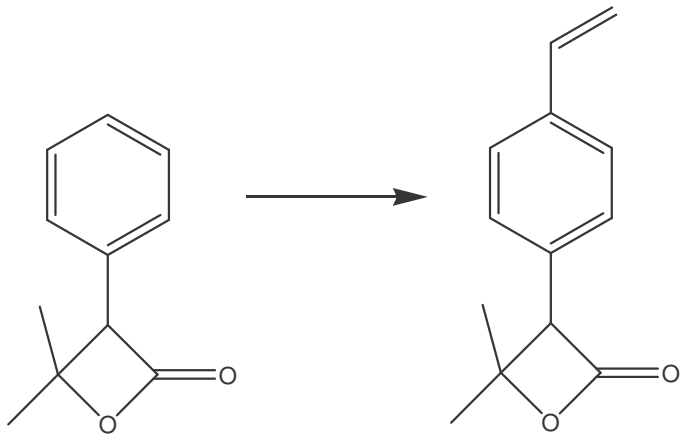

2.4
Model Compound

2.12
Styrene Derivative

Figure 2.29: Proposed monomer (2.12) version of the β-lactone (2.4) model compound.

The synthesis of **2.12** was accomplished by following the path to the model compound (**2.4**).

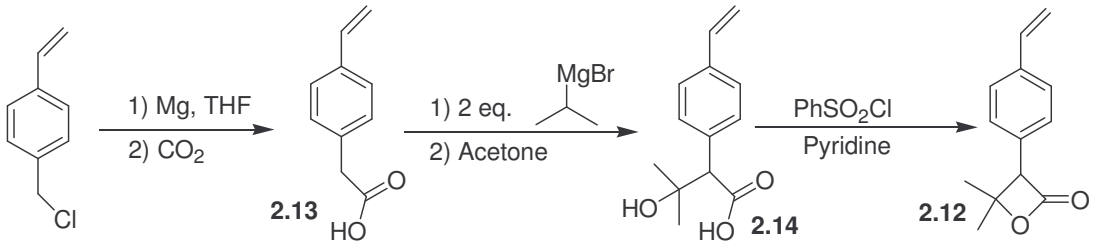

Figure 2.30: Synthesis of polymerizable beta-lactone.

The synthesis of the desired monomer **2.12** takes one more step than the synthesis of the model lactone (**2.4**). The synthesis started with 4-vinylbenzylchloride which was reacted with magnesium to form the Grignard reagent. The Grignard was reacted with carbon dioxide to produce the desired acid **2.13**. The dianion was formed and reacted with

acetone to give **2.14**, which was cyclized to the desired monomer (**2.12**) (**Fig. 2.30**). The next step was to form a functioning resist polymer from compound **2.12**.

Polymer Synthesis and Lithographic Evaluation

Styrene monomers can be polymerized by radical, anionic and cationic polymerization techniques. The most common method is radical polymerization. Radical polymerization is relatively easy compared to anionic or cationic polymerizations as both anionic and cationic typically require scrupulously dry environments. Cationic and anionic polymerization would also not likely be compatible with the very reactive β-lactone functional group.

One of the most common radical initiators used in the polymerization of styrenes is azoisobutyronitrile (AIBN). The first polymer made with compound **2.12** was the homopolymer (**2.15**) (**Fig. 2.31**).

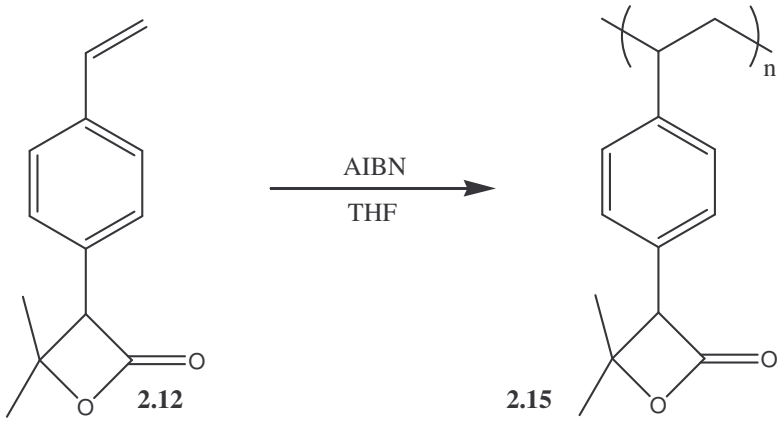

2.12 **2.15**

Figure 2.31: Radical polymerization of 2.12 to form homopolymer 2.13.

To test the lithographic capabilities of **2.15**, the polymer had to formulated to produce a photoresist. A basic photoresist formulation consists of polymer resin, photoacid generator (PAG) and a casting solvent. The typical casting solvent used is propylene glycol methyl ether acetate (PGMEA). An ideal casting solvent is one that readily solubilizes polymers and PAGs, possesses a moderately high boiling point (PGMEA bp = 145 °C) to allow controlled evaporation during spin coating and is non-toxic. Highly developed photoresist formulations include base additives, which limit diffusion of the photo generated acid into the unexposed regions. However, for simple proof of concept imaging experiments such additives were not needed.

The β-lactone polymer (**2.15**) was dissolved in PGMEA to give a 15% w/w solution of polymer in solvent and 3% by weight PAG (triphenylphosphonium nonaflate) was added. The photoresist solution was spin coated onto a silicon wafer and irradiated with 248 nm light. Following post exposure baking at 100 °C for 90 seconds and development in standard tetramethyl ammonium hydroxide (TMAH) the polymer failed to fully dissolve (**Fig. 2.32**).

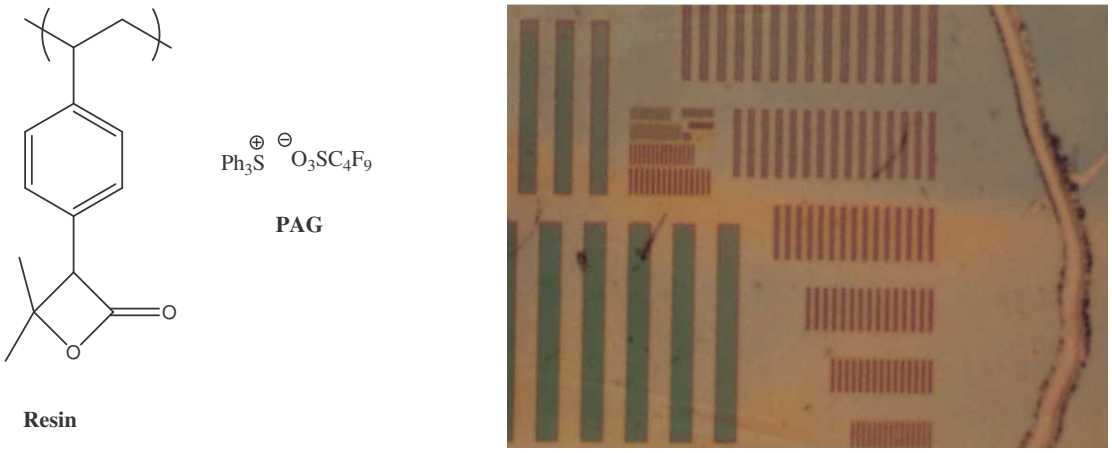

igure 2.32: Formulation of polymer 2.15 and resulting contact image.

The picture shown in **Fig. 2.32** indicates that the photoresist did develop slightly, but not all the way down to the silicon surface. The scratch on the right side of the image indicates that photoresist remains in the exposed regions, which means that the resist suffers from poor dissolution properties.

Copolymer Synthesis and Lithographic Evaluation

To improve the dissolution properties of the resin a base soluble comonomer was added to produce a copolymer. Most commercial resists are only partially protected. An example is the common *t*-boc protected poly-(*p*-hydroxystyrene) used commercially for 248 nm applications, which is not 100% *t*-boc protected.[30]

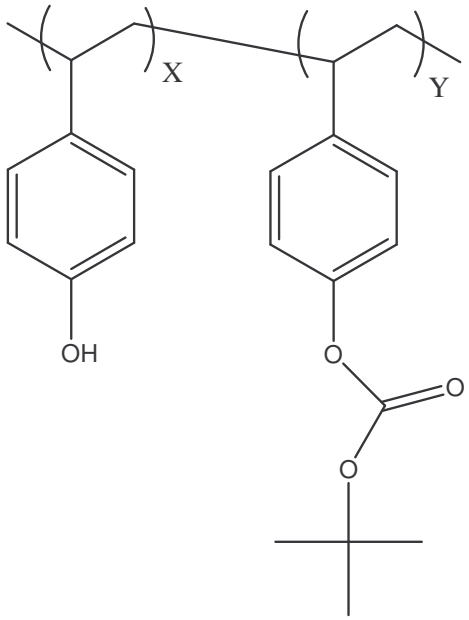

Figure 2.33: Typical 248nm resist in partially protected PHOST.

The unprotected phenol serves to improve the imaging performance. The free hydroxyl group improves adhesion to the substrate and, more importantly, is hydrophilic. The increased hydrophilicity of the polymer increases the wetting of the polymer with the aqueous developer. This allows for more interaction of the polymer with the aqueous developer and improves its dissolution properties.

The ideal copolymer for successful imaging of a photoresist based on the beta-lactone **2.12** would be a copolymer of *p*-hydroxystyrene and **2.12** (**Fig. 2.34**).

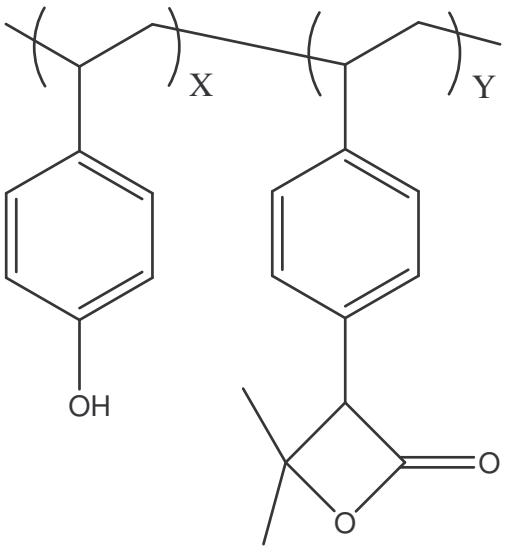

Figure 2.34: Ideal copolymer to improve imaging performance of β-lactone based photoresist.

The homopolymerization of *p*-hydroxystyrene has been reported, however it does not generate very good polymer and the monomer is very unstable.[31] The industrial method for preparing PHOST utilizes the 4-acetoxystyrene monomer (**Fig. 2.35**).

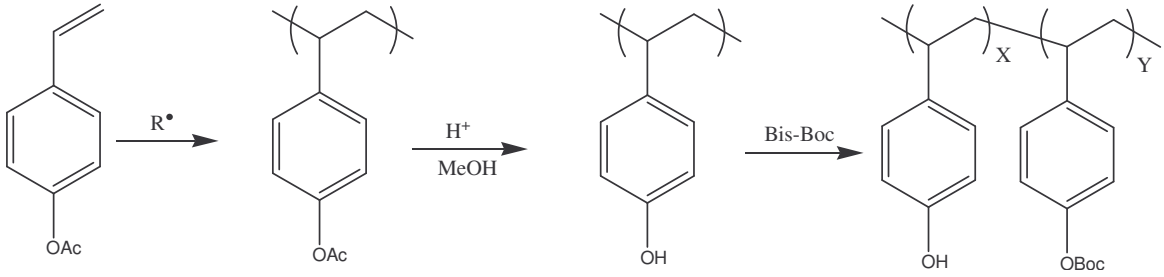

Figure 2.35: Typical industrial synthesis of PHOST.

First, the acetoxystyrene monomer is polymerized to form acetoxy-protected PHOST. The acetoxy is then hydrolyzed off to produce high quality PHOST. The PHOST is then *t*-boc protected to the desired copolymer ratio. Unfortunately, this synthetic route to a copolymer of hydroxystyrene and β-lactonestyrene (**2.12**) is not feasible. Selective hydrolysis of the acetoxy, versus the β-lactone, is not possible. To achieve the desired polymer for imaging applications, two different approaches can be imagined: different protecting groups could be employed, or a different comonomer could be used in place of the hydroxystyrene monomer, one that could be used to produce an ideal copolymer with the β-lactonestyrene (**2.12**).

Use of Protecting Groups for Ideal Copolymer Synthesis

Two different protecting groups for hydroxystyrene were investigated. The first was a silicon protecting group. Silicon protecting groups are widely used in organic synthesis, and are easily removed with acid or a fluoride source. Acid deprotection is not advantageous in this case due to the likelihood of the acid reacting with the β-lactonestyrene. However, removal of silicon protecting groups with a mild fluoride reagent looked promising.

t-Butyldimethylsilane as a Protecting Group for *p*-Hydroxystyrene Monomer

The use of *t*-butyldimethylsilylchloride as protecting group for PHOST has been previously reported.[32,33,34] The synthesis of the TBMDS protect hydroxystyrene was completed in two steps (**Fig. 2.36**).

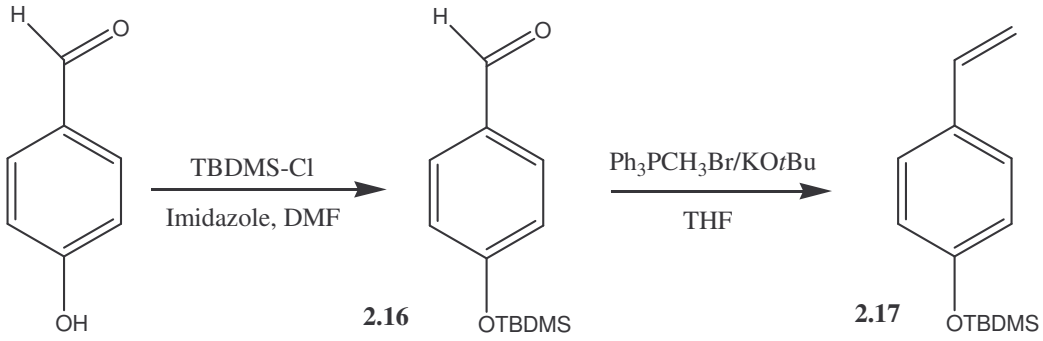

Figure 2.36: Synthesis of TBDMS protected *p*-hydroxystyrene.

Commercially available *p*-hydroxybenzaldehyde was protected with TBDMS-Cl and imidazole in THF to produce 4-*t*-butyldimethylsiloxybenzaldehyde (**2.16**). A Wittig reaction with triphenylmethylphosphonium bromide and **2.16** produced the desired 4-*t*-butyldimethylsiloxystyrene (**2.17**).

The homopolymer of **2.17** was made via radical polymerization (**Fig. 2.37**), using AIBN as the initiator, to produce TBDMS-protected PHOST (**2.18**).

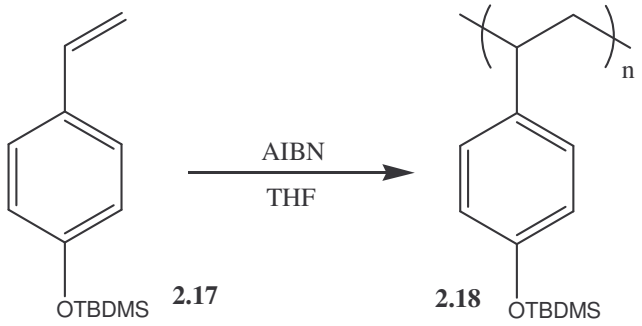

Figure 2.37: Polymerization of TBMDS protected hydroxystyrene to produce TBDMS-protected PHOST.

A common reagent used to deprotect TBDMS groups is tetrabutylammonium fluoride (TBAF). When polymer **2.18** was treated with TBAF the TBDMS protecting group was cleanly removed from the polymer as monitored by proton NMR. To test the compatibility of TBAF with the β-lactone functional group, a sample of the β-lactone model compound was treated with TBAF. The solution was monitored by thin layer chromatography which showed rapid decomposition of the model β-lactone. Given such rapid decomposition of the beta-lactone model compound, it was obvious that TBAF would not be a suitable reagent for the deprotection of the TBDMS group.

Fluoride sources other than TBAF can be used to remove a TBDMS group. One example is KF on basic alumina and sonication to quickly removed TBDMS groups from phenols.[35] This method was tested on the β-lactone model compound and no decomposition of the lactone was observed by thin layer chromatography. However, when the TMBDMS polymer was treated with KF/Al_2O_3 it failed to cleanly deprotect the TBDMS group (**Fig. 2.38**).

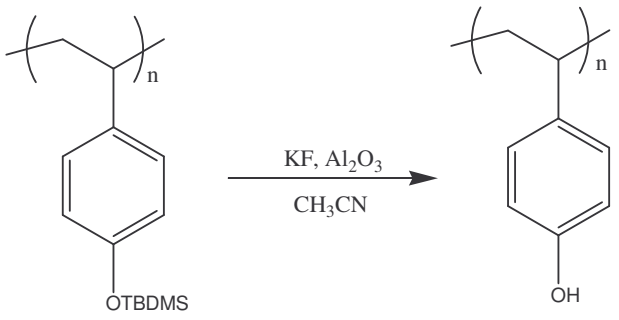

Figure 2.38: KF on alumina failed to quantitatively remove the TBDMS protecting group.

The difficulty in finding a reagent that would successfully remove the TBDMS protecting group without decomposing the β-lactone prompted the search for a different protecting group.

Benzyl Protection of *p*-Hydroxystyrene Monomer

The benzyl group is commonly used as a protecting group for an alcohol. Benzyl groups can be removed under relatively mild conditions by hydrogenation with pd on carbon.[36,37] 4-Benzyloxystyrene (**2.20**) was synthesized (**Fig. 2.39**) in a manner similar to that used for compound **2.18**.

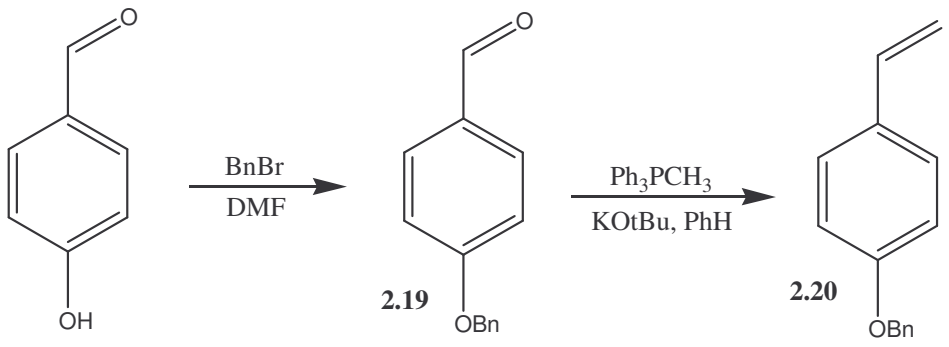

Figure 2.39: Synthesis of 4-benzyloxystyrene.

Commercially available 4-hydroxybenzaldehyde was reacted with benzyl bromide to give 4-benzyloxybenzaldehyde (**2.19**). The aldehyde was reacted with the ylide of triphenylmethylphosphonium bromide to give the corresponding styrene (**2.20**). Radical copolymerization of **2.12** and **2.20** was carried out using AIBN as the radical initiator (**Fig. 2.40**).

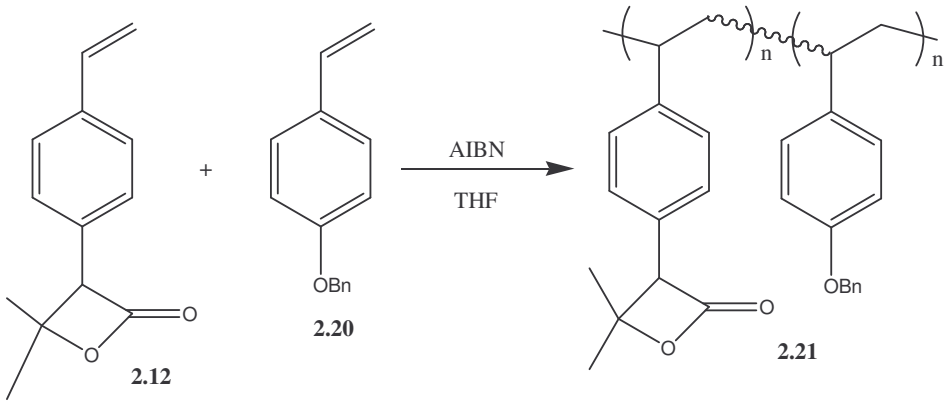

Figure 2.40: Radical copolymerization of 4-benzyloxystyrene (2.20) and β-lactone (2.12) with AIBN.

Before the benzyl protected PHOST (**2.21**) was synthesized the beta-lactone (**2.4**) model compound was subjected to hydrogenation conditions of 70 psi hydrogen at 50 °C for 4

days. Thin layer chromatography indicated the β-lactone suffered no decomposition. However, subjecting the benzylated polymer (**2.21**) to 65 psi of H_2 at 50 °C for 3 days resulted in no observable deprotection by proton NMR. Due to the lack of success in finding a suitable protecting group, the protecting group strategy was abandoned in favor of incorporation of a different comonomer.

Incorporation of Base Soluble Comonomer

Producing a polymer that mimics a common 248 nm polymer (partially *t*-boc protected PHOST) proved difficult through the protection and deprotection schemes, and efforts were turned to a monomer that did not need protection schemes. A monomer that had seen early use in development of 157 nm resists was a 1,1,1-3,3,3-hexafluoropropan-2-ol substituted styrene (HFASTY) monomer (**Fig. 2.41**).[38,39,40,41] HFASTY was used early in 157nm resist for two reasons. The hexafluoroalcohol group has roughly the same acidity (pK_a =11) as that of phenol (pK_a=10), and the hexafluoroalcohol reduces the absorbance of the monomer at 157 nm.

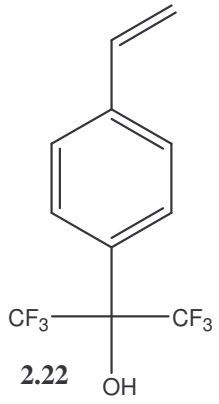

2.22

Figure 2.41: 1,1,1,3,3,3-Hexafluoro-2-(4-vinylphenyl)-propan-2-ol (HFASTY) monomer used at 157 nm lithography.

HFASTY was synthesized by two methods, via a Grignard reaction and through lithium halogen exchange (**Fig. 2.42**).

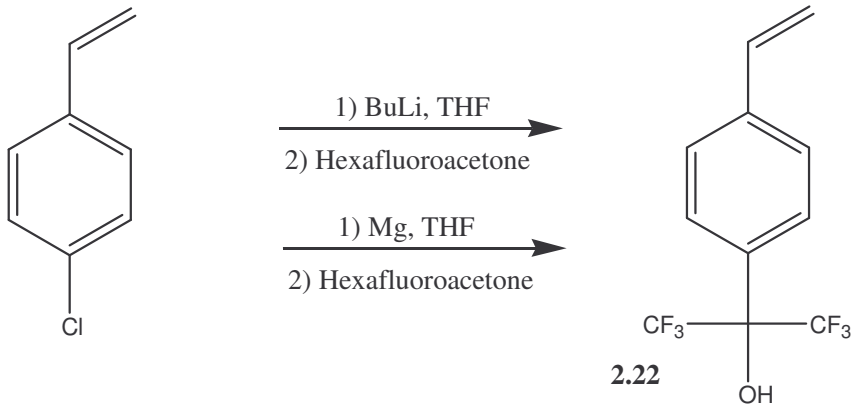

Figure 2.42: Synthesis of HFASTY (2.22) via Grignard and hexafluoroacetone.

Synthesis of HFASTY via the Grignard of the corresponding *p*-halostyrene[42,43] resulted in a higher yield and more purer product. The only benefit of the lithium halogen exchange method is it results in less polymerization of the monomer since the reaction done at cold temperatures (-78 °C).

Several copolymers of HFASTY and β-lactone styrene were synthesized via free radical polymerization (**Fig. 2.43**).

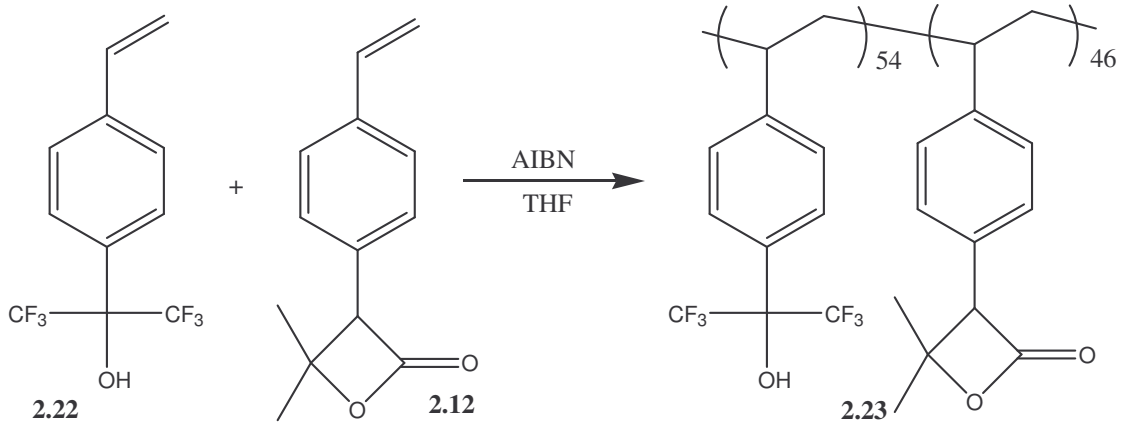

Figure 2.43: Copolymerization of HFASTY (2.22) with beta-lactone styrene (2.12).

A co-polymer ratio of 54% HFASTY and 46% β-lactone styrene proved to be a ratio that produced the best imaging results.

Copolymer Imaging

Imaging of copolymer **2.23** was done at International SEMATECH with the assistance of Jordan Owens. Exposures were done at 248 nm and standard tetramethylammonium hydroxide was used as the developer.

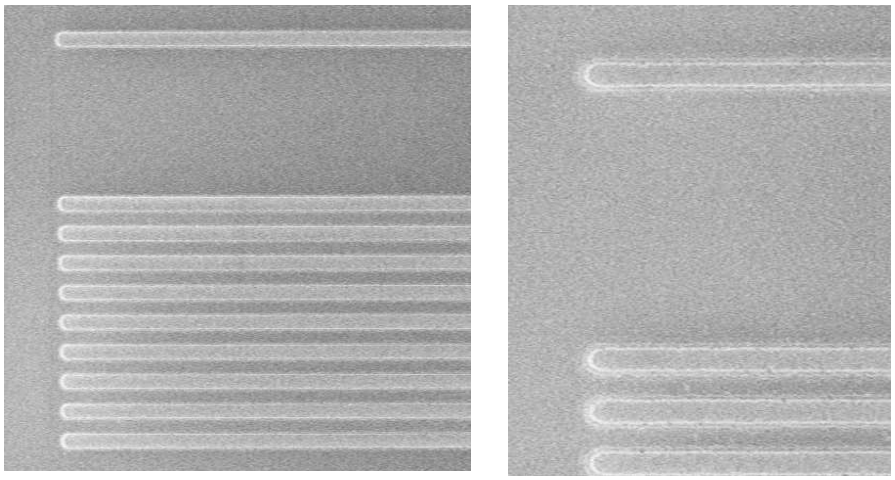

Figure 2.44: 500 and 300 nm nested lines of co-polymer 2.23. PAB 90 °C for 90 secs, PEB 90 °C for 90 secs, 6% TPS-NF, 104 mJ/cm^2.

Imaging experiments resolved dense lines down to 300nm (**Fig. 2.44**). Commercial 248 nm resists print approximately 130nm lines, but these imaging experiments provided a good proof of concept for developing non-outgassing photoresists.

As mentioned earlier, outgassing is a very important issue for 157 nm lithography. Even though theses experiments were carried out using polystyrene polymer based photoresists and were imaged using 248 nm exposures, it still proves that a viable non-outgassing resist can be developed.

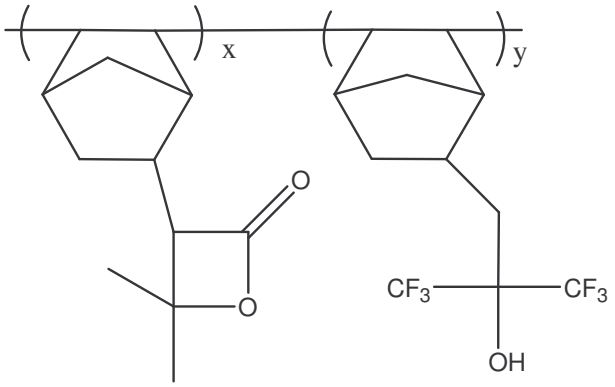

Figure 2.45: Proposed 157 nm photoresist incorporating the mass persistent β-lactone solubility switch.

Incorporation of the beta-lactone functionality onto a norbornene ring and used in a co-polymer with NBHFA could potentially provide as a mass persistent 157 nm photoresist (**Fig. 2.45**).

The goals of the project were to design a new solubility switching group that would function as a non-outgassing resist. If industrial interest in such a photoresist is sufficient, resist suppliers could produce a material for the desired application. Using the chemical knowledge gained in the development of a mass persistent resist (**2.23**) as a guide to more advanced resist systems.

---

[10] Kunz, R. R.; Downs, D. K. *J. Vac. Sci. Technol. B*, **1999**, *17*, 3330-3334.

[11] Houlihan, F. M.; Rushkin, I. L.; Hutton, R. S.; Gabor, A. H.; Medina, A. N.; Malik, S.; Neiser, M.; Kunz, R. R.; Downs, D. K. *Proc. SPIE* **1999**, *3678,* 264-274.

[12] Hein, S.; Angwood, S.; Ashworth, D.; Basset, S.; Bloomstein, T.; Dean, K.; Kunz, R. R.; Miller, D.; Patel, S.; Rich, G. *Proc. SPIE* **2001**, *4345,* 439-447.

[13] Dektar, J. L.; Hacker, N. P. *J. Am. Chem. Soc.*, **1990**, *112*, 6004-6015.

[14] Kane, V. V.; Doyle, D. L.; Ostrowski, P. C. *Tetrahedron Letters*, **1980**, *21*, 2643-2646.

[15] Adam, W.; Baeza, J.; Liu, J. C. *J. Amer. Chem. Soc.,* **94**, 2000 (1972)

[16] Weston, A. W.; DeNet, R. W. *J. Amer. Chem. Soc.,* **73**, 4221 (1951)

[17] Chung, K., Takata, T., Endo, T. *Macromolecules*, **1997**, *30*, 2532-2538.

[18] Strunz, G. M.; Lal, G. S. *Can. J. Chem.* **1982**, *60*, 2528-2530.

[19] Lightstone, F. C.; Bruice, T. C. *Bioorganic Chemistry*, **1998**, *26*, 193-199.

[20] Illumanti, G.; Mandolini, L. *Acc. Chem. Res.* **1981**, *14*, 95-102.

[21] Chang, S. J.; McNally, D.; Shary-Tehrany, S.; Hickey, S. M. J.; Boyd, R. H. *J. Amer. Chem. Soc.* **1970**, *92*, 3109-3118.

[22] Schleyer, P. V. R.; Williams, J. E.; Blanchard, K. R. *J. Amer. Chem. Soc.* **1970**, *92*, 2377-2386.

[23] Liu, X.; Wang, M.; Li, Z.; Li, F. *Macromol. Chem. Phys.* **1999**, *200*, 468-473.

[24] Strunz, G. M., Lal, G. L. *Can. J. Chem.* **1982**, *60*, 2528-2530.

[25] Duda, A., Penczek, S. *Macromolecules*, **1995**, *28*, 5981-5992.

[26] Odian G., . *Principles of polymer Chemistry,* John Wiley and Sons: USA, 1991.

[27] Pinnow, M. J., *et. al., Polymeric Materials Science and Engineering*. **2002**, *87*, 403-404

[28] Pinnow, M. J., *et. al., Design and Synthesis of Mass Persistent Photoresists.* Poster Presentation. **2nd International Symposium on 157nm Lithography**, Dana Point, CA, May 16, 2001.)

[29] Kim, J. B. and Lee, J. J. *Polymer,* **43**, 2002,1963-1967

[30] Ito, H. *IBM J. Res & Dev.* **2001**, *45*, 683-695.

[31] Kato, M. *J. Polym. Sci. Part A-1*. **1969**, *7*, 2415-2427.

[32] Do, Y.; Kim, Y. *Macromol. Rapid Commun.* **2000**, *21*, 1148-1155.

[33] Kim, K. H.; Jo, W. H.; Kwak, S.; Kim, K. U.; Hwang, S. S.; Kim, J. *Macromolecules*, **1999**, *32*, 8703-8710.

[34] Ito, H., Knebelkamp, A., Lundmark, S. B., Nguyen, C. V., Hinsberg, W. D. *J. Polym. Sci. Part A*, **2000**, *38*, 2415-2427.

[35] Schmittling, E. A., *Et. Al.*, *Tetrahedron Lett.* **1991**, 7207-7210.

[36] Venuti, M. C.; Loe, B. E.; Jones, G. H.; Young, J. M. *J. Med. Chem.* **1988**, *31*, 2132-2136.

[37] Greene, T. W.; Wuts, P. G. M. *Protecting Groups in Organic Synthesis 2nd Ed.* John Wiley and Sons: USA, 1991.

[38] Ito, H.; Wallraff, G. M.; Brock, P.; Fender, N.; Truong, H.; Breyta, G.; Miller, D. C.; Sherwood, M. H.; Allen, R. D. *Proc. SPIE-Int. Soc. Opt. Eng.* **2001**, *4345*, 273-284
.

[39] Fujigaya, T.; Sibasaki, Y.; Ando, S.; Kishimura, S.; Endo, M.; Sasago, M.; Ueda, M. *Chem. Mater.* **2003**, *15*, 1512-1517.

[40] Hall, D. S., Osborn, B., Patterson, K., Burns, S. D., Willson, C. G.; *Proc. SPIE-Int. Soc. Opt. Eng.* **2001**, *4345*, 1066-1072.

[41] Fedynyshyn, T. H.; Mowers, W. A.; Kunz, R. R.; Sinta, R. F.; Sworin, M.; Cabral, A.; Curtin, J. *Polymeric Materials Science and Engineering*, **2002**, *87*, 398-399.

[42] Leebrick, J. R. and Ramsden, H. E. *J. Org. Chem.*, **23**, 953 (1958)

[43] Pike, R. M. *J. Polymer Sci.,* **40**, 577 (1959)

Chapter 3 - Negative Tone Mass Persistent Photoresists

During integrated circuit production, many different patterns need to be produced. A cross-section of a finished device shows two common features that need to be fabricated, vias and metal layers (**Fig. 3.1**).[44]

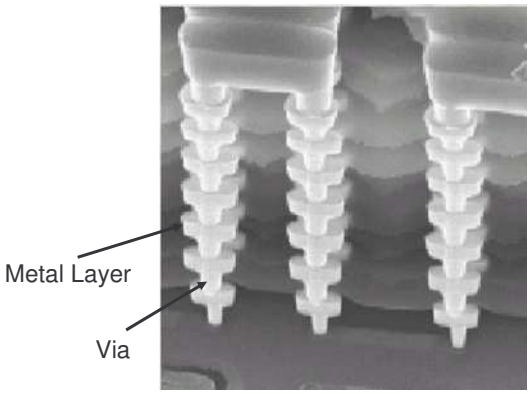

Figure 3.1: Cross section of a chip showing metal layers and vias inside a modern computer chip.

Metal layers are essentially the interconnecting wires used in the construction of an integrated circuit. Vias are metal pillars that connect the different metal layer stacks to each other and, subsequently, to the gate's sources and drains of the transistor. To print a variety of features, vias and lines for example, different photomasks can be used. The photomask for vias is shown in **Fig. 3.2**.

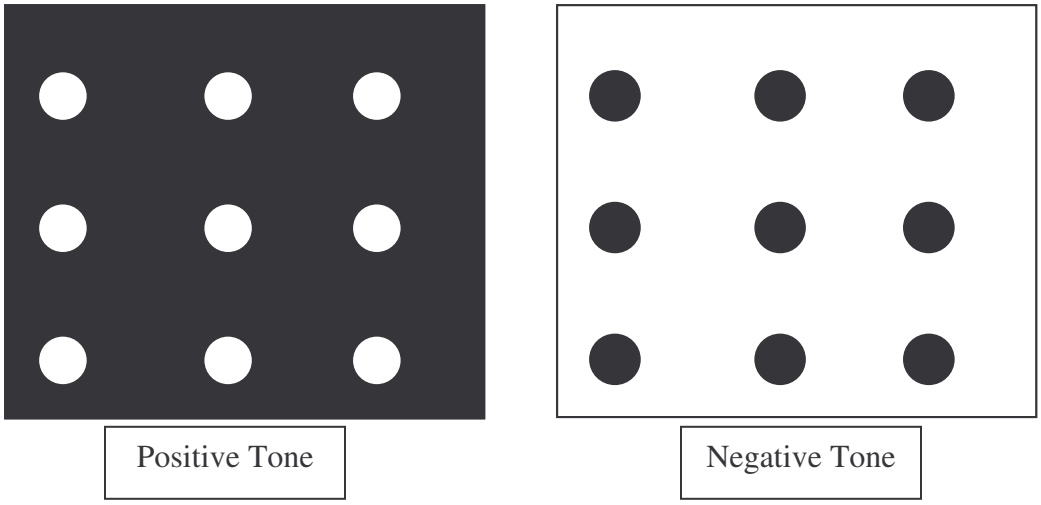

Figure 3.2: Diagram of positive and negative tone photomasks used to fabricate vias. Black represents chrome and white represents glass.

The fabrication of vias is best accomplished using a positive tone resist system. Looking at the representative positive and negative photomasks (**Fig. 3.2**) that would be used to produce vias it is easy to understand why positive tone is preferred. The larger the area of the wafer that is exposed to light, the more likely a particle falling on the mask or wafer during imaging will generate a defect. In the case of the negative tone mask, used for the fabrication of vias, the majority of photomask is transparent, and therefore has a higher probability of a defect occurring. Whereas the positive tone scheme only the small vias are exposed to light and most particles fall in an area that is not to be exposed anyway.

For the fabrication of lines, such as those used in metal layers, the density of the pattern often dictates the resist scheme used. When printing dense lines the geometry of

the feature dictates the tone used.[45] Positive tone resists are best for narrow resist lines, whereas narrow trenches are best printed using a negative tone resist. The printing of isolated features is potentially the best use for a negative tone system.

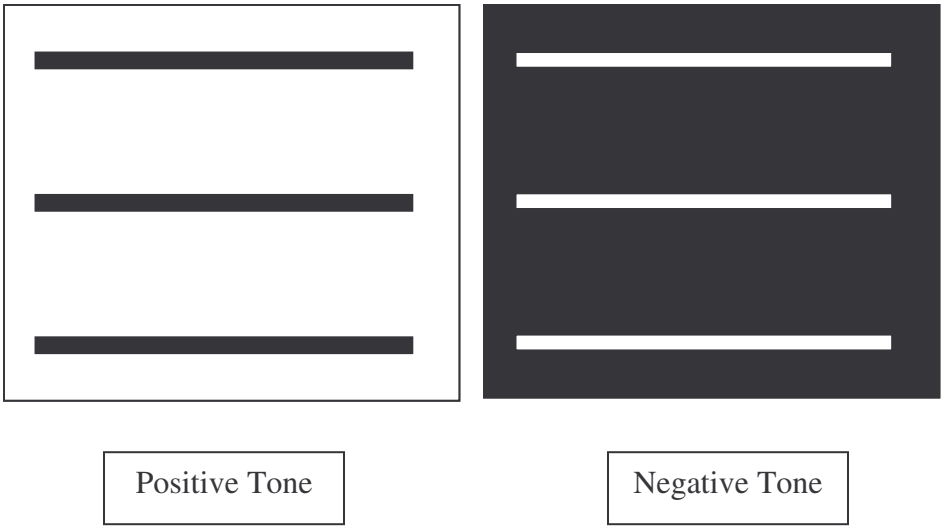

Figure 3.3: Diagram of positive and negative tone photomasks used to fabricate metal layers. Black represents chrome and white represents glass.

If an isolated line is desired, the majority of the photomask would be exposed with light in the case of the positive tone resist (**Fig. 3.3**). However, in the case of the negative tone resist only the desired lines are exposed. Again by only having a small part of the mask transmit light, the chance of particulates or other defects on the mask causing a defect in the resulting image is reduced.

Negative Tone Photoresist Solubility Switches

A negative tone photoresist, when exposed to acid and baked becomes less soluble in developer. Traditionally there have been two ways to accomplish this solubility switch. One is through cross-linking the polymer.

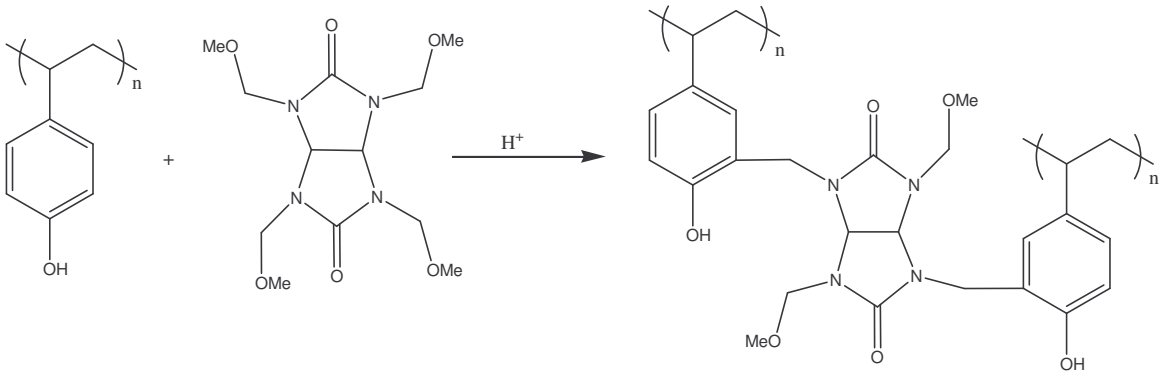

Figure 3.4: Crosslinking method for negative tone solubility switch.

One common cross-linking method involves the use of tetramethoxymethyl glycoluril which in the presence of acid will cross-link phenol resins (**Fig. 3.4**) through electrophilic aromatic substitution.[46] The acid catalyzed cross-linking of the polymer results in a dramatic increase in molecular weight, rendering the polymer insoluble in the developer. While cross-linking does result in a solubility change, the cross-linked polymer feature often swells, which is detrimental to the imaging performance of the resist.

Another common negative tone solubility switch is the use of a polarity in the polymer.[47,48] One example of such a polarity switch is the acid catalyzed formation of base insoluble lactones from hydroxy acids (**Fig. 3.5**).[49]

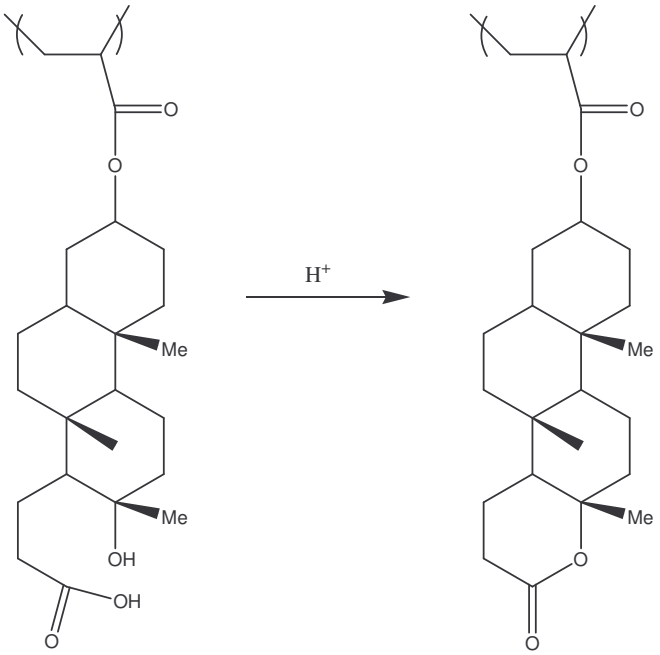

Figure 3.5: Polarity switch for a negative tone resist via lactone formation from a hydroxy acid.

The main downfall of the hydroxy acid system is the inherit resist instability. Lactonization occurs so readily that the photoresist often undergoes this solubility switch even when stored. Any potentially commercial photoresist must have sufficient shelf life to insure consistent imaging performance over time.

Synthesis of a Negative Tone Resist System via Lactonization of γ,δ- and δ,ε-Unsaturated Carboxylic Acids

The synthesis of a negative tone mass persistent resist originated from the experimental results described in Chapter 2. During the screening of model compounds it was determined that five and six member lactones would not ring open when treated with acid (**Fig. 3.6**).

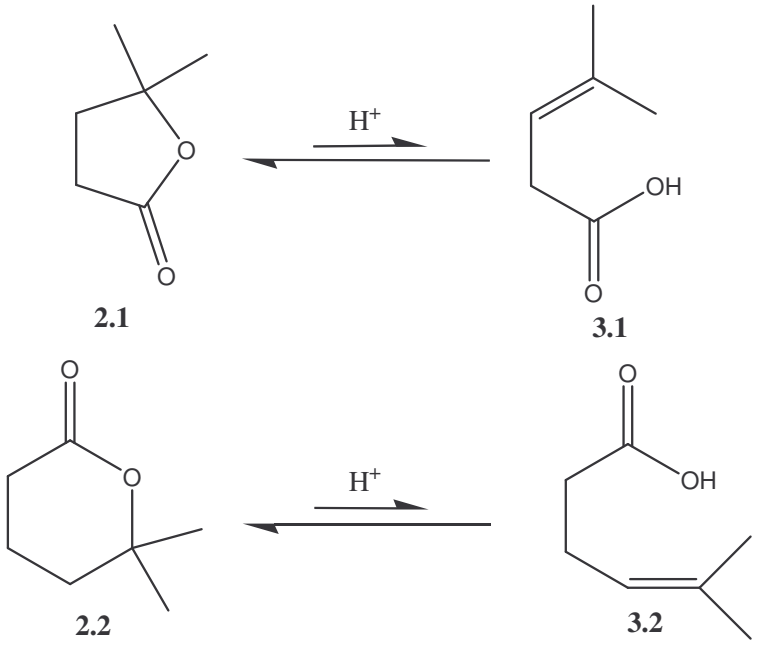

Figure 3.6: Ring opening of five (2.1) and six (2.2) member lactones failed. The equilibrium lies strongly with the ring closed lactone.

It was reasoned that if the base soluble ring opened lactone (**3.1**, **3.2**) was treated with acid it would ring close to the base insoluble lactone (**2.1**, **2.2**). To determine whether or not the desired ring closing reaction would occur, the ring opened lactones (**3.1**, **3.2**) would need to be synthesized.

Synthesis of Ring Opened Lactones

Initial literature searches for the synthesis of **3.1** and **3.2** turned up very little precedent. The synthesis of **3.1** has been reported in the process of studying the Grob fragmentation.[50,51] The synthesis of **3.1** is fairly straight forward and is adopted from the previously reported synthesis. Starting from commercially available 2-oxo-

cyclopentanecarboxylic acid ethyl ester (**3.3**) deprotonation with sodium hydride followed by methylation with methyl iodide provided **3.4** (**Fig. 3.7**). Protection of the carbonyl with ethylene glycol gave the acetal **3.5** (**Fig. 3.7**).

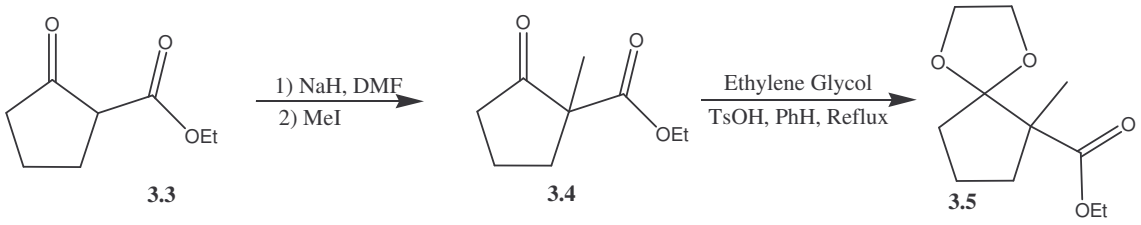

Figure 3.7: Synthesis of six membered ring opened lactone (3.2).

Reduction of the ester group with lithium aluminum hydride (LAH) produced the alcohol (**3.7**) (**Fig. 3.8**), and hydrolysis of the acetal with aqueous acid furnished **3.8** (**Fig. 3.8**).

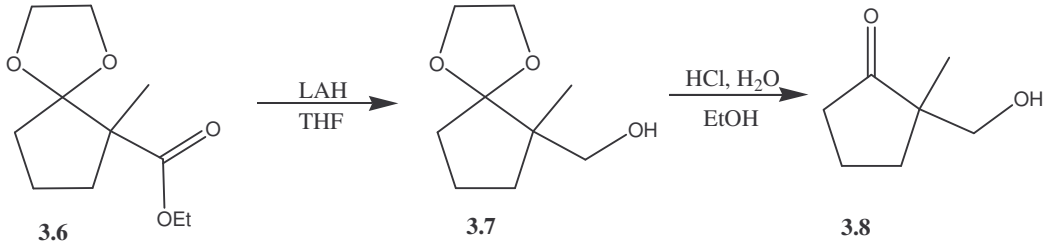

Figure 3.8: Synthesis of six member open lactone (3.2) continued.

Tosylation of the alcohol (**Fig. 3.9**) gave the precursor (**3.9**) to the desired ring opened lactone (**3.2**).

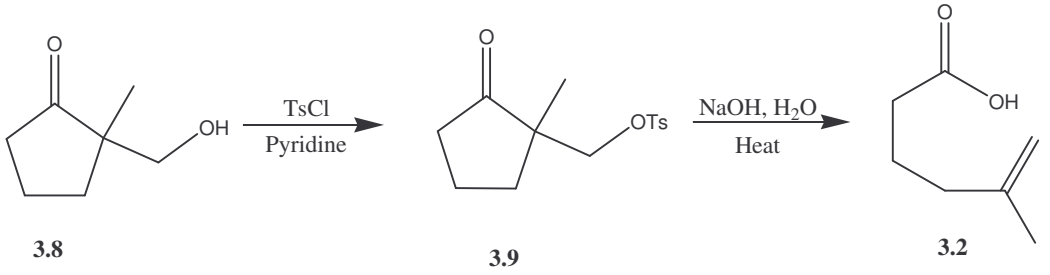

3.8 **3.9** **3.2**

Figure 3.9: Synthesis of six member open lactone (3.2) continued.

Heating **3.9** in aqueous base gave the desired product **3.2** via the Grob fragmentation (**Fig. 3.9**). Subsequent literature searching found a reduction procedure that removes the need for the acetal protecting there by reducing the length of the synthesis by two steps.[52]

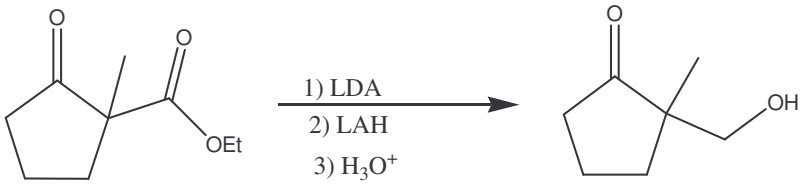

3.4 **3.8**

Figure 3.10: Selective reduction of the ester via enolate formation as a protecting group.

Treatment of **3.4** with one equivalent of lithium diisoproplyl amine (LDA) formed the enolate of the carbonyl, addition of LAH reduced the ester and acidic work yielded the desired β-hydroxy ketone (**3.4**). This allowed for a quicker synthesis of the desired ring opened product.

Ring Closing NMR Experiment

In a manner similar to the testing carried out in the screening of the ring opening lactones discussed in Chapter 2, **3.2** was treated with acid to determine whether it ring closes to form the corresponding lactone (**2.2**). Upon treatment of **3.2** with triflic acid it ring closed to form the base insoluble lactone (**2.2**) (**Fig. 3.11**).

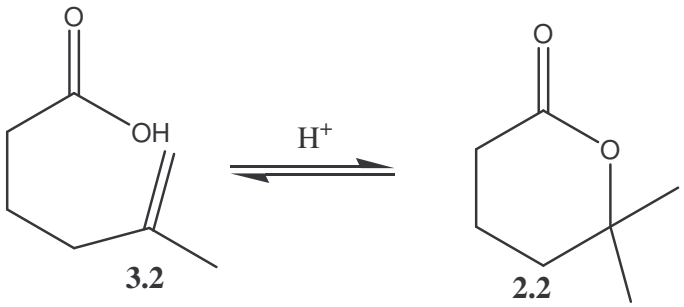

Figure 3.11: Acid catalyzed ring closing of 3.2 to the corresponding six member lactone (2.2).

While the successful ring closure was an encouraging result there was a problem with the Grob fragmentation pathway. The final product **3.2** was always accompanied by an impurity that was never fully removed from the desired material through traditional purification techniques. This impurity proved problematic as producing monomers and polymers from this material also incorporated the impurity into the polymers. If a negative tone polymer was to be based on the ring closure of **3.2** or **3.1** a new synthesis was needed.

Improved Synthesis of Ring Opened Lactones

It is conceivable the desired olefin could be installed in **3.1** and **3.2** via a Wittig reaction with the corresponding γ- or δ-keto acid.

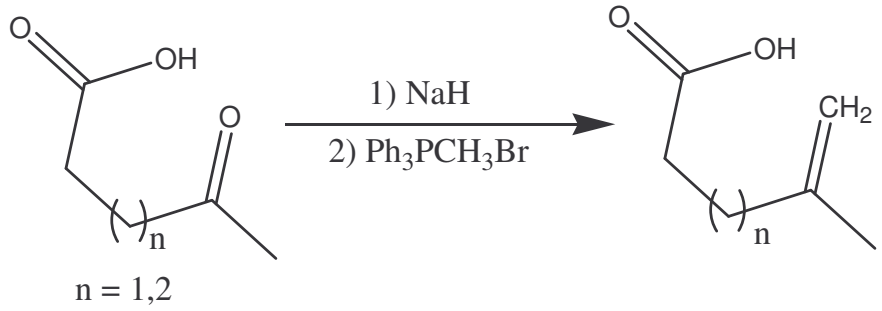

Figure 3.12: Synthesis of ring opened lactones via Wittig reaction.

A Wittig reaction was carried out on the keto acid precursor to produce the desired ring opened lactones (**3.1**, **3.2**) (**Fig. 3.12**). Deprotonation of the carboxylic acid with sodium hydride, followed by addition of the corresponding ylide derived from methyltriphenylphosphonium bromide, yielded the desired compounds. Purification by distillation produced very pure product for subsequent ring closing studies.

Acid Catalyzed Ring Closing to From Lactones

Acid catalyzed ring closing of **3.1** and **3.2** was tested with triflic acid in deuterated chloroform. Both **3.1** and **3.2** reacted quickly (<10 min) at room temperature with 5% triflic acid to form the ring closed lactones (**2.1**, **2.2**). Time resolved NMR data was obtained using 5% methane sulfonic acid in deuterated DMSO. The initial NMR was

taken after 4 minutes of reaction time and each additional spectra was taken after a 114 second delay (**Fig. 3.13 and 3.14**).

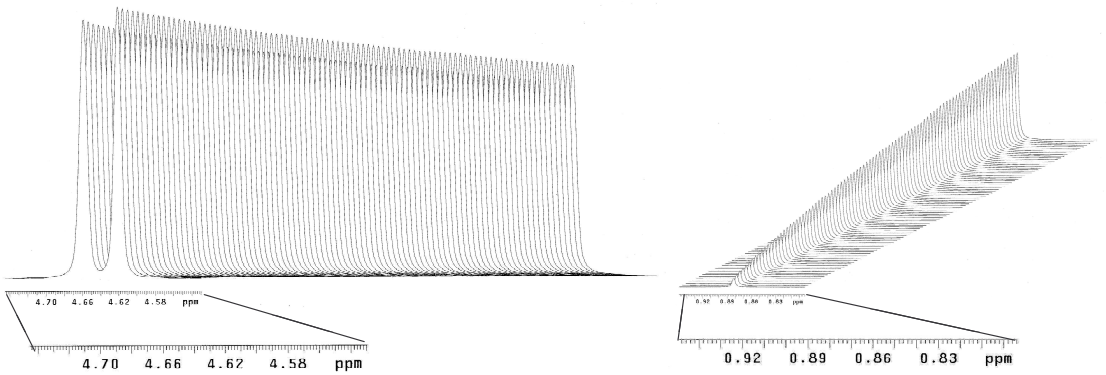

Figure 3.13: Ring closing NMR experiment of 3.1 with triflic acid. The olefin peaks (~4.6ppm) disappear while the gem-dimethyl peaks (~0.9ppm) grow in.

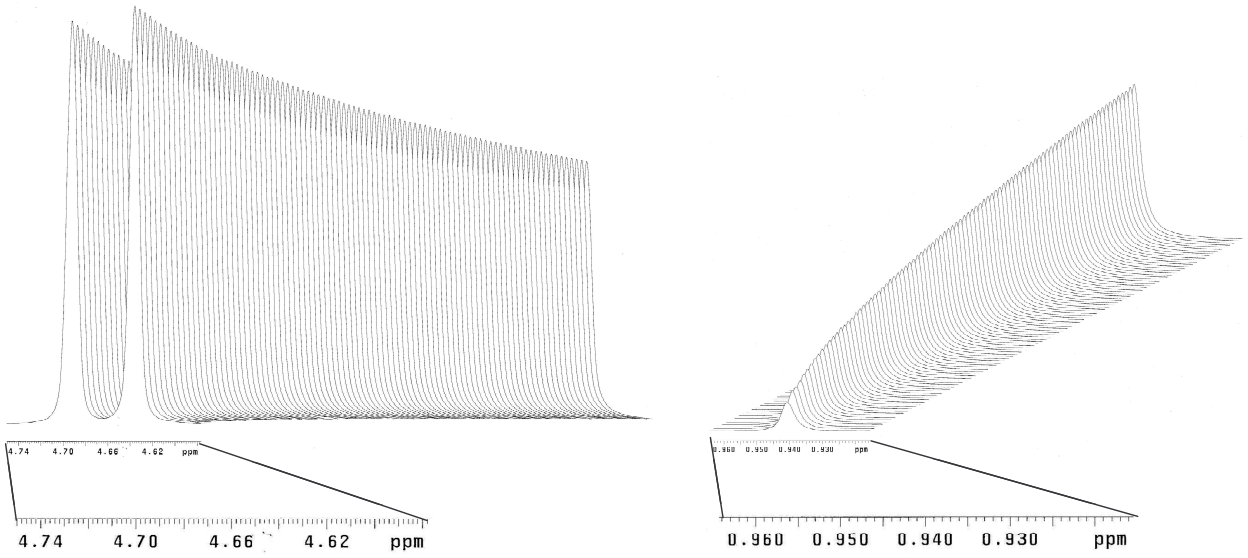

Figure 3.14: Ring closing NMR experiment of 3.2 with triflic acid. The olefin peaks (~4.6ppm) disappear while the gem-dimethyl peaks (~0.9ppm) grow in.

The successful ring closing of both **3.1** and **3.2** to the base insoluble lactones and the one step synthesis to obtain pure product allowed for successful synthesis of a monomer for ring opened lactone resist systems.

Negative Tone Monomer Synthesis

To make a photoresist based on this negative tone solubility switch, a monomer was required that incorporated this functional group. Synthesis of a ring opened lactone monomers (**3.1**, **3.2**) is possible with literature precedence by the alkylation of carboxylic acids on the α-carbon.[53]

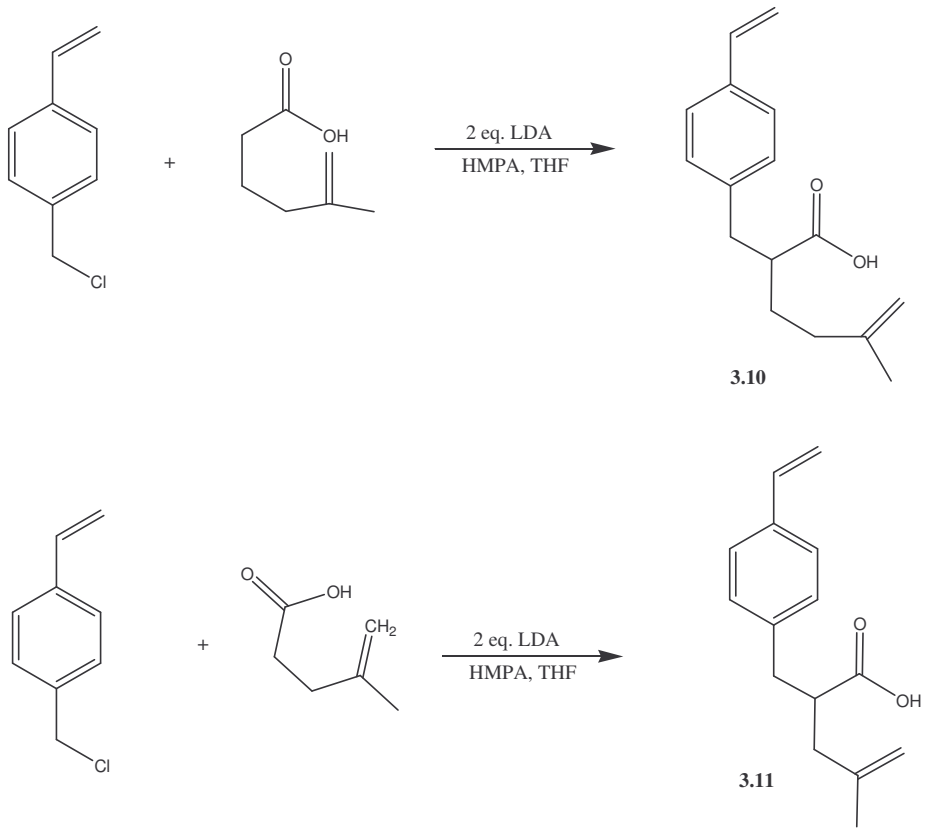

Figure 3.15: Synthesis of styrene monomers with the ring opened lactone attached.

Reaction of corresponding carboxylic acid with two equivalents of lithium diisopropyl amide forms the di-anion. Addition of 4-vinylbenzyl chloride alkylates alpha to the carbonyl, which upon quenching, results in the desired monomers (**3.10**, **3.11**) (**Fig. 3.15**).

Polymerization and Lithographic Evaluation

Radical polymerization of (**3.10**) with AIBN produced the homopolymer (**3.12**). However, imaging experiments with **3.12** never resulted in a resist that successfully printed.

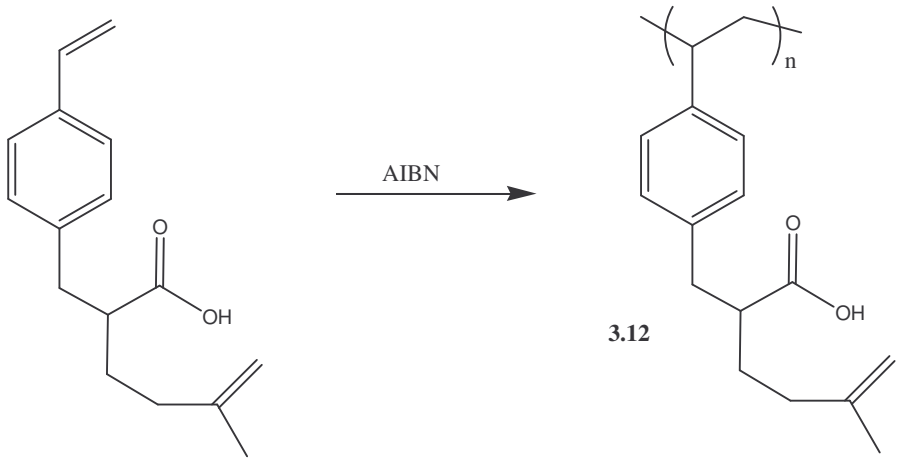

Figure 3.16: Radical polymerization of 3.10 with AIBN.

Due the increased acidity of the carboxylic acid (pK_a ~4.5) relative to a phenol (pK_a~10) the homopolymer (**3.12**) is very soluble in base. To render the homopolymer sufficiently insoluble in developer, a very high percentage of the ring opened lactones have to be closed to the base insoluble lactone. To reduce the amount of acid content in

the polymer, and subsequently the solubility in developer, a copolymer (**3.13**) of **3.10** (27%) and styrene (73%) was synthesized (**Fig. 3.17**).

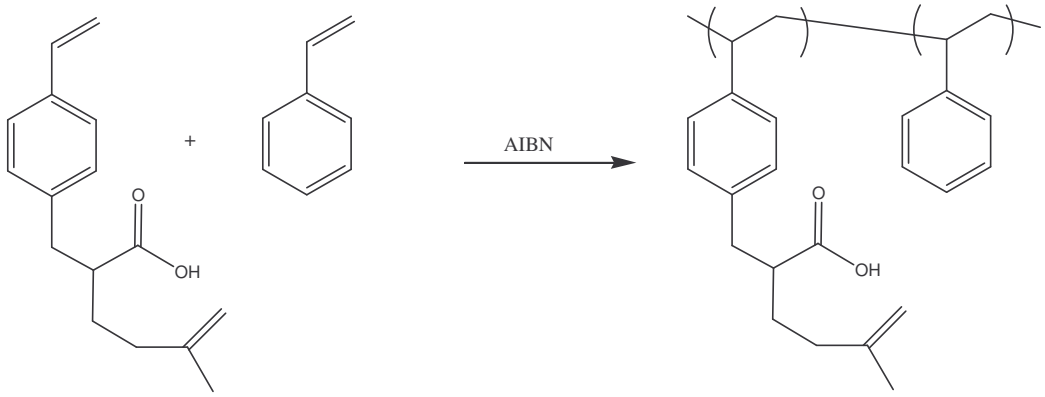

3.13

Figure 3.17: AIBN radical polymerization of 3.10 with styrene.

Imaging experiments indicated that copolymer (**3.13**) had reduced solubility in aqueous base developer and exhibit the desired solubility switch necessary for imaging. However, the incorporation of the hydrophobic styrene monomer resulted in adhesion failure from the silicon wafer during development. To improve the adhesion of the polymer a third monomer was added to the polymerization. The third monomer added was the base soluble HFASTY monomer used as the comonomer in the positive tone resist discussed in Chapter 2.

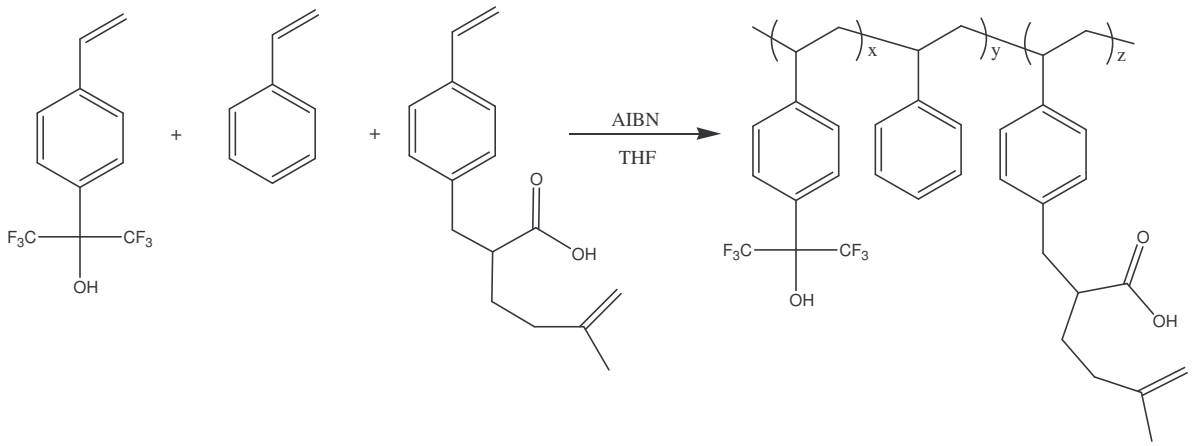

Figure 3.18: Radical polymerization of HFASTY, styrene and 3.10 to produce an imageable terpolymer.

Two different copolymers (**3.14**, **3.15**) were synthesized and through the use of fluorine NMR (internal fluorine standard), the copolymer ratios were calculated. The terpolymer ratios of **3.14** are 42% HFASTY, 31% styrene, 27% **3.10** and the terpolymer ratios of **3.15** are 16%, 73%, 11% **3.10**. Terpolymer **3.14** dissolved too fast whereas terpolymer **31.5** dissolved too slowly during initial imaging experiments. A 50/50 blend of the two polymers produced a resin (**3.16**) that had sufficient base solubility, adhesion to the silicon wafer and displayed the desired solubility switch during imaging.

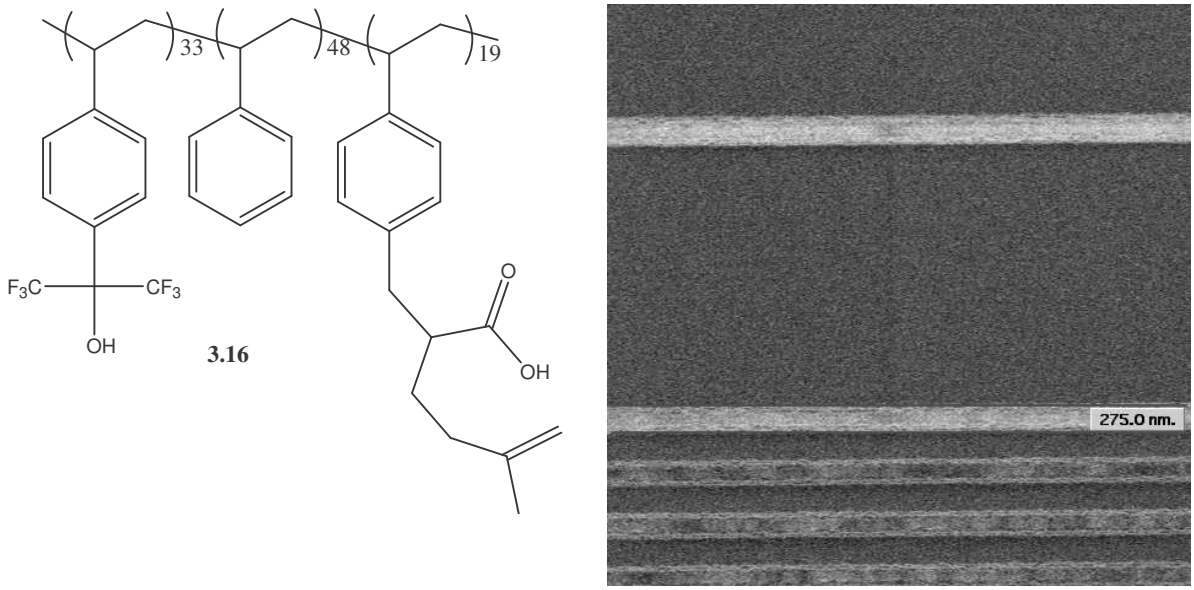

Figure 3.19: Dense 275 nm lines of terpolymer 3.16. PAB 90° C for 90 s, PEB 110° C for 90 s, 6% TPS-NF, 110 mJ/cm^2

The 50/50 blend resulted in a terpolymer ratio of 33% HFASTY, 48% styrene and 19% **3.10**. Imaging of the blend polymer formulation at 248nm exposure produced 275 nm nested lines (**Fig. 3.19**). This imaging was very encouraging since it was the first time it was printed on a quality exposure tool. Resist formulation and processes tweaking would increase the resolution capabilities of the resist platform. However, the goals of this project are purely proof of concept and not to display high resolution imaging.

While the six membered open lactone platform yielded a good proof of concept image, results from polymers made from the five membered open lactone polymer platform were disappointing. Tweaking the terpolymer ratio such that proper dissolution

and adhesion criteria are met has proved to be difficult. Obtaining the correct polymer ratio for these terpolymers is difficult, as a small change in acid content has a very large affects on the dissolution behavior of the polymers.

In conclusion, a negative tone mass persistent resist system has been demonstrated based on what was learned in the ring opening studies of five and six membered lactones. The chemistry was initially demonstrated using 248 nm exposure, but the alkylation chemistry should lend itself to incorporation of **3.1** and **3.2** into norbornane monomers for use in the design of 193 or 157nm photoresists (**Fig. 3.20**).

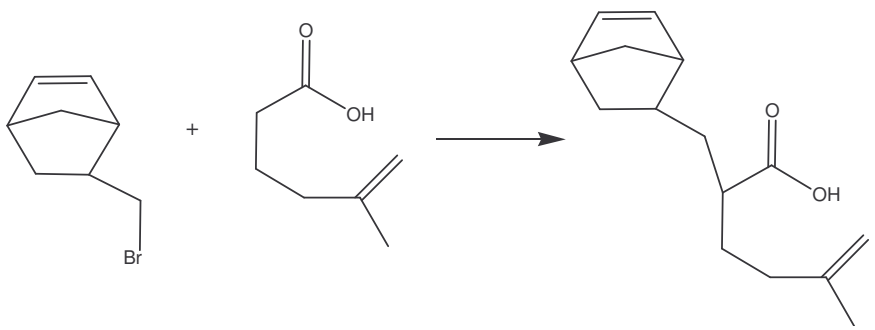

Figure 3.20: Proposed monomer synthesis incorporating negative tone solubility switch for use at 193 or 157nm lithography.

There are currently very few negative tone 193 nm photoresists available. The ring closing of lactones described above, incorporated into norbornane polymers, may offer solutions for current imaging challenges in 193 nm lithography.

[44] http://www.tsmc.com

[45] Brunner, T. A.; Fonseca, C. *Proc. SPIE-Int. Soc. Opt. Eng.* **2001**, *4690*, 76-83

[46] Conley, W.; Brunsvold, W.; Ferguson, R.; Gelorme, J.; Holmes, S.; Martino, R.; Petryniak, M.; Rabidoux, P.; Sooriyakumaran, R.; Sturtevant, J. *Proc. SPIE-Int. Soc. Opt. Eng.* **1993**, *1925*, 120-126.

[47] Cho, S.; Vander Heyden, A.; Byers, J.; Willson, C. G. *Proc. SPIE-Int. Soc. Opt. Eng.* **2000**, *3999*, 62

[48] Sooriyakumaran, B.; Davis, C. E.; Larson, P. J.; Brock, R. A.; DiPietro, R. A.; Wallow, T. I.; Connor, E. F.; Sundberg, L.; Breyta, G.; Allen, R. D. *Proc. SPIE-Int. Soc. Opt. Eng.* **2004**, *5376*, 71-78.

[49] Yokoyama, Y.; Hattori, T.; Kimura, K.; Tanaka, T.; Shiraishi, H. *Proc. SPIE-Int. Soc. Opt. Eng.* **2001**, *4345*, 58

[50] Eschenmoser, A.; Frey, A. *Helvetica Chimica Acta.*, **1952**, *35*, 1660-1666.

[51] Heinz, U.; Adams, E.; Klintz, R.; Welzel, P. *Tetrahedron*, **1990**, *46*, 4217-4230.

[52] Sreekumar, C.; Darst, K. P.; Still, W. C. *J. Org. Chem.*, **1980**, *45*, 4264-4263.

[53] Pfeffer, P. E.; Silbert, L. S.; Chirinko Jr., J. M. *J. Org. Chem.*, **1972**, *37*, 451-458.

Chapter 4 – Materials for Top Surface Imaging

As discussed in Chapter 1, one of the more pressing issues faced when designing a resist for 157 nm photolithographic applications is the transparency of the base resin. To combat this issue a lot of work has been put forth to find a resin that is suitably transparent for use at 157 nm exposures. The two types of resins that have been utilized for 157 nm lithography are fluoropolymers and siloxane polymers.

Siloxane Polymers

Siloxane polymers have been reported to have absorbance as low as 0.06 μm^{-1}.[54] While unfunctionalized siloxanes proved to be very transparent, functionalization of the siloxanes (**Fig. 4.1**) for use as a photoresist increases the absorbance of the resin dramatically.[55] As a result of these absorbance issues, along with the inherently low T_g of siloxane polymers, these systems failed to produce high resolution imaging.

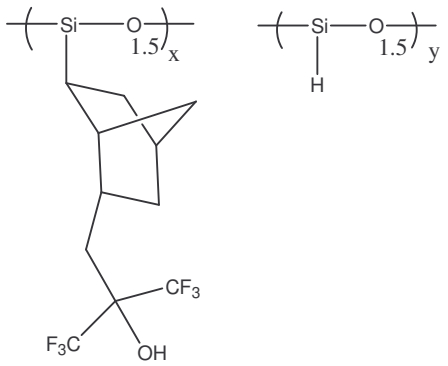

Figure 4.1: Functionalized siloxane resin used for 157 nm imaging.

Fluorinated Polymers

The use of fluorinated materials has been shown to be effective towards producing a transparent 157 nm photoresist system. Three common polymers are used in 157 nm photoresists: fluorinated acrylates, fluorinated norbornenes and fluorinated cyclic polymers.

Fluorinated Acrylates

Fluorinated acrylates have been investigated by several groups as potential 157 nm photoresists.[56,57] Two types of acrylates have been pursued, those involving the α-triflouromethylacrylates (**Fig. 4.2**) and acrylates using fluorinated side chains (**Fig. 4.3**).

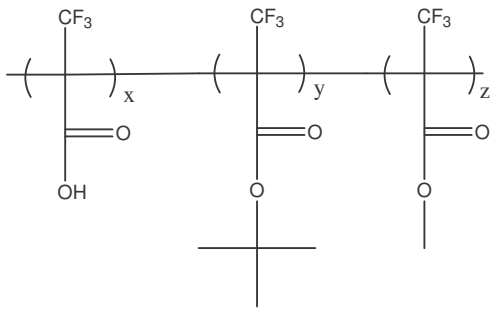

Figure 4.2: α-Trifluoroacrylate platform used for 157 nm lithography.

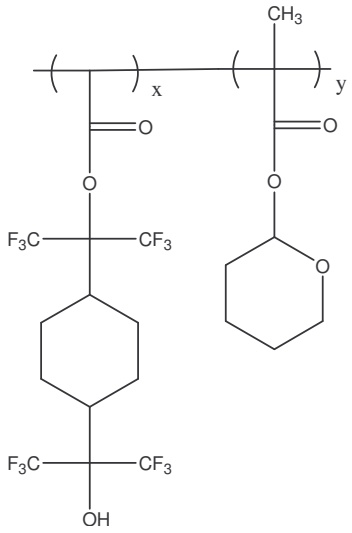

Figure 4.3: Acrylate platform using fluorinated side chains for 157 nm lithography.

Fluorinated acrylates do show improved transparency over their nonfluorinated counterparts; however the acrylate platforms failed to produce high resolution imaging.[58,59] Another issue faced by the acrylate platforms is their low etch resistance. The etch resistance of acrylates is often increased by placing an etch resistant moiety on a side chain on one of the monomer(s). These incorporated etch resistant side chains to the polymer often increases the absorbance, in turn further diminishing imaging performance.

Fluorinated Norbornenes

The second type of fluorinated resin used for 157 nm photolithography is a fluorinated polynorbornene. The most common norbornene derivative has a hexafluoroisopropanol moiety substituted at the two position of norbornane (**Fig 4.4**).

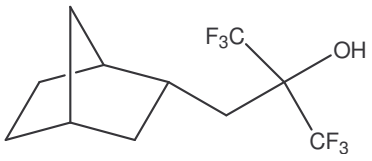

Figure 4.4: Norbornane with hexafluoroisopropanol functional group.

First reported for use at 157 nm by Patterson, *et al*. the hexafluoroisopropanol (HFA) group proved to be useful for two reasons.[60] First, the HFA moiety has a pK_a value of 10.5 which is similar to the pK_a of poly-(*p*-hydroxystyrene) (pK_a = 10) (PHOST).[61] Secondly, it achieves this acidity without having to use any functional groups that will add to the absorbance of the polymer. The acidic groups used in 248 nm (phenol) and 193 nm (carboxylic acid) resists are both absorbing at 157 nm. The phenol as well as the carboxylic acid rely on resonance stabilization of the anion into the aromatic ring and carbonyl for their inherit acidity (**Fig. 4.5**). Since aromatic rings and carbonyls are absorbing at 157 nm these do not make good candidates for 157 nm resist materials.

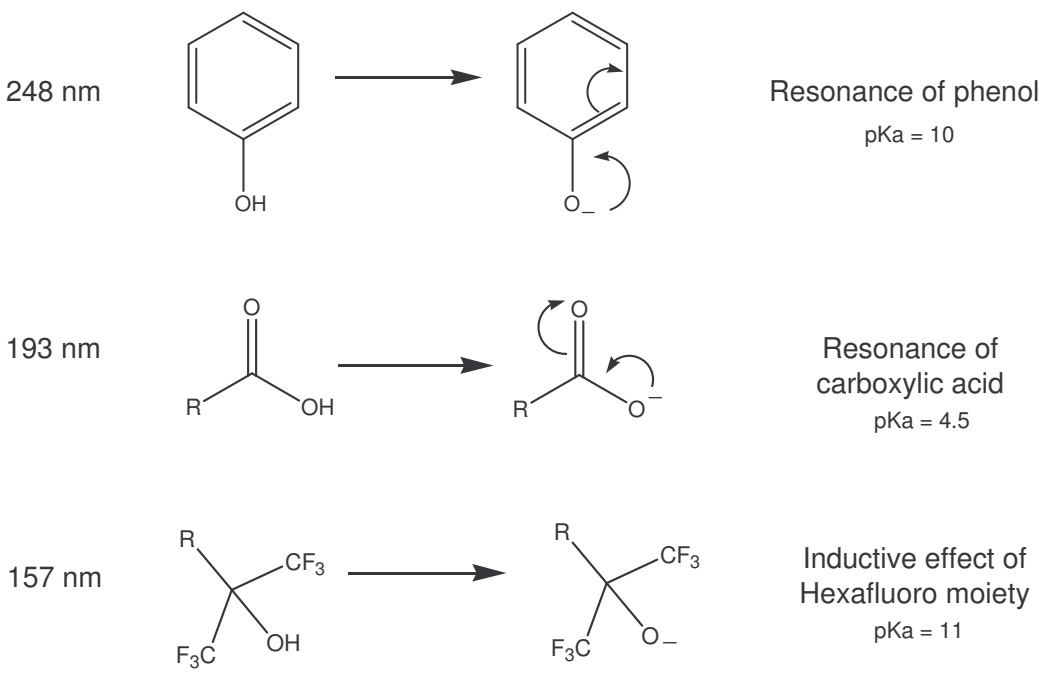

Figure 4.5: Acidic groups used at various different lithographic exposure wavelengths.

However, the inductive effect of fluorine in the HFA moiety provides acidity comparable to that of phenol, while incorporating highly transparent functional groups. Fluorine provides the necessary acidity, but also significantly decreases the overall absorbance of the monomer. The absorbance of a homopolymer made from norbornenehexafluoroalcohol (NBHFA) is 1.15 μm^{-1}, whereas polynorbornene has an absorbance of 6.10 μm^{-1} (**Fig. 4.6**).[62]

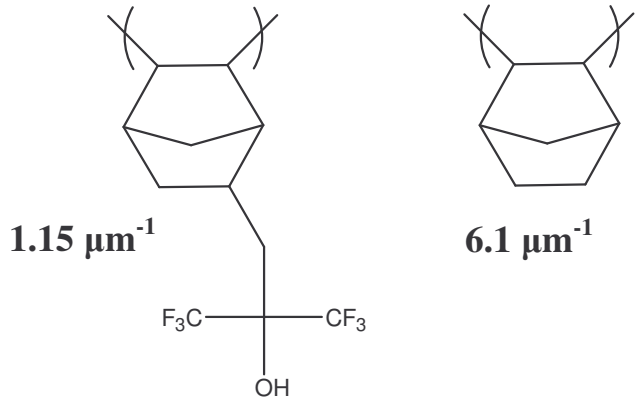

Figure 4.6: Polynorbornenehexafluoroalchol and polynorbornane with their corresponding absorbances.

As a result of its low absorbance, polynorbornenehexafluoroalcohol (PNBHFA) resin has been used extensively for 157 nm applications and has produced promising imaging results[6364656667]. Even with an absorbance as low as 1.15 μm^{-1}, the imaging of PNBHFA still suffers from having too high an absorbance at 157 nm. As a result, there remains a need to push the absorbance of the bulk resin below 1 μm^{-1}.

Asahi Polymer

In 2002, another fluorinated resin for use at 157 nm lithography was introduced by Asahi Glass.[68] The Asahi Glass resin is made via radical cyclization to form a highly fluorinated resin (**Fig. 2.4**). As a result of this high level of fluorination, the absorbance of the polymer is less than 0.5 μm^{-1}. Due to its low absorbance the resin has been tested extensively for 157 nm resist applications. The caveat to its low absorbance is that the Asahi polymer has very low etch resistance.

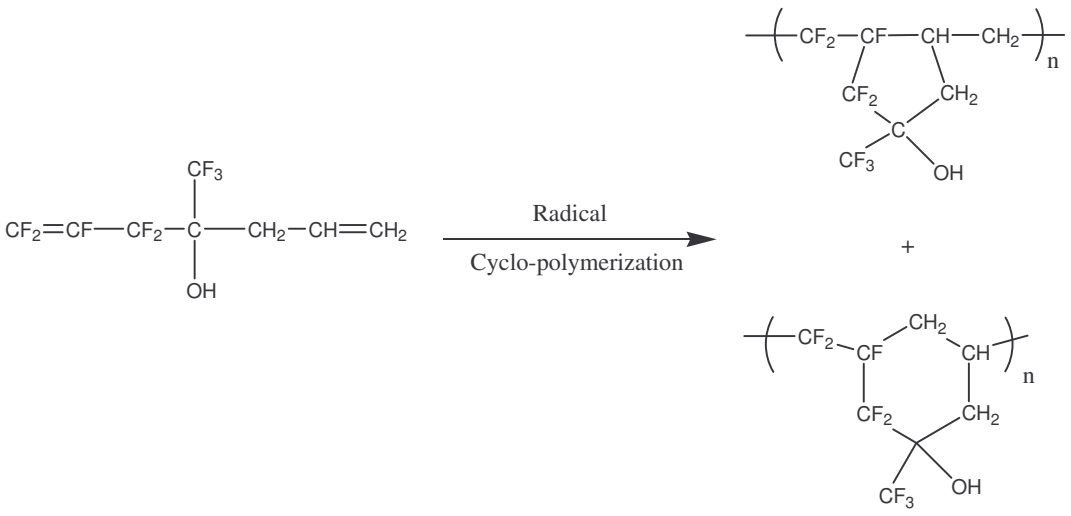

Figure 4.7: Asahi 157 nm photoresist resin made via radical cyclopolymeriztion.

Similar to the acrylate systems, etch resistant functional groups can be appended to the polymer via side chains to improve the etch resistance. However, this will increase the absorbance of the resin, reducing its imaging performance from the added absorbance when compared to the PNBHFA resin. Even though progress was being made in the search for a suitably transparent 157 nm photoresist resin, no one resin has emerged that provided all the characteristics needed for an ideal 157 nm photoresist. A potential solution to a transparent resin is another imaging process called thin layer imaging (TLI), which does not have resin transparency as a requirement for its design.

Thin Layer Imaging (TLI)

Thin layer imaging processes have been investigated since the early 1980's as an alternative to a tradition single layer resist process. Thin layer imaging is unique because it only uses the uppermost portion of the film to produce the three dimensional relief

image. A bilayer resist process (**Fig. 4.8**) is a common example of a thin layer imaging process.

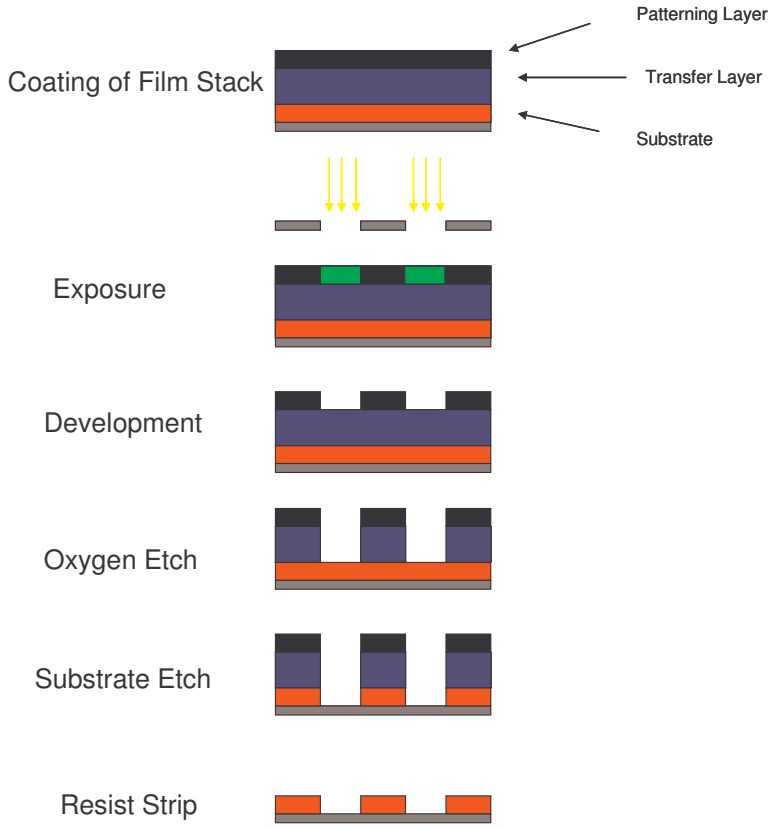

Figure 4.8: Bilayer photoresist scheme.

In a bilayer scheme, two polymers are coated on top of the substrate. The bottom layer is referred to as a transfer layer and is composed of an organic polymer. The top layer is referred to as the patterning layer and is relatively thin compared to the transfer layer. The patterning layer is a silicon-based photoresist. The patterning layer is imaged like a standard photoresist, to expose the transfer layer. The wafer is then subjected to an oxygen reactive ion etch (RIE). The oxygen etch quickly reacts with the organic transfer layer producing carbon dioxide and water. However, the silicon-containing patterning

layer reacts with the oxygen plasma to form silicon dioxide, which resists oxygen etching. Since only the thin patterning layer needs to be imaged, the transparency of such a thin film is less critical as compared to the transparency of standard photoresist layer.

CARL Process

A variation of a standard bilayer process called Chemical Amplification of Resist Lines (CARL) (**Fig 4.9**) was pioneered by Infineon.[69]

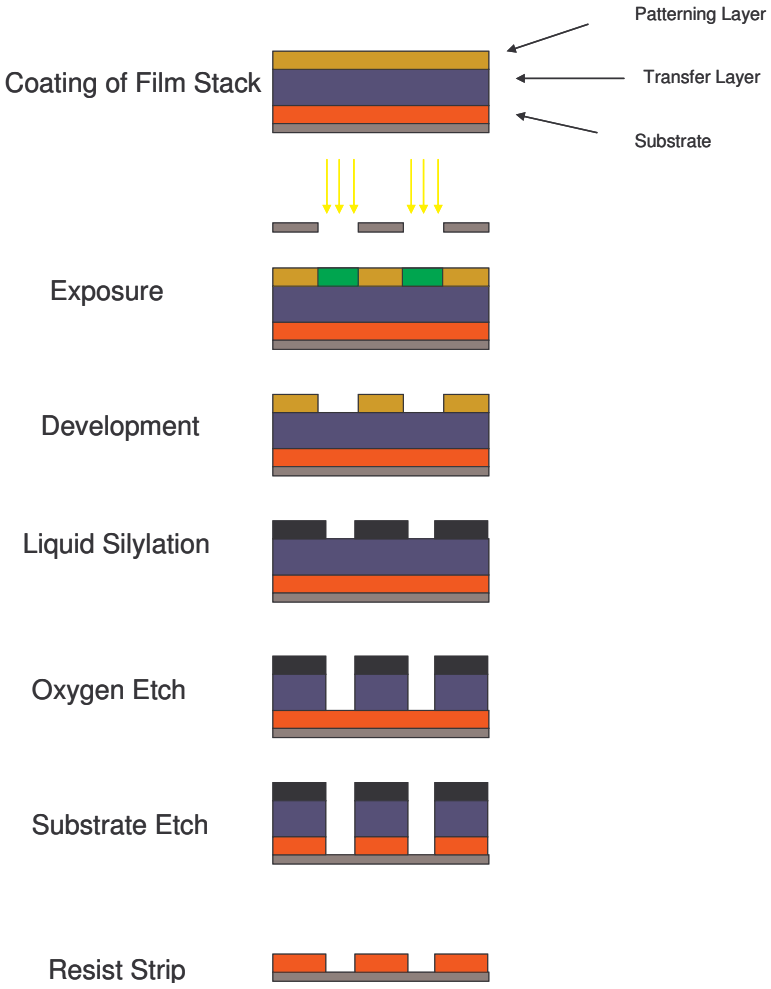

Figure 4.9: CARL bilayer resist scheme.

The CARL process involves one more step than a traditional bilayer process. After the patterning layer is exposed and developed, the wafer is exposed to a liquid phase silylation process. This extra silylation step introduces the necessary silicon content into the remaining (unexposed) patterning layer. What makes the CARL process unique is during the silylation step, the resist lines swell which effectively shrinks the previously exposed/developed regions. The silylation process is done by adding a bifunctional amino-terminated siloxane (CARL reagent) into an anhydride styrene copolymer (patterning layer) (**Fig. 4.10**).

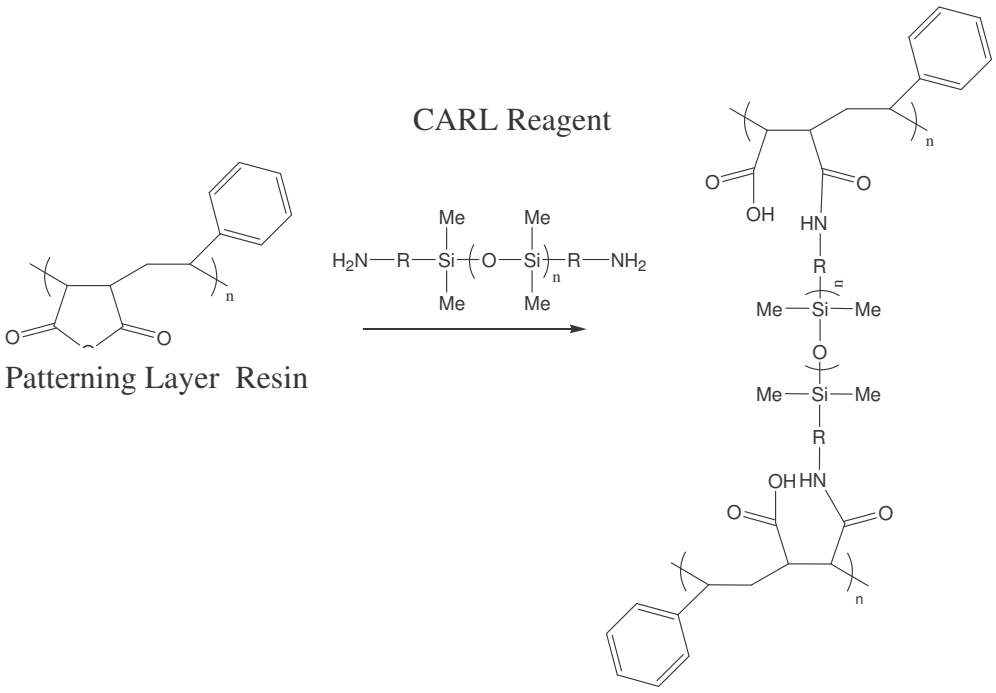

Figure 4.10: Reaction of CARL reagent with patterning layer.

The CARL reagent crosslinks the patterning layer and the swelling can be controlled by changing the silylation time. The swelling effectively allows for images to be patterned that are higher resolution that a normal exposure process is capable of. Unfortunately,

the major drawback is the extra process steps that the CARL system introduces as compared to traditional lithography.

Top Surface Imaging (TSI)

Top surface imaging (TSI) is another thin layer resist process that incorporates the etch chemistry of a bilayer process while only using a single resist layer found in a traditional lithography process (**Fig. 4.11**).

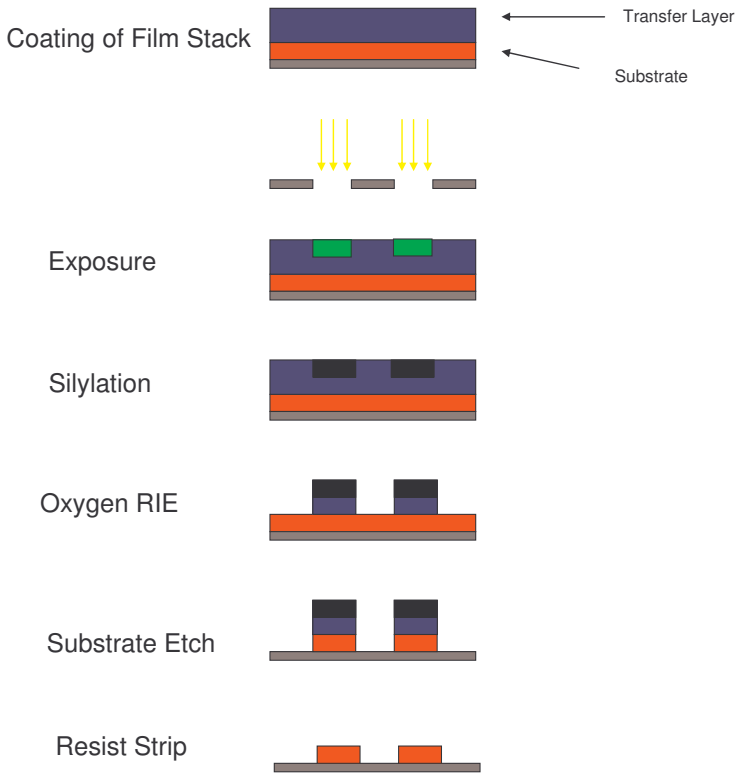

Figure 4.11: Top surface imaging (TSI) lithography scheme.

After the photoresist layer is coated, the resist is selectively exposed through a photomask. The wafer is exposed to a gas phase silylating agent that selectively silylates the exposed

regions. This incorporation of silicon into the resist forms the necessary etch barrier for the three dimensional relief image to be transferred with an oxygen RIE. Since only a thin layer of the resist is required for etch transfer, the polymer does not have to be very transparent at the applicable wavelength. Even though both bilayer and top surface imaging are more process intensive due to the extra coating and/or silylation steps, both are desirable as they relax the demanding transparency requirements for a 157 nm photoresist.

Liquid Phase Silylation

In top surface imaging, the introduction of the silylating agent can be accomplished via two methods: liquid phase or gas phase. Liquid phase is perhaps the easiest method as gas phase silylation requires the extensive use of more equipment. Liquid phase silylation allows for a wide variety of silylating agents to be used, as the volatility is not an issue for the silylating reagents. The most common liquid phase silylating reagent used is hexamethylcyclotrisilazane (HMCTS).[70,71,72] However, several other silylating reagents have been evaluated for liquid phase silylation: tetramethyldisilazane (TMDS), hexamethyldisilazane (HMDS), bis(dimethylamino)dimethylsilane (BDMADS), bis(dimethylamino)methylsilane (BDMAMS) (**Fig. 4.12**).

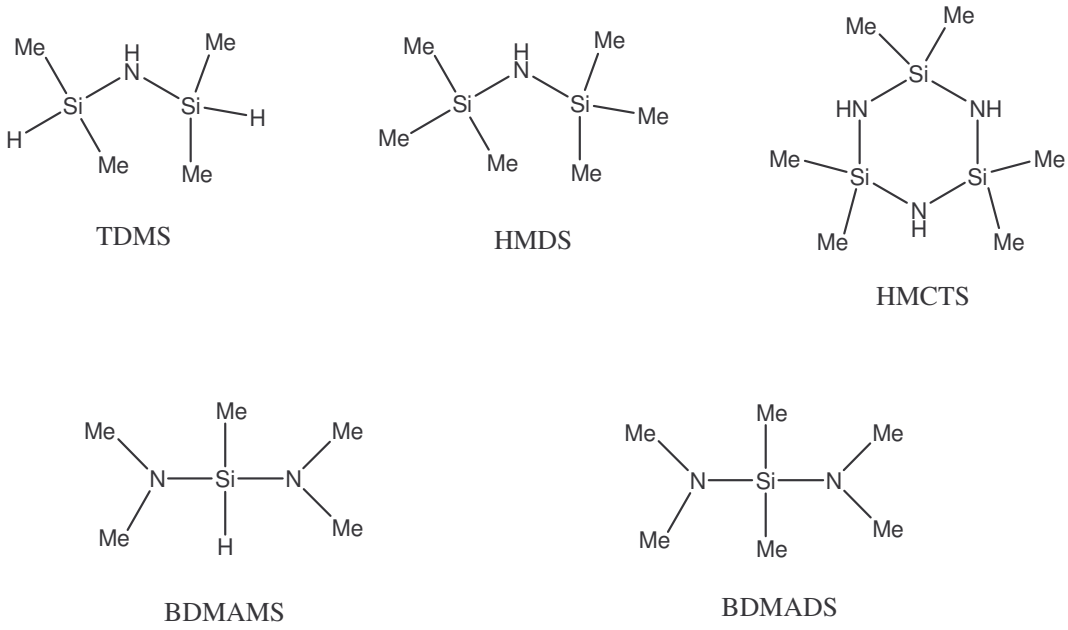

Figure 4.12: Silylation reagents evaluated for liquid phase silylation processes.

The choice of silylating agent for the liquid phase silylation reaction is affected by several factors including time, temperature and solvent concentration.

Time and Temperature Dependence of Liquid Phase Silylation

The use of HMCTS in novolac films was introduced by Shaw and co-workers in the late 1980's (**Fig. 4.13**).

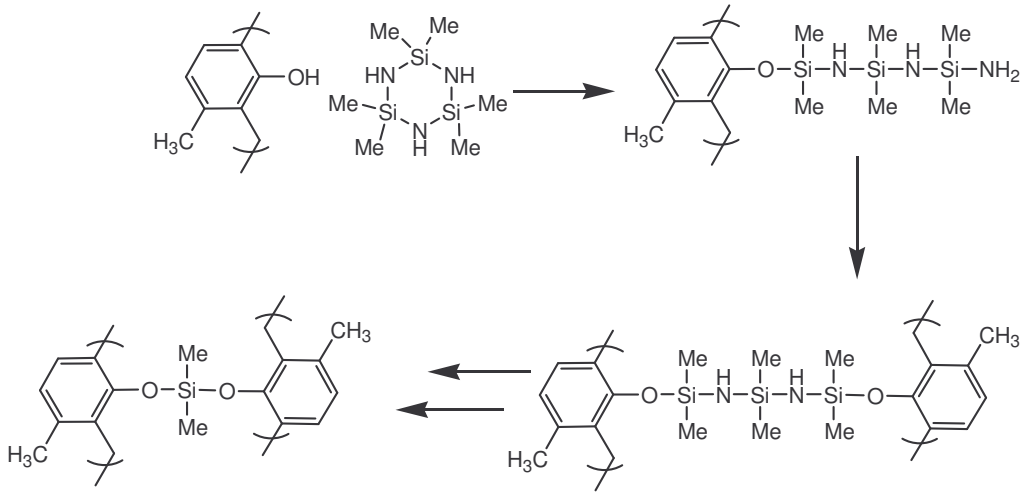

Figure 4.13: Liquid phase silylation of novolac with HMCTS.

Their report states that the rate of silylation doubles with every 10° C increase in the silylation bath temperature. It was found that for novolac films, a silylation temperature of 40° C provides efficient silylation, while remaining below the T_g of the novolac resin. Baik and co-workers also reports silylation of novolac with BDMADS at 35° C gives efficient silylation.

Concentration Dependence of Liquid Phase Silylation

During liquid phase silylation, the silylation agent is often diluted in a carrier solvent(s). Both the silylating agent concentration and the specific carrier solvent are critical in the silylation process. The solvent most commonly used is xylenes. N-methylpyrolidone (NMP) and propylene glycol methyl ether acetate (PGMEA) have been used as co-solvents to enhance the diffusion of the silylating agent into the novolac film. The concentration of the co-solvent varies from 2% (NMP) to 50% (PGMEA). If too

much co-solvent is used the top of the film will be dissolved away during the liquid phase silylation process. The effect of the silylating agent concentration is less pronounced than the co-solvent concentration. Typical silylating agent concentration usually ranges from 10-30% with 10% being the most common concentration.

The major problem with liquid phase silylation is the formation of defects. Water contamination in the silylation bath can result in the formation of oligomers or polymeric siloxanes (**Fig. 4.14**).

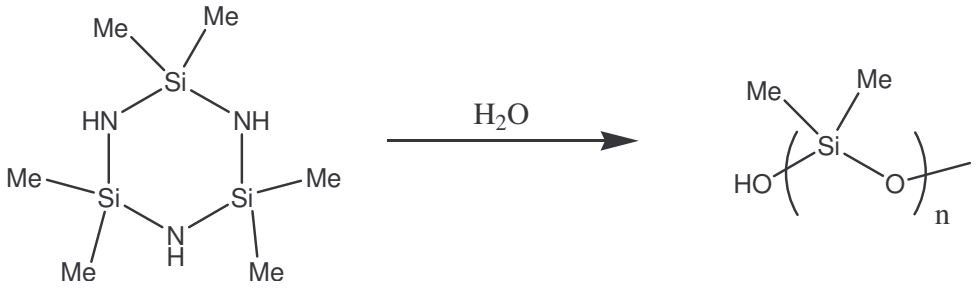

Figure 4.14: Reaction of HMCTS with water to form oligosiloxanes.

The oligosilanes can precipitate out from solution onto the wafer, resulting in unintentional silicon deposition, resulting in defects after etch transfer. As a result, gas phase silylation has been investigated as well, since it has the potential to significantly reduce these types of defects.

Gas Phase Silylation

The other method for introducing the silylating reagent is via a gas phase reaction. One benefit of gas phase silylation is that the silylation chemistry is cleaner and results in fewer defects that are problematic with the liquid phase silylation techniques. In order to

do gas phase silylation a volatile silylating agent is required. Common silylating agents used are hexamethyldisilazane (HMDS) and dimethylsilyldimethylamine (DMSDMA). Other silylating agents used are trimethylsilyl dimethylamine (TMSDMA) and tetramethyl disilazane (TMDS) (**Fig. 4.15**).

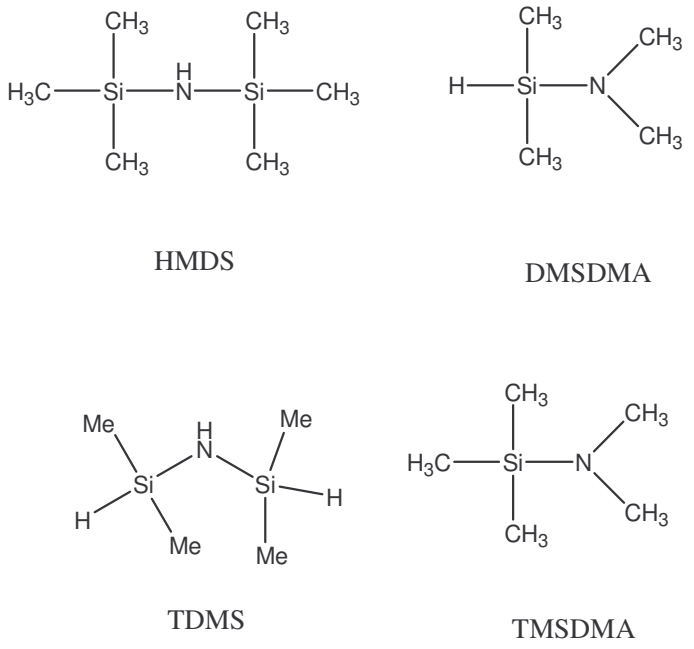

Figure 4.15: Common silylating agents used in top surface imaging.

A gas phase silylation process called Diffusion Enhanced SIlylating REsist (DESIRE) system was introduced in the mid 1980's.[73,74,75] The DESIRE process uses HMDS as the active silylating agent and novolac/DNQ as the resin. The first step of the process is to irradiate the DNQ/novolac, producing indene carboxylic acid in the exposed regions (**Fig. 4.16**).

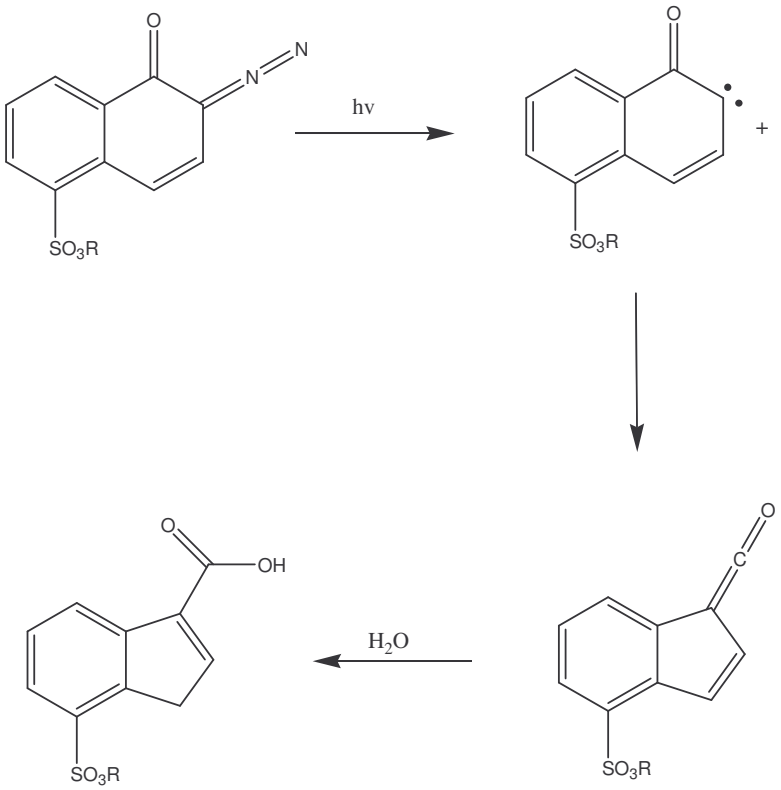

Figure 4.16: Exposure of DNQ with light and subsequent hydrolysis to indene carboxylic acid.

After the indene carboxylic acid is produced in the exposed regions, the wafer is heated, which does two things. It both drives the water from the wafer as well as thermally decomposing the unexposed DNQ to the ketene. Without the presence of water the ketene reacts with the phenols of the novolac which results in a cross-linked resin (**Fig. 4.17**).

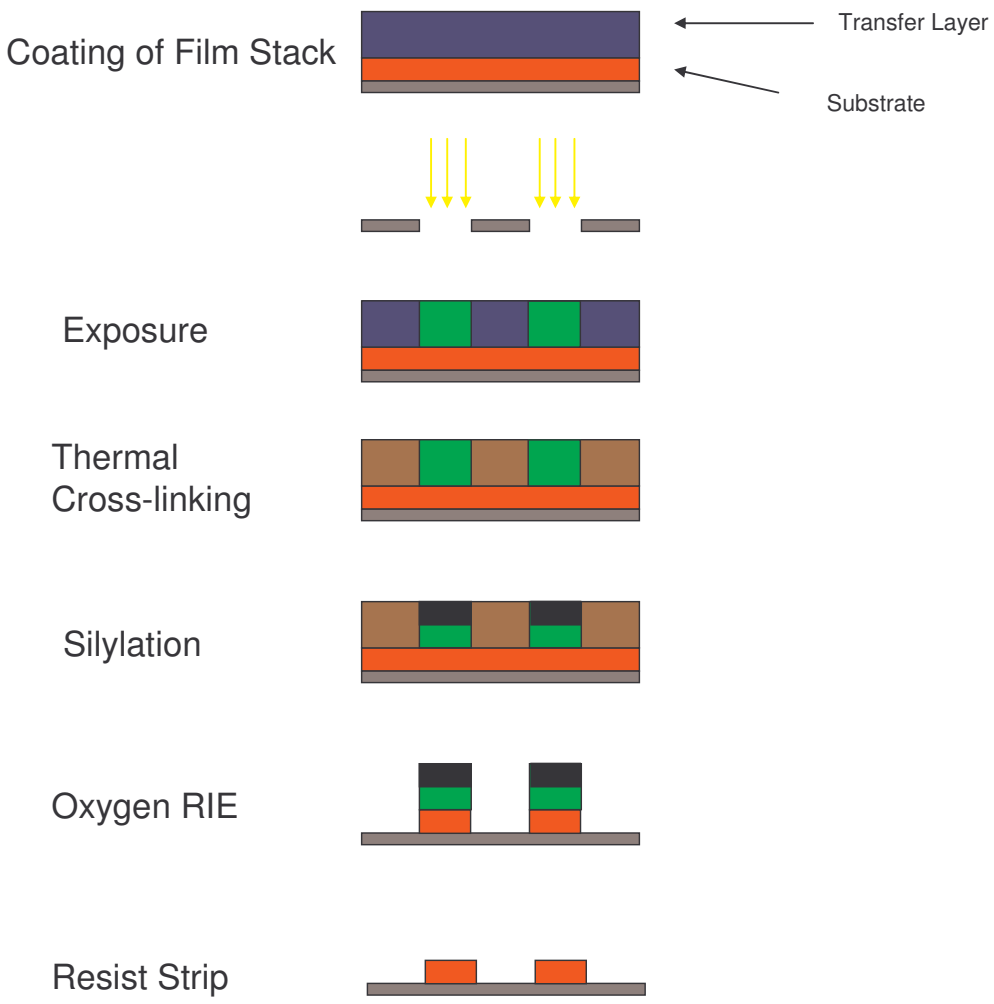

Figure 4.17: Scheme of DESIRE imaging process.

Gas phase silylation with HMDS selectively silylates the exposed regions due to the enhanced diffusion of silylating agent into the exposed regions relative to the cross-linked regions. An oxygen RIE produces the desired relief image.

A process similar to the DESIRE process was introduced by Hiroshi Ito and co-workers at IBM.[76] Their system used a *t*–boc protected poly-(*p*-hydroxystyrene)

(PHOST) resin which had been developed for 248 nm lithography as a chemically amplified resist. The *t*-boc-PHOST could be deprotected using a photoacid generator (PAG) (**Fig. 4.18**).

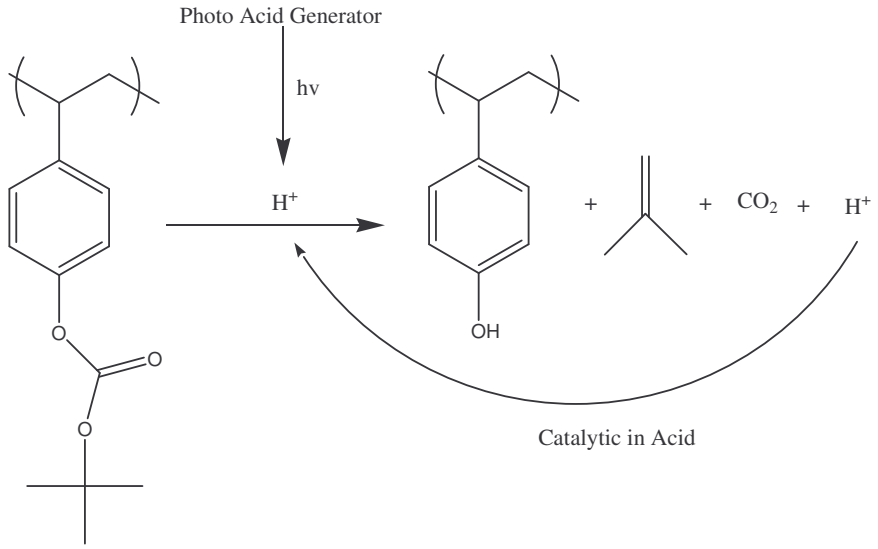

Figure 4.18: Photoacid catalyzed deprotection of *t*-boc styrene.

The deprotected phenol gives a reactive site for silylation reactions. This process is referred to as a "digital zero volume change" TSI process. It is digital because the resin exists in only two states after exposure, protected and deprotected. Therefore, silylation only occurs in the exposed regions whereas the DESIRE process relies on diffusion rates to dictate selective silylation. The term "zero volume" is derived from the fact that deprotection of the resin decreases film thickness due to the loss of mass associated with the volatilization of its protecting groups. Upon silylation the mass balance is restored by the silylating reagent, resulting in "zero volume" change. The original process used

HMDS as the silylating reagent, but recent work has also incorporated the use of DMSDMA as a silylating reagent.

Designing a Top Surface Imaging Resist

A resist used in top surface imaging must meet several requirements. The majority of the design requirements relate to the resin properties.

- The resin needs a reactive site for silylation, *i.e.* alcohol
- After silylation resin must have at least 12% (by weight) of silicon for sufficient oxygen RIE resistance
- The resin itself must provide enough etch resistance for substrate etch
- Resin film must have sufficiently high T_g to withstand processing conditions (*i.e.* PAB, PEB)

Most importantly the resin needs to have a reactive site for silylation to occur. Often this site is a pendant alcohol that can react with a variety of different silylating reagents that are commonly used in organic synthesis. After silylation occurs, the resin needs to have a minimum 12%, by weight, silicon in the resist. That has been empirically determined to be the critical weight percent silicon to provide sufficient oxygen etch. The base polymer must provide etch resistance as well. Even though the oxygen etch is resisted by the silicon incorporated at the top of the resist this is only used to provide the three dimensional relief image. The base polymer also must be able to resist the desired etch

chemistry used in etching (patterning) the substrate layer. The T_g of the resin is also important as silylation affects resin T_g (**Fig. 4.19**).

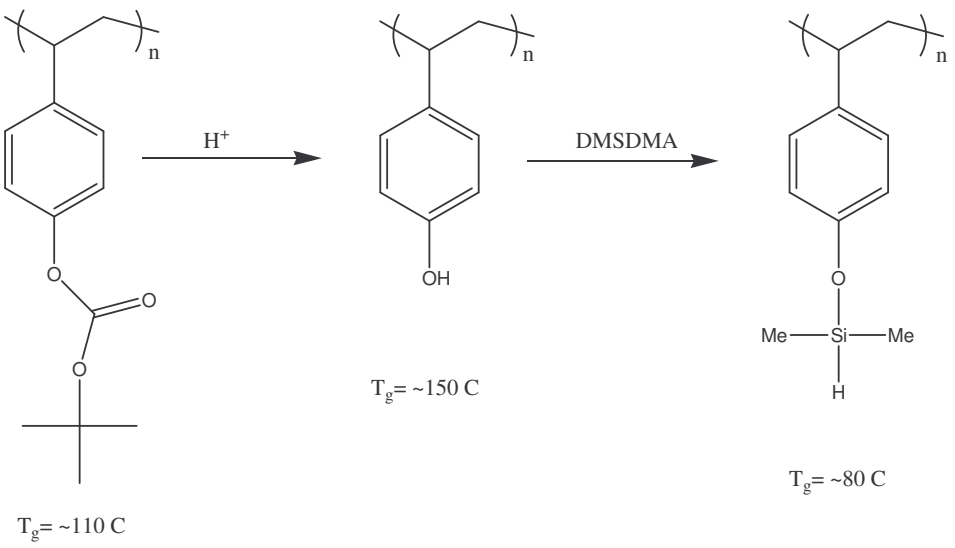

Figure 4.19: Effective of silylation on T_g of PHOST.

The effect of resin T_g with respect to silylation has been demonstrated by the silylation of PHOST with DMSDMA.[77] The T_g of fully *t*-boc protected PHOST is ~110° C. When exposed to acid and baked to remove the *t*-boc protecting group the T_g of PHOST is ~150° C. This increase in T_g can be attributed to the increase of hydrogen bonding of the free hydroxyl groups. During silylation with DMSDMA, the free hydroxyl groups are silylated and the T_g of the resin drops to less than 80°C when it is fully silylated. This is rationalized by the loss of hydrogen bonding between the repeat units and also by the incorporation of low T_g side chain. The siloxy bonds are non-polar and cause the T_g of the silylated polymer to drop below that of *t*-boc protected PHOST. This dramatic T_g drop can become a concern since the silylation process often takes place at elevated

temperatures. If this temperature is above the resin T_g, then the polymer material will flow, possibly resulting in a blend region of silylated and unsilylated material. This blending of silylated and unsilylated regions has been targeted as a cause for one of the most problematic issue with top surface imaging, namely line edge roughness.

Line Edge Roughness in Top Surface Imaging

The major issue with current TSI platforms is the inherit amount of line edge roughness (LER) associated with the process. An example of high line edge roughness is the imaging *t*-boc-PHOST (**Fig. 4.20**). The scanning electron microscope (SEM) image clearly shows the sidewalls of the images are very rough and this is what is referred to as LER. LER is quantitatively defined as the amount of 3 σ deviation from the defined line edge, and is measured in nanometers.

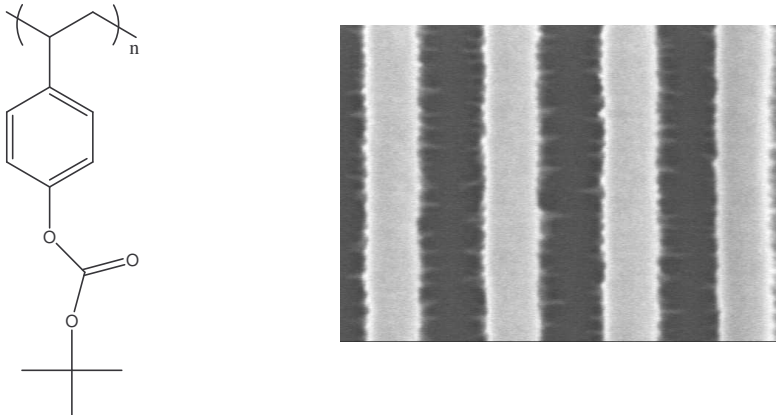

Figure 4.20: Line edge roughness typical of top surface imaging of PHOST.

An imaging system with high LER leads to decreased uniformity of the features being transferred into the substrate, which can lead to defects in the final device. The 2003

ITRS roadmap (**Fig. 4.21**) indicates that current resist platforms need to have less than 2.6-3.0 nm of line width roughness (LWR). [78]

Year of Production	*2003*	*2004*	*2005*	*2006*	*2007*	*2008*	*2009*
Technology Node		*hp90*			*hp65*		
DRAM ½ Pitch (nm)	*100*	*90*	*80*	*70*	*65*	*57*	*50*
MPU/ASIC Metal 1 (M1) ½ Pitch (nm)	120	107	95	85	76	67	60
MPU/ASIC ½ Pitch (nm) (un-contacted gate)	107	90	80	70	65	57	50
MPU Gate in resist Length (nm)	65	53	45	40	35	32	28
MPU Gate Length after etch (nm)	45	37	32	28	25	22	20
Resist Characteristics *							
Resist meets requirements for gate resolution and gate CD control (nm, 3 sigma) **	◆ 4.0	3.3	2.9	2.5	2.2	2.0	1.8
Resist thickness (nm, imaging layer) ***	250–400	220–360	200–320	170–250	160–220	140–200	130–180
*Ultra thin resist thickness (nm)***	120–150	120–150	120–150	100–150	100–130	100–130	80-120
PEB temperature sensitivity (nm/C)	2.5	2	2	1.5	1.5	1.5	1.5
Backside particles (particles/m^2 at critical size, nm)	2000 @ 150	2000 @ 150	1500 @ 100	1500 @ 100	1500 @ 100	1500 @ 100	1000 @ 50
Defects in spin-coated resist films† #/cm^2	0.02	0.01	0.01	0.01	0.01	0.01	0.01
(size in nm)	60	55	50	45	40	35	30
Defects in patterned resist films, gates, contacts, etc. #/cm^2	0.07	0.06	0.05	0.04	0.04	0.03	0.03
(size in nm)	60	55	50	45	40	35	30
Line Width Roughness (nm, 3 sigma) <8% of CD ******	◆ 3.6	3.0	2.6	2.2	2.0	1.8	1.6

Manufacturable solutions exist, and are being optimized
Manufacturable solutions are known
Interim solutions are known
Manufacturable solutions are NOT known

Figure 4.21: 2003 ITRS roadmap for lithography.

LWR is very similar to LER and is defined as the 3 sigma of deviation from the defined line width. Due to these stringent requirements, and the fact that most TSI resists have increased LER, TSI has not been adopted in large scale manufacturing processes.

There are examples of a smooth imaging TSI process. Work completed by Mark Sommervell during his thesis work focused on optimizing TSI resists for 193nm lithography.

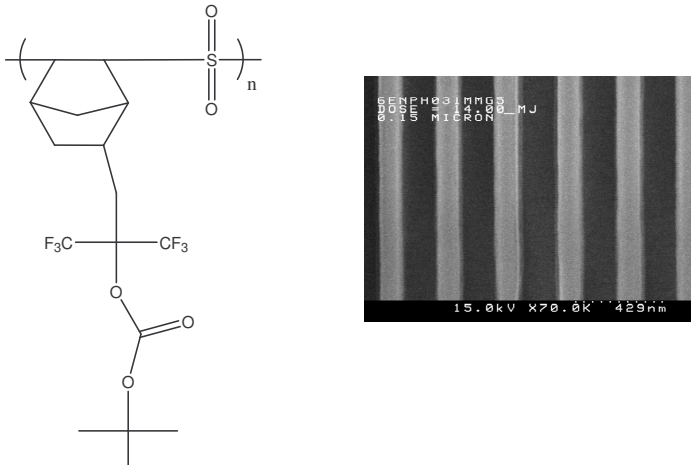

Figure 4.22: Example of minimal LER in TSI resist imaging.

This resist system used a co-polymer of norbornenehexafluoroalcohol (NBHFA) and sulfur dioxide (**Fig. 4.22**). The SEM images of this resist system demonstrated low LER imaging performance. While this resist performed well, it was not the ideal resist. Three main reasons this resist proved to be less than ideal were: excessive outgassing from the polymer, low substrate etch resistance and the use of the hexafluoro alcohol moiety required silylating agents that are difficult to synthesize or procure.

When using PNBHFA, a disilane based silylating agent is required to achieve sufficient silicon content, 12% by weight of the resin. Dimethylsilane does not have enough silicon to reach 12% so the added silicon content of the disilane is needed. The

main drawback of such a silylating agent is the extreme danger in synthesizing it, as reported by Wheeler and co-workers.[79]

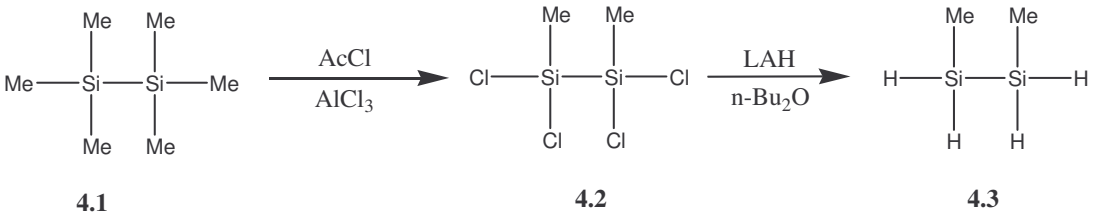

4.1 **4.2** **4.3**

Figure 4.23: Synthesis of dimethylamino dimethydisilane.

The synthesis begins with commercially available hexamethyldisilane, reacted with acetyl chloride and aluminum trichloride to produce tetrachlorodimethyldisilane (**4.2**). A lithium aluminum hydride reduction (LAH) of **4.2** produces dimethyl disilane **4.3** (**Fig. 4.23**).

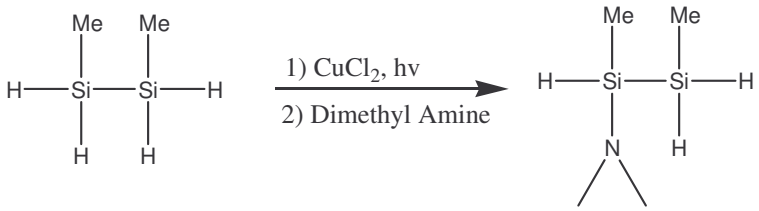

4.3 **4.4**

Figure 4.24: Synthesis of dimethylamino dimethyldisilane continued.

A light initiated radical reaction with copper chloride and **4.3** forms chlorodimethyl disilane, which is reacted *in-situ* with dimethyl amine to form dimethylamino dimethyldisilane **4.4** (**Fig. 4.24**). The synthesis is very dangerous due to pyrophoric nature of **4.3**.

New Materials for Improved TSI Imaging

To address the issue of LER a collaboration was started with Andrew Jamieson, a fellow graduate student in our research group. Our main hypothesis was that LER in TSI materials might be attributed to the T_g drop associated with silylation. Two approaches were envisioned to yield the high T_g materials. The first was synthesizing high T_g materials that upon silylation, the T_g of the polymer would remain above the silylation process temperature. The second approach was to use a different silylation chemistry, such that silicon incorporation into the film would not lower the resin T_g.

Synthesis of High T_g Resin Materials

A survey for high T_g polymeric materials began. It has been reported by Turner and co-workers that styrene and maleimide co-polymers have very high T_gs (> 200°C). [80] The reported synthesis of the maleimide was accomplished by the addition of *p*-aminophenol to maleic anhydride in toluene. Stirring the solution at room temperature afforded the desired maleanilic acid (**4.5**) (**Fig. 4.25**).

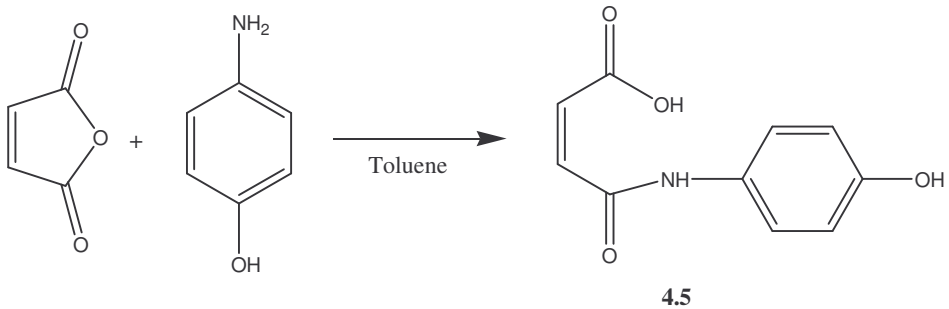

4.5

Figure 4.25: Synthesis of *p*-acetoxy-*N*-phenylmaleimide.

Cyclization of **4.5** in acetic anhydride with catalytic sodium acetate produced *N*-4-acetoxyphenyl maleimide (**Fig. 4.26**).

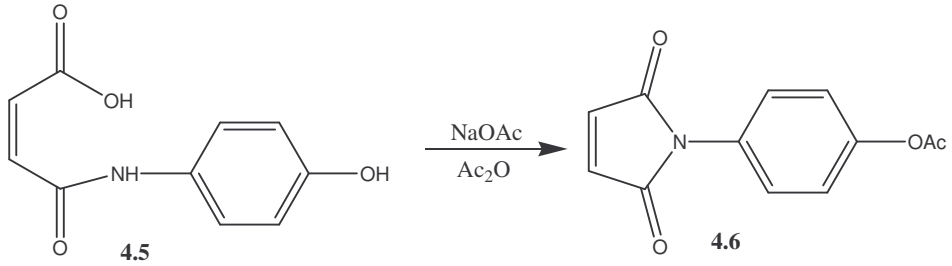

Figure 4.26: Synthesis of *p*-acetoxy-*N*-phenylmaleimide continued.

Radical co-polymerization of **4.6** with acetoxy styrene produced the acetoxy-protected co-polymer of *N*-(*p*-hydroxy)phenylmaleimide and *p*-acetoxystyrene (**4.7**) (**Fig. 4.27**).

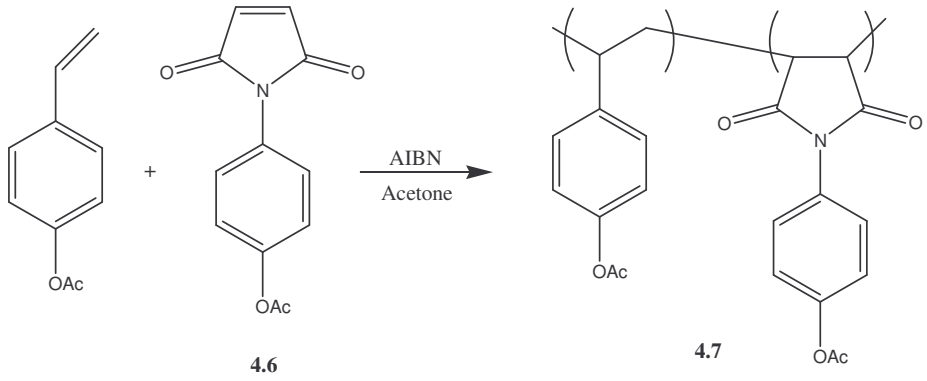

Figure 4.27: Co-polymerization of *p*-acetoxy-*N*-phenylmaleimide with *p*-acetoxystyrene.

In order to produce a photoresist material with the required solubility switch, the acetoxy protecting groups would need to be removed and replaced with *t*-boc. The removal of the acetoxy groups was accomplished by acid hydrolysis in methanol (**Fig. 4.28**) to form the phenol derivative **4.8**.

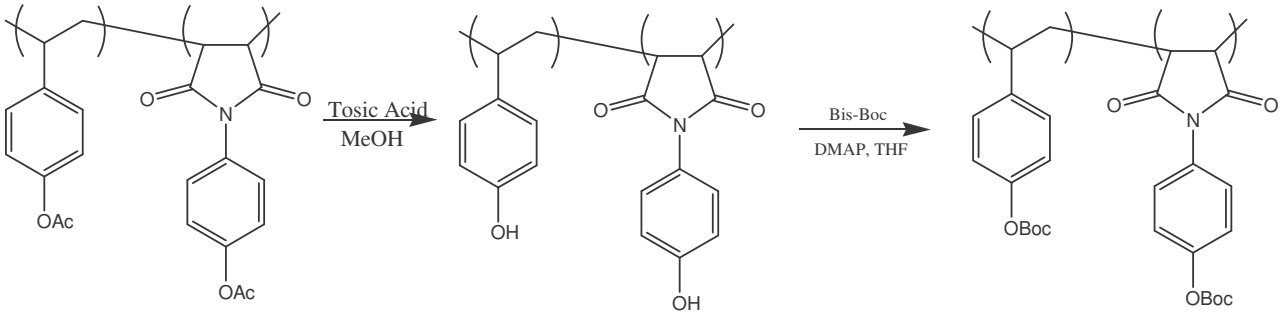

Figure 4.28: Hydrolysis of acetoxy protecting groups, followed by *t*-boc protection, of PHOST-co-maleimide polymer.

After hydrolysis the corresponding phenolic polymer, was protected with *t*-boc to give an imagable polymer (**4.9**) (**Fig. 4.28**).

Imaging of High T_g Polymer

Once the polymer was synthesized the next step was to test its imaging performance. The polymer was imaged using 248 nm exposure at International SEMATECH. The SEM image shows that this polymer which after silylation, has a T_g in excess of 150° C, still displays significant line edge roughness.

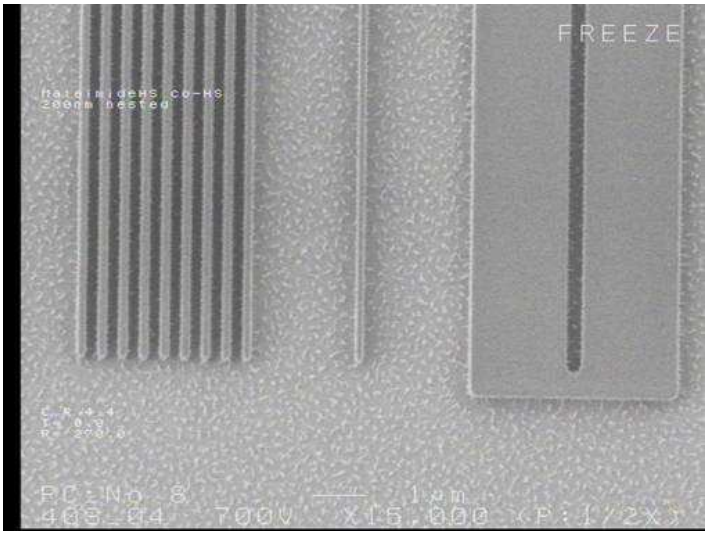

Figure 4.29: SEM with LER evident upon imaging a high T_g polymer in the TSI process.

Knowing that this high T_g resin had failed to reduce LER, the focus shifted to change the T_g effects of the silylating reagent and determine if it can improve the imaging performance.

New Silylation Chemistry

Another proposal to improve TSI process LER was the use of novel silylation chemistry. Since the siloxy bond formed in the silylation of the resin is non-polar, it is possible for the silylated areas to phase separate from the base resin. If the side chains after silylation were more polar and did not phase separate, the silylated areas may then be more defined and as a result show less LER. One method of incorporating silicon without forming siloxy bonds uses an isocyanate as the reactive group for silylation. This would result in a urethane linkage with a more polar side chain that should result in a higer T_g domain (**Fig. 4.30**).

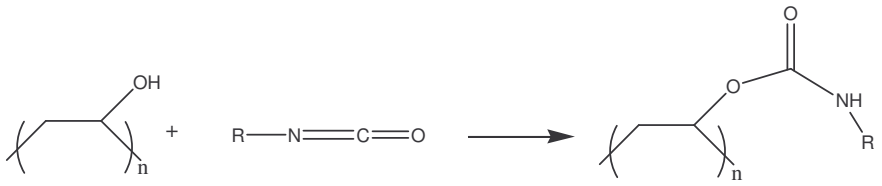

Figure 4.30: Reaction of isocyanate with polyvinyl alcohol to form urethane linkage.

To install the necessary etch resistance, the R group must be a silicon-containing group. The synthesis of such an isocyanate was accomplished following a literature procedures of Tsuge and co-workers.[81,82] Commercially available trimethylsilylmethyl chloride was reacted with sodium azide in hexamethylphosphoramide (HMPA) to form **4.10**. Treatment of **4.11** with triphenylphosphine formed the nitrogen ylide, which was reacted with carbon dioxide to produce the desired trimethylsilylmethyl isocyanate (TMSMIS) (**4.11**) (**Fig. 4.31**).

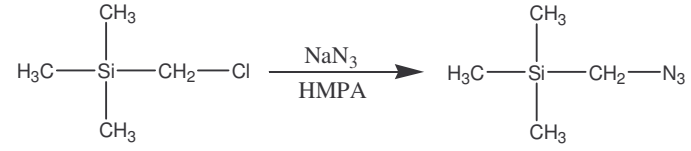

4.10

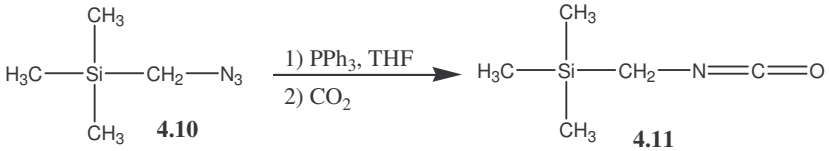

4.10 **4.11**

Figure 4.31: Synthesis of silicon containing isocyanate.

One disadvantage of the isocyanate approach is dealing with the 12% by weight silicon requirement. Amino silylation proceeds via a Sn2 reaction mechanism in which

the amine (usually dimethyl amine) is exchanged with the reactive alcohol. However, when using an isocyanate there is no leaving group thus the weight percent amount of silicon that is added to the polymer is less.

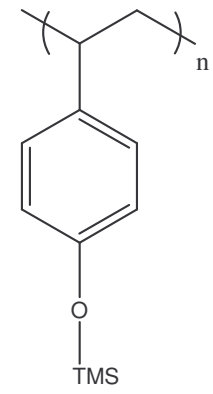

14.5% Silicon

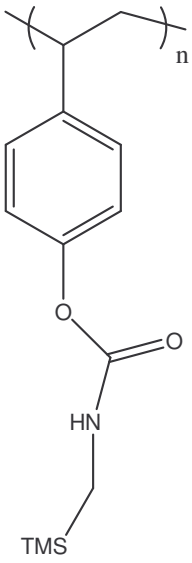

11.2% Silicon

Figure 4.32: Weight percent silicon in PHOST using DMSDMA and TMSMIS as silylating agents.

A typical silylation of PHOST with TMSDMA incorporates 14.5% weight percent silicon, which is above the threshold level needed for sufficient etch resistance. If PHOST is silylated with TMSMIS, only 11.2% silicon is incorporated, well below the 12% requirement (**Fig. 4.32**). Compounding the problem is that these numbers assume 100% silylation, which is rarely achieved. The use of an isocyanate will require a new polymer material such that the final silicon content is greater than 12% by weight.

Polymer Synthesis

An ideal polymer for use with isocyanates would have more than one reactive site (alcohol) per monomer repeat unit, effectively doubling the amount of silicon added to the polymer. An ideal monomer would be a norbornene diol (NB-diol).

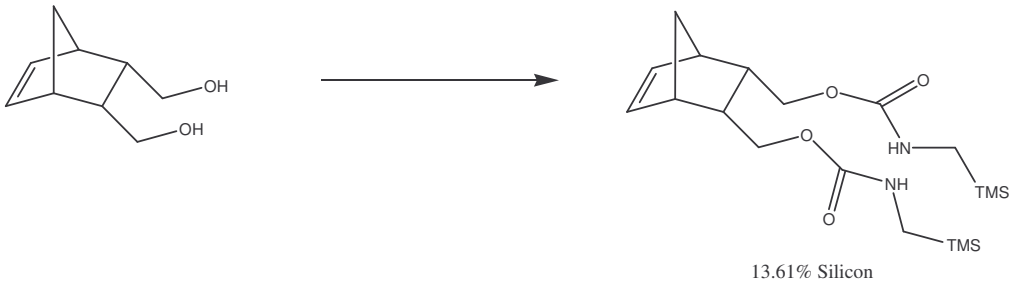

Figure 4.33: Weight percent silicon of NB-diol when silylated by TMSMIS.

Upon complete silylation, this norbornene diol would have 13.6% weight silicon incorporated into the polymer (**Fig. 4.33**). The synthesis of this monomer was accomplished via the Diels-Alder reaction of cyclopentadiene with maleic anhydride to form **4.12** (**Fig. 4.34**).

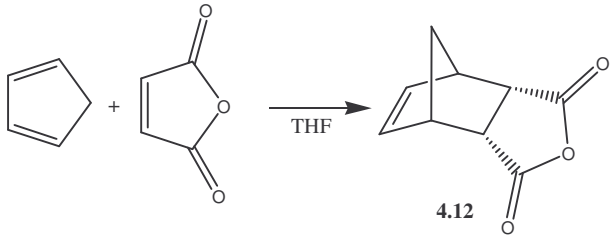

Figure 4.34: Diels-Alder reaction of cyclopentadiene with maleic anhydride.

It was believed that the *endo*-diol would prohibit polymerization of the norbornene due to chelation of the catalyst by the *endo*-diol functional group. Hennis and co-workers reported that palladium catalysts failed to polymerize *cis-endo*-2,3-

norbornenedimethylester. [83] However, they reported the palladium catalyzed polymerization of the *cis-exo*-2,3-norbornenedimethylester proceeded normally (**Fig. 4.35**).

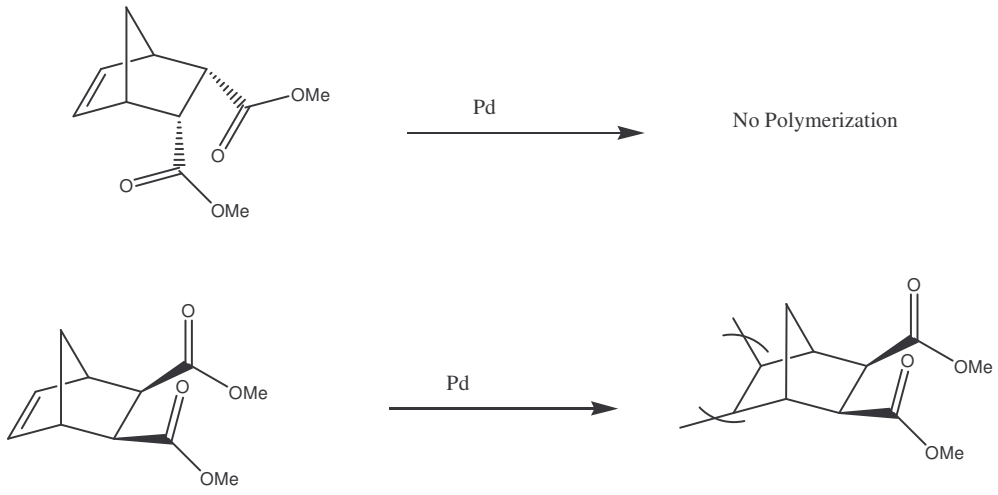

Figure 4.35: Literature precedence for polymerization reactivity of *endo* and *exo* norbornene isomers.

Evidence was also reported for the chelation of a Pt complex by the both the double bond of the norbornene ring and the carbonyl of the *endo* ester (**Fig. 4.36**). However, the chelation of a metal center with both the double bond and the carbonyl was not observed with the *exo* version of the monomer.

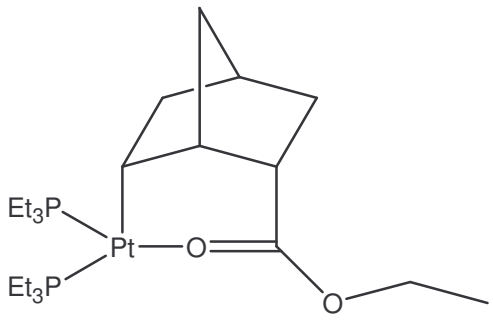

Figure 4.36: Platinum complex with *endo*- norbornene ester showing chelation of ester carbonyl with metal center.

According to this reported data, the ideal norbornene monomer is an *exo-cis*-diol. The *exo*-diol was synthesized by heating **4.12** which thermally isomerizes the anhydride to the exo Diels-Alder product **4.13** (**Fig. 4.37**). [84]

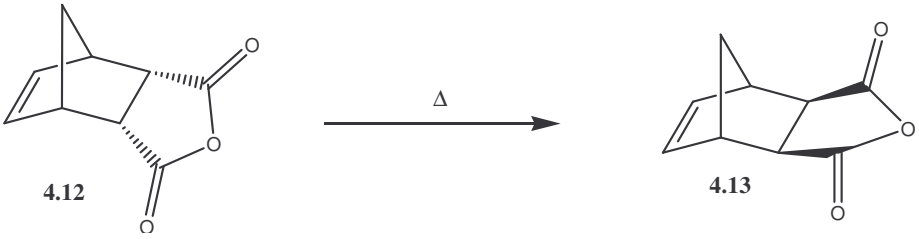

Figure 4.37: Thermal isomerization from *endo* isomer to *exo* isomer.

Compound **4.13** was then reduced to the corresponding diol **4.14** with LAH, then *t*-boc protected to form the desired monomer **4.15** (**Fig. 4.38**).

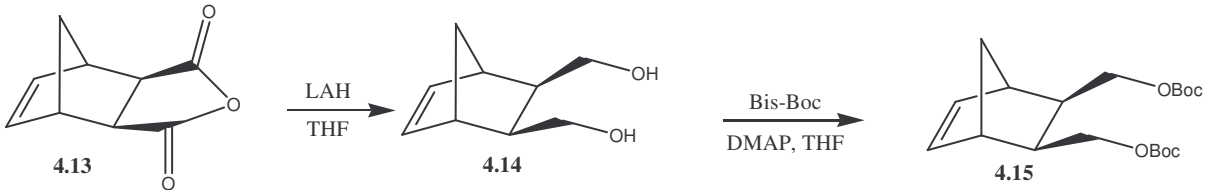

Figure 4.38: Synthesis of t-boc protected NB-diol, LAH reduction followed by t-boc protection.

The palladium catalyst used for the polymerization of **4.15** is an allyl palladium species generated *in-situ* (**Fig. 4.39**). [85,86,87,88]

Figure 4.39: In-situ synthesis of allyl palladium catalyst.

The polymerization of **4.15** with the palladium catalyst produced an insoluble polymer. The authors reported their studies with the ester. The diol may have different reactivities so the *endo* isomer was synthesized (**Fig. 4.40**).

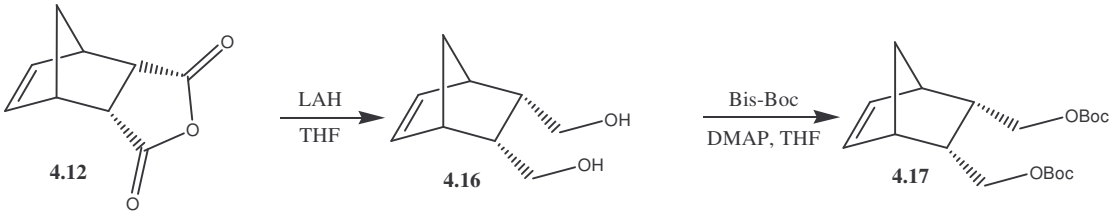

Figure 4.40: Synthesis of *t*-boc protected *endo*-NB-diol, LAH reduction followed by *t*-boc protection.

The *t*-boc protected *endo*-diol (**4.17**) polymerized using the palladium catalyst and produced a polymer soluble in organic solvents.

Isocyanate Reactivity in Polymer Films

During diol polymer synthesis, poly-(vinyl alcohol) (PVA) was used as a test polymer for silylation with TMSMIS (**4.11**). Even though poly-(vinylalcohol) does not meet all of the TSI resin characteristics, namely substrate etch resistance, it should clearly

demonstrate whether or not silylation with the isocyanate is occurring. Since PVA is not soluble in many organic solvents it was coated out of water and baked to drive off the water. The silylation of the PVA film was carried out in a gas phase silylation chamber design to monitor in real time the film properties during silylation. [89]

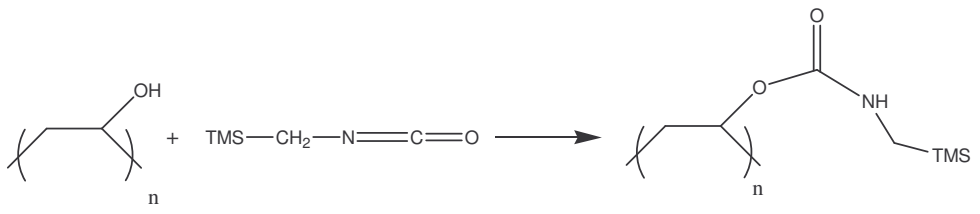

Figure 4.41: Reaction of TMSMIS with PVA as a proof of concept.

The chamber was designed to introduce a volatile silylating agent while monitoring the film thickness by variable angle scanning ellipsometery (VASE) in real time. When silylation occurs, the film thickness increases as the silylating agent is incorporated. Silylation was carried out at several temperatures and the thickness of the film grew dramatically indicating incorporation of the isocyanate into the film (**Fig. 4.42**).

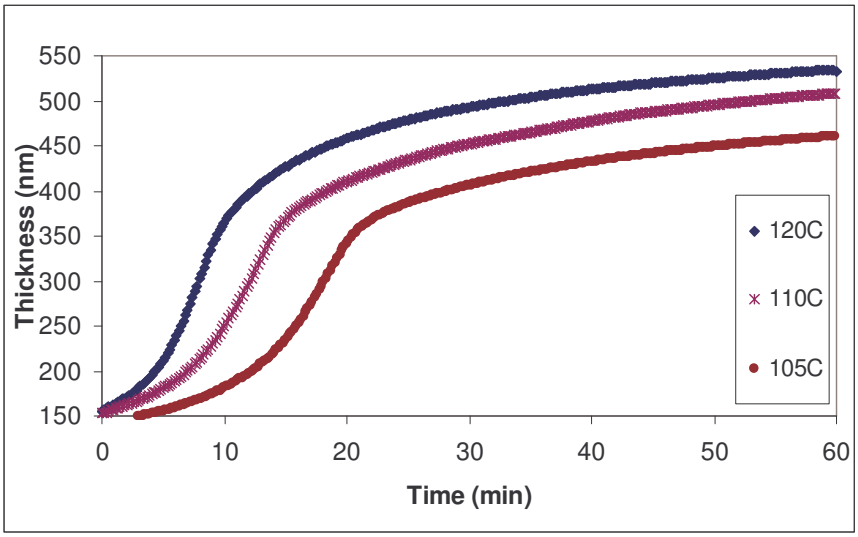

Figure 4.42: TSI resin thickness as a function of time as silylation was carried out at different temperatures.

An IR of the film before and after silylation indicates the formation of a carbonyl resonance and the change of the OH stretch to an amide stretch (**Fig. 4.43**).

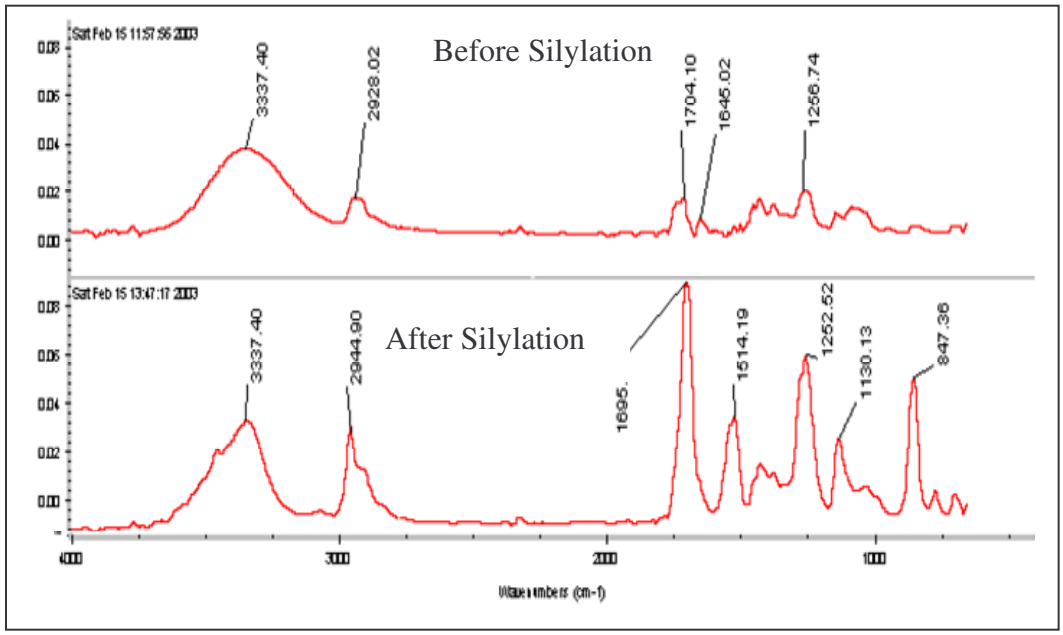

Figure 4.43: IR of PVA film before and after silylation with TMSMIS.

These results were encouraging and indicated the TMSMIS was reactive in the film. However, the film was cast from water, which is a cause for concern. Isocyanates react rapidly with water and it is very difficult to completely remove water from PVA. Therefore, it was conceivable that TMSMIS (**4.11**) reacted with water in the film instead of the alcohol of the PVA. To determine if the isocyanate reacted with the PVA or water, a *t*-boc protected PVA was synthesized according to the work published by Jiang and co-workers.[90]

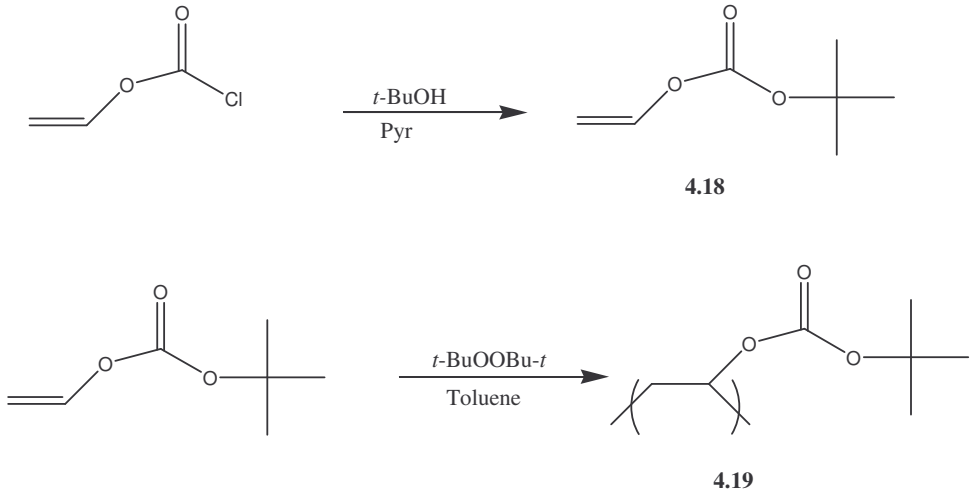

Figure 4.44: Synthesis of *t*-boc protected PVA.

A solution of **4.19**, with photoacid generator in propylene glycol methyl ether acetate (PGMEA) as the solvent, was spin coated onto a wafer. Coating the polymer out of an organic solvent should aid in eliminating water from the film. The resin was exposed, producing acid, and baked to remove the *t*-boc protecting group, resulting in a relatively

dry PVA film. Isocyanate was then introduced into the chamber and no reaction (film thickness change) with the PVA was observed. This was a surprising result in lieu of the previous experiment, coupled with the fact that isocyanates react readily with alcohols. It was thus concluded that the isocyanate reacted exclusively with residual water in the PVA film cast from water. To reach the final goal of using isocyanates for TSI, more investigation was required regarding the reactivity of the TMSMIS (**4.11**).

Isocyanate Reactivity in Solution

To address the lack of reactivity of TMSMIS with PVA, the isocyanate was studied in solution using FT-IR. The isocyanate was added to a solution of dry THF with an equal molar amount of dry methanol (**Fig. 4.45**).

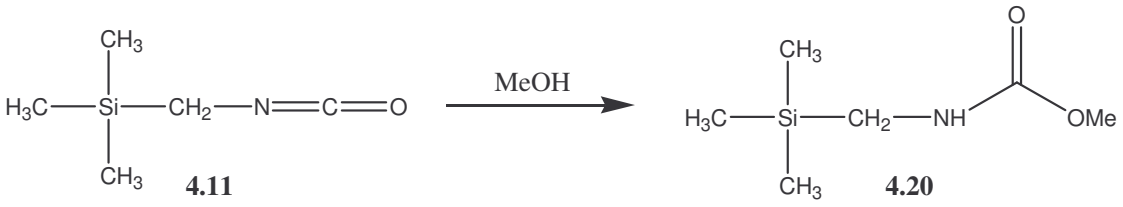

4.11 **4.20**

Figure 4.45: Reaction of TMSMIS with methanol.

The reaction was stirred at room temperature and monitored via FT-IR. Even after stirring for 22 hrs no formation of **4.20** was observed.

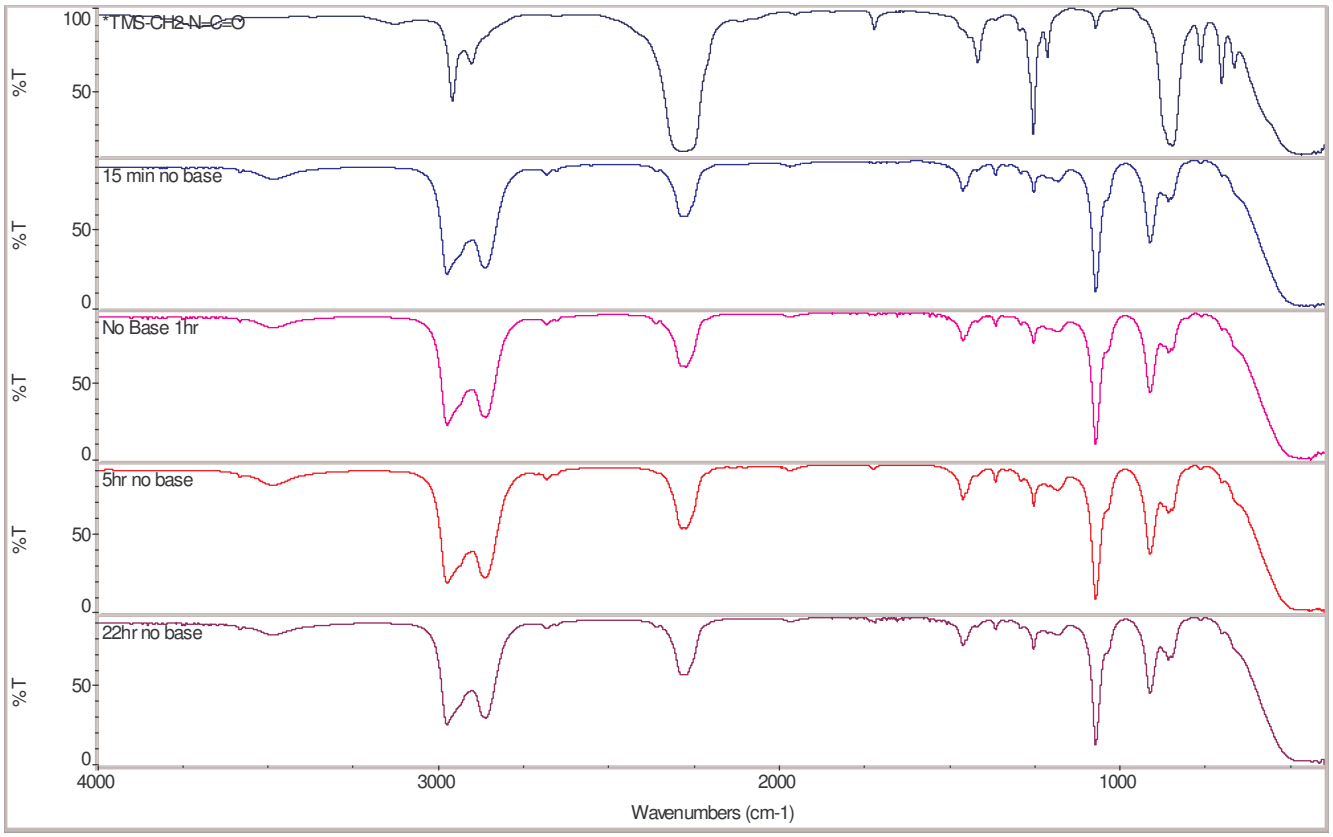

Figure 4.46: IR showing no reaction of MeOH with TMSMIS at room temperature.

Since the reaction of isocyanates with alcohols is catalyzed by a tertiary amines the same experiment was carried out using five mole percent triethylamine as a catalyst. Surprisingly even after 22 hrs again no reaction was observed.

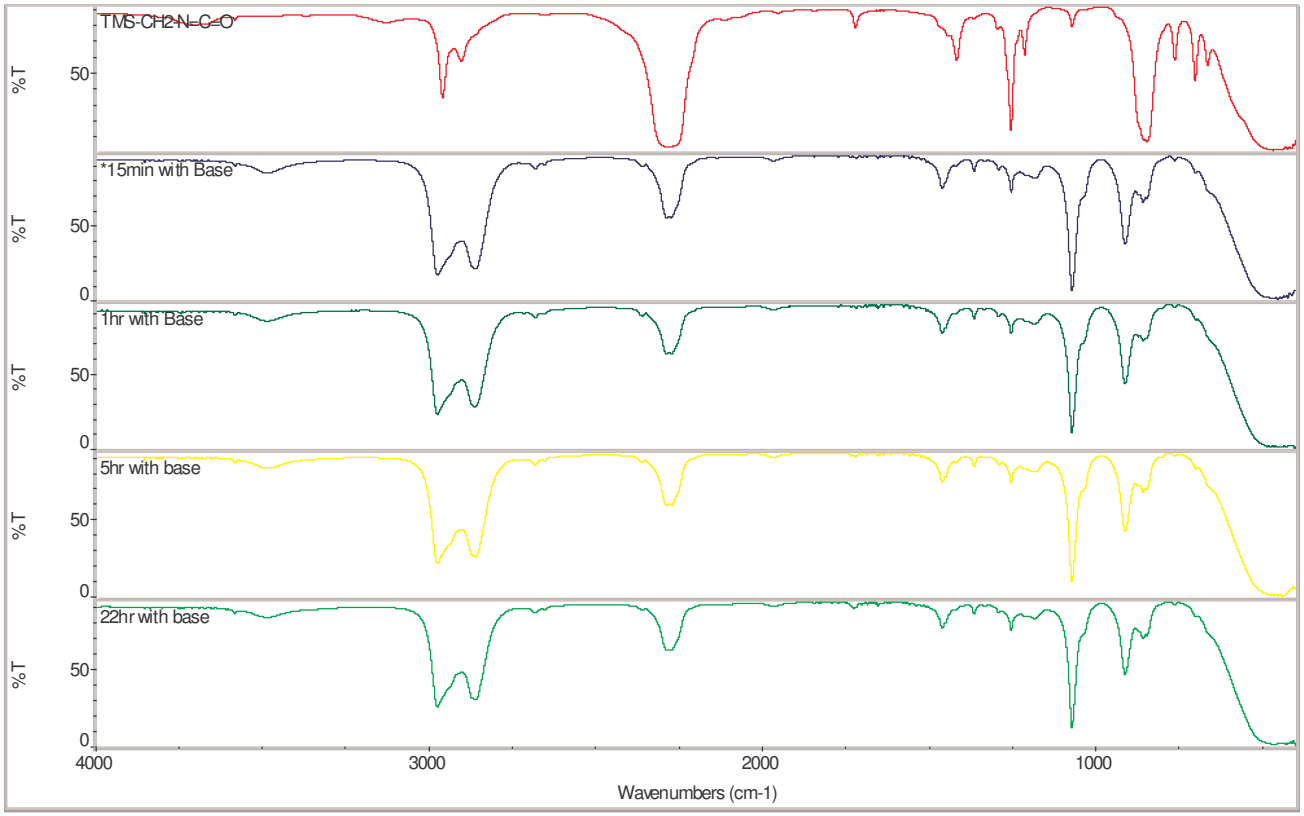

Figure 4.47: Experimental IR showing no reaction of MeOH with TMSMIS at room temperature using triethylamine as a base catalyst.

It is known that silicon has an unusual electronic property, known as the "beta" effect. Silyl groups are able to stabilize beta carbocations through hyperconjugation of the C-Si bond.[91] It is not clear whether the beta effect was prohibiting the isocyanate reaction with the alcohol, since the isocyanate nitrogen is beta to the silicon atom. To address this issue, the carbon analog of the isocyanate was synthesized by the same method described earlier (**Fig. 4.31**).

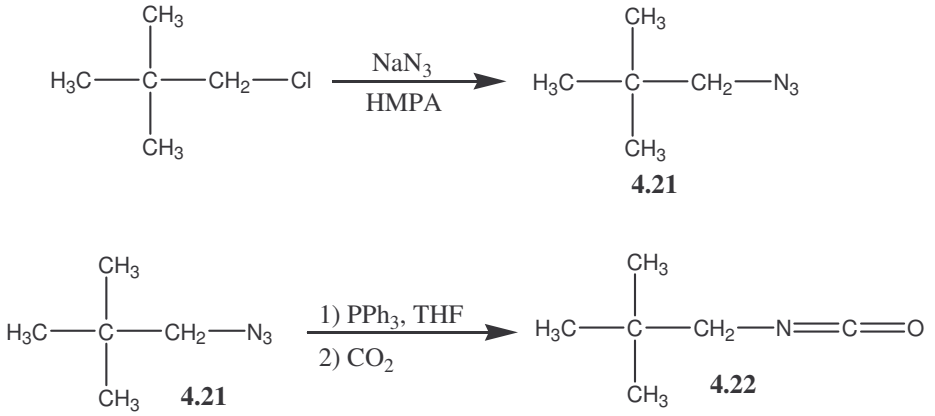

Figure 4.48: Synthesis of the carbon analogue of TMSMIS.

Compound **4.22** was tested in solution with methanol, and again failed to react after one hour. Dimethylaminopyridine (DMAP) was also used as a catalyst but failed to promote any reaction (**Fig. 4.48**).

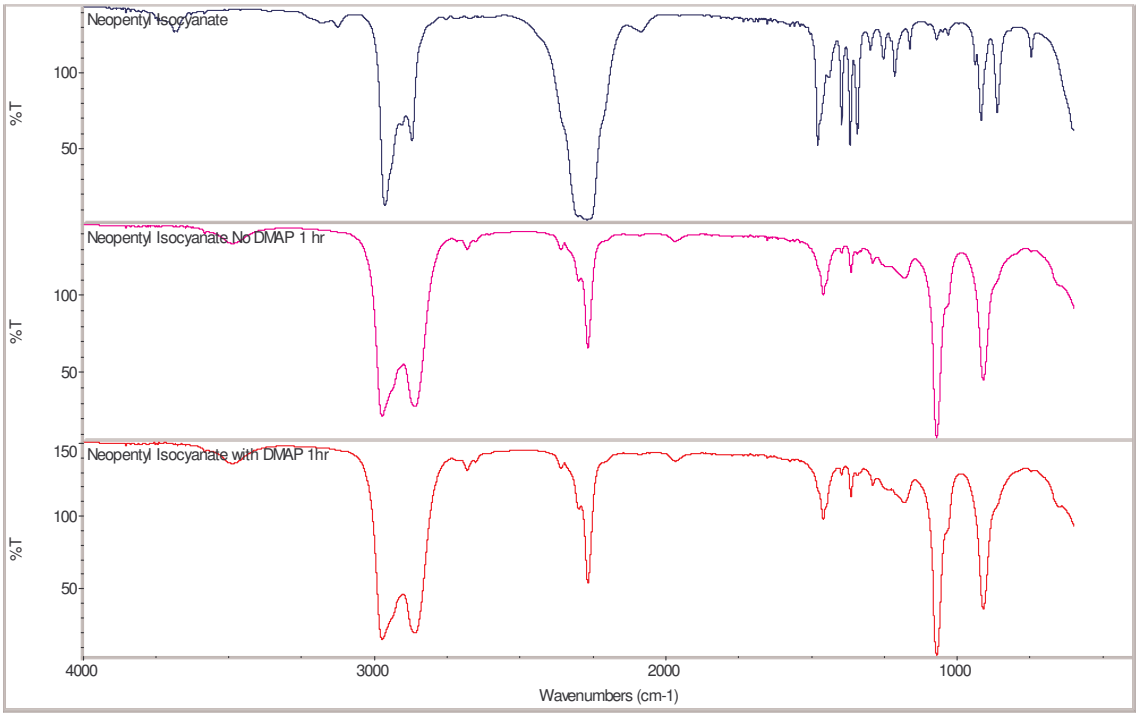

Figure 4.49: Carbon analog of TMSMIS with MeOH, with and without base catalyst.

Given that both the silicon and carbon analogues failed to react with methanol, steric hindrance was thought to be a reason for the lack of the isocyanates reactivity. To determine whether steric effects were an issue, an isocyanate was synthesized with more distance between the bulky TMS group and the isocyanate functional group. The elongated isocyanate was synthesized via the same method use for both **4.11** and **4.22** (**Fig. 4.49**).

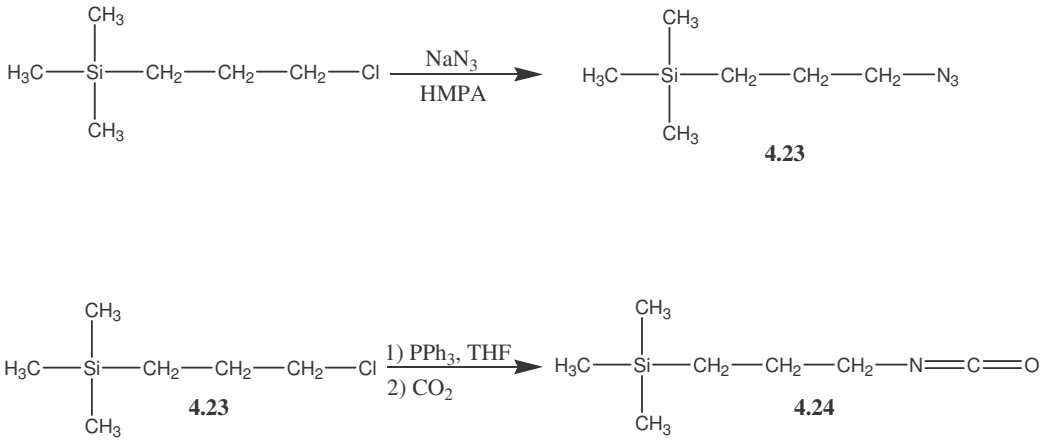

Figure 4.50: Synthesis of less sterically hindered TMS containing isocyanate.

Compound **4.24** was tested in the same manor as the TMSMIS (**4.11**) and again failed to show any reactivity toward methanol both with (**Fig. 4.50**) and without (**Fig. 4.51**) triethylamine as a catalyst.

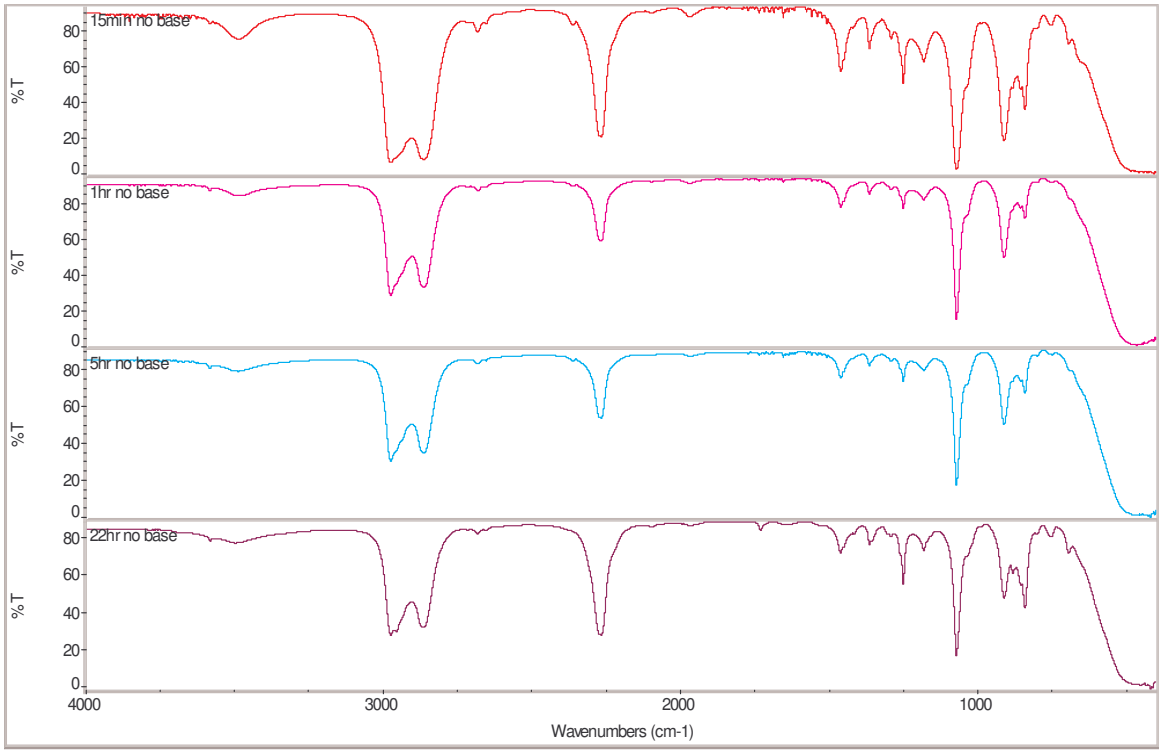

Figure 4.51: Reaction of 4.24 and methanol without base catalyst.

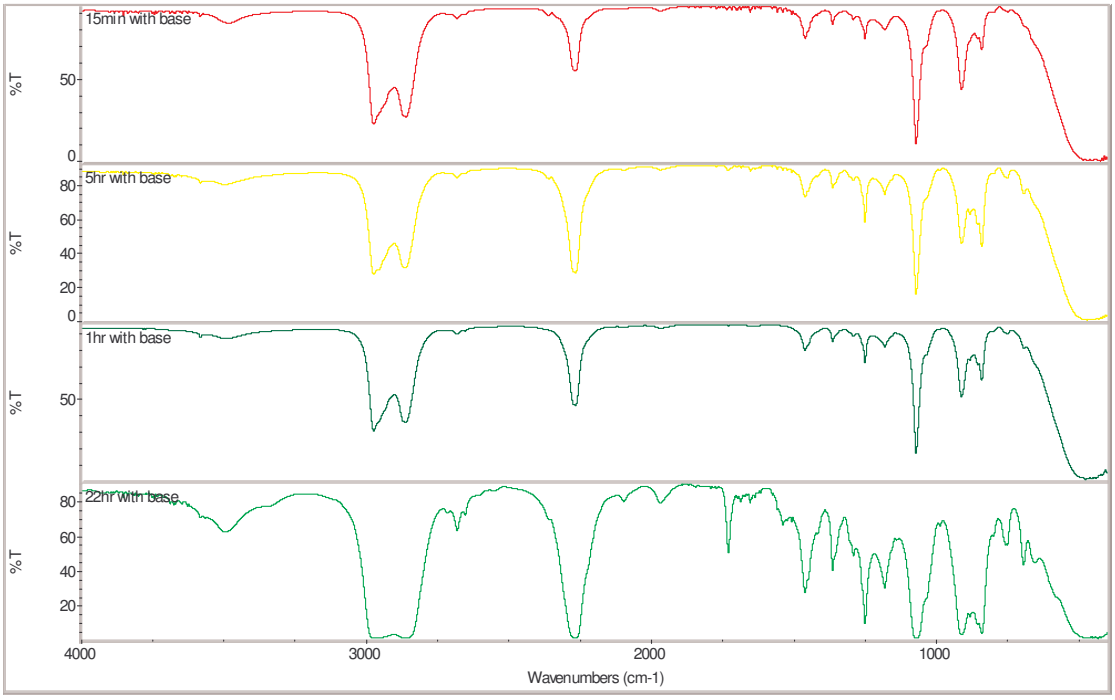

Figure 4.52: Reaction of 4.24 with methanol using triethyl amine as a catalyst.

Throughout all these experiments, only the least sterically hindered isocyanate reacted. At 22hrs at room temperature with triethylamine a small carbonyl stretch is observed in the IR (**Fig. 4.51**).

Since the isocyanates were slow to react at room temperature, TMSMIS (**4.11**) was heated in the presence of methanol. These reactions were carried out in an NMR tube using deuterated benzene as the solvent, and the tube was heated to 50°C.

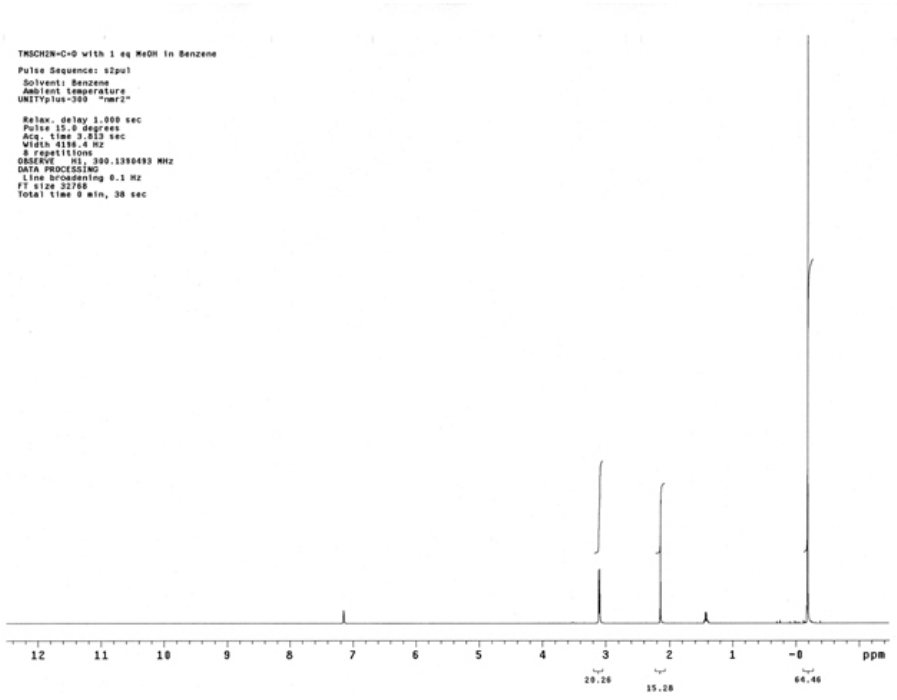

Figure 4.53: NMR of TMSMIS (4.11) with MeOH before heating.

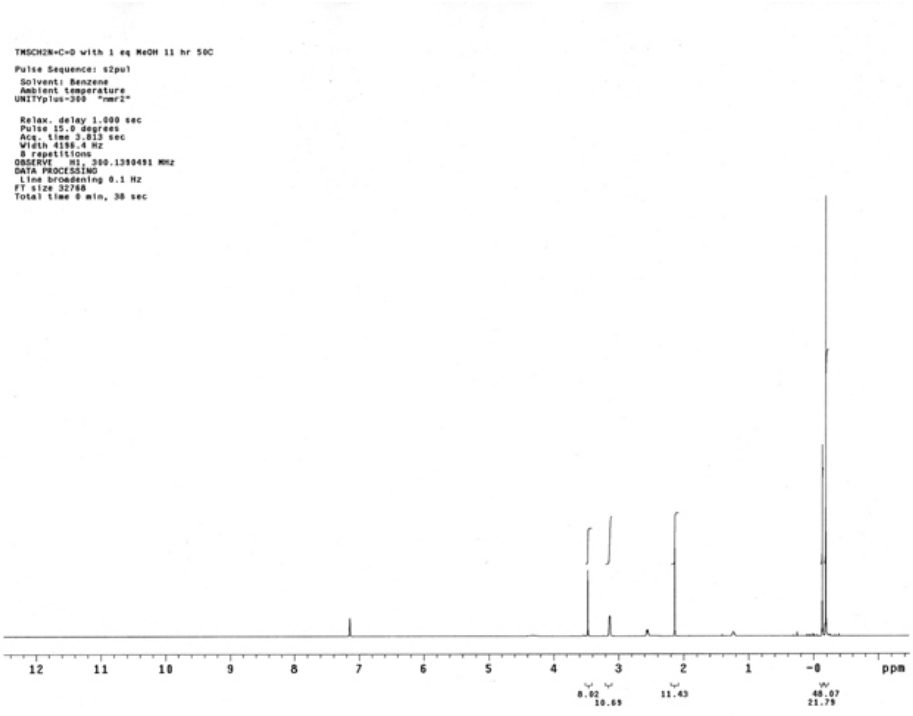

Figure 4.54: NMR of TMSMIS (4.11) reacting with MeOH for 11hrs at 50C.

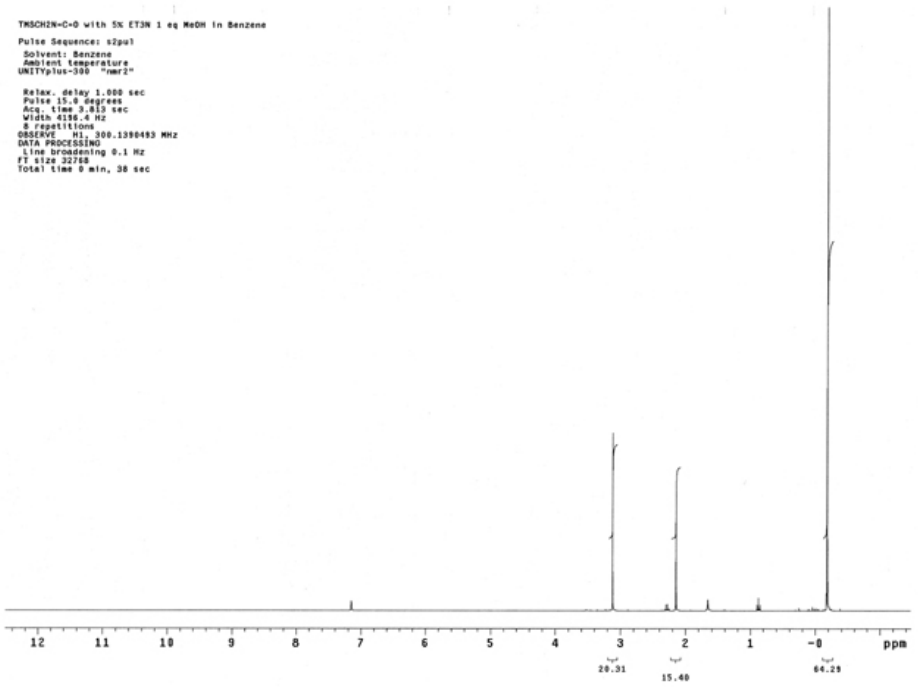

Figure 4.55: NMR of TMSMIS (4.11) with MeOH and 5% triethyl amine.

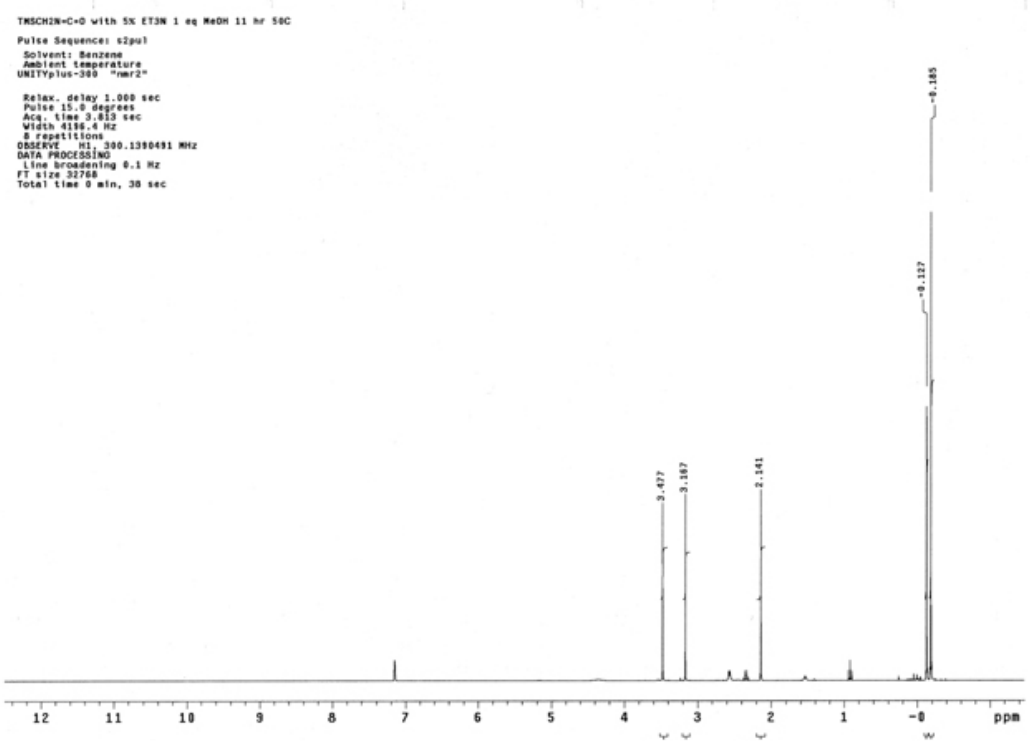

Figure 4.56: NMR of TMSMIS (4.11) reacting with MeOH and 5% triethyl amine for 11hrs at 50C.

Heating at 50°C for 11hrs with (**Fig. 4.55**) and without (**Fig. 4.54**) base catalyst TMSMIS (**4.11**) failed to react to completion. In conclusion, the silylation use of TMSMIS (**4.11**) for TSI was not achieved. While there is precedence for the reactivity of isocyanates with polymer films.[92] The reactivity of the isocyanate both in the gas phase and in solution is too slow to be of any use. The literature precedence uses methyl isocyanate which is more volatile and have a higher pressure during gas phase silylation. This higher pressure means there is a higher concentration of isocyanate available for reacting with the polymer film.

---

[54] Kunz, R.R. *et al*., Proc. SPIE 3678, 13 (**1999**).

[55] Tran, H. V. PhD Thesis, University of Texas at Austin, **2002**.

[56] Bae, C. Y.; Douki, K.; Yu, T.; Dai, J.; Schmaljohann, D.; Koerner, H.; Ober, C. K. *Chem. Mater.* **2002**, *14*, 1306-1313.

[57] Trinque, B. T.; *et. al. J. Vac. Sci. Technol. B.* **2002**, *20*, 531-536.

[58] Trinque, B. C., Chiba, T., Hung, R. J., Chambers, C. R., Pinnow, M. J., Osburn, B. P., Tran, H. V., Wunderlich, J., Hsieh, Y., Thomas, B. H., Shafer, G., DesMarteau, D. D., Conley, W., Willson, C. G. *J. Vac. Sci. Technol. B*, **2002**, *20*, 531-536.

[59] Trinque, Brian PhD Thesis, University of Texas at Austin, 2003.

[60] Patterson, K.; Yamachika, M.; Hung, R.; Brodsky, C.; Yamada, S.; Somervell, M.; Osborn, B.; Hall, D.; Dukovic, G.; Byers, J.; Conley, W.; Willson, C. G. *Proc. SPIE-Int. Soc. Opt. Eng.* **2000**, *3999*, 365-374.

[61] Ishikawa, T., Kodani, T., Yoshida, T., Moriya, T., Yamashita, T., Toriumi, M., Araki, T., Aoyama, H., Hagiwara, T., Furukawa, T., Itani, T., Fujii, K., *Journal of Fluorine Chemistry*, **2004**, *125*, 1791-1799.

[62] Osborn, Osborn PhD Thesis, University of Texas at Austin, 2004.

[63] Hung, R. J.; Tran, H. V.; Trinque, B. C.; Chiba, T.; Yamada, S.; Sanders, D. P.; Connor, E. F.; Grubbs, R. H.; klopp, J.; Frechet, J. M. J.; Thomas, B. H.; Shafer, G. J.; DesMarteau, D. D., Conley, W.; Willson, C. G. *Proc. SPIE-Int. Soc. Opt. Eng.* **2001**, *4345*, 385-395.

[64] Li, W., Varanasi, P. R.; Lawson, M. C.; Kwong, R. W.; Chen, K.; Ito, H.; Truong, H.; Allen, R. D.; Yamamoto, M.; Kobayashi, E.; Slezak, M. *Proc. SPIE-Int. Soc. Opt. Eng.* **2003**, *5039*, 61-69.

[65] Ito, H.; Hinsberg, W. D.; Rhodes, L. F.; Chang, C. *Proc. SPIE-Int. Soc. Opt. Eng.* **2003**, *5039*, 70-79.

[66] Crawford, M. K.; Farnham, W. B.; Feiring, A. E.; Feldman, J.; French, R. H.; Leffew, K. W.; Petrov, V. A.; Qiu, W.; Schadt III, F. L.; Tran, H. V.; Wheland, R. C.; Zumsteg, F. C. *Proc. SPIE-Int. Soc. Opt. Eng.* **2003**, *5039*, 80-92.

[67] Tran, H. V.; Hung, R. J.; Chiba, T.; Yamada, S.; Mrozek, T.; Hsieh, Y.-T.; Chambers, C. R.; Osborn, B. P.; Trinique, B. C.; Pinnow, M. J.; MacDonald, S. A.; and Willson, C. G. *Macromolecules*, **2002**, *35*, 6539-6549.

[68] Kodama, S.; Kaneko, I.; Takebe, Y.; Okada, S.; Kawaguchi, Y.; Shida, N.; Ishikawa, S.; Toriumi, M.; Itani, T. *Proc. SPIE-Int. Soc. Opt. Eng.* **2002**, *4690*, 76-83.

[69] Sebald, M.; Sezi, R.; Leuschner, R.; Ahne, H.; Birkle, S. *Microelectr. Eng.* **1990**, *11*, 531-534.

[70] Baik, K.; Van den hove, L.; Roland, B. *J. Vac. Sci. Technol. B.* **1991**, 3399-3405.

[71] Hartney, M. A.; Kunz, R. R.; Eriksen, L. M.; LaTulip, D. C. *Optical Engineering* **1993**, 2382-2387.

[72] Shaw, J. M.; Hatzakis, M.; Babich, E. D.; Paraszczak, J. R.; Whitman, D. F.; Stewart, K. J. *J. Vac. Sci. Technol. B.* 1989, *7*, 1709-1716.

[73] Roland, B., Lambaerts, R., Jakus, C., Coopmans, F., *Proc. SPIE-Int. Soc. Opt. Eng.* **1987**, *771*, 69-76.

[74] Coopmans, F., Roland, B., Lombaerts, R. *Microelectronic Engineering*, **1986**, *5*, 291-297.

[75] Garza, C. M., *Proc. SPIE-Int. Soc. Opt. Eng.* **1988**, *920*, 233-240.

[76] Ito, H.; MacDonald, S. A.; Miller, R. D.; Willson, C. G. U.S. Patent 4,552,83, (1985).

[77] Sommerville, Mark PhD Thesis, University of Texas, 2000.

[78]http://public.itrs.net/Files/2003ITRS/Litho2003.pdf

[79] Wheeler, D., Hutton, R., Boyce, C., Stein, S., Cirelli, R., Taylor, G., *Proc. SPIE-Int. Soc. Opt. Eng.* **1995**, *2438*, 762-774.

[80] Turner, S. R., Arcus, R. A., Houle, C. G., Schleigh, W. R. *Polymer Engineering and Science*, **1986**, *26*, 1096-110.

[81] Tsuge, O., Kanemasa, S., Matsuda, K., *J. Org. Chem.*, **1984**, *49*, 2688-2691.

[82] Tsuge, O., Kanemasa, S., Matsuda, K., *Chemistry Letters*, **1983**, 1131-1134.

[83] Hennis, A. D., Polley, J. D., Long, G. S., Sen, A. *Organomettallics*, **2001**, *20*, 2802-2812.
[84] Craig, D. *J. Am. Chem. Soc.* **1951**, *73*, 4889-4892.

[85] Okoroanyanwu, U. Ph.D. Dissertation, The University of Texas at Austin, 1997.

[86] Risse *et al, Makromol. Chem., Rapid Commun*., **1991**, 12, 255

[87] Goodall, B. L. *et al*. *International patent,* WO 9733198 (1997)

[88] Mathew, J. P., Reinmuth, A., Melia, J., Swords, N., Risse, W. *Macromolecules*, **1996**, *29*, 2755-2763.

[89] Jamieson, Jamieson PhD Thesis, University of Texas at Austin, 2004.

[90] Jiang, Y., Frechet, J. M. J., Willson, C. G., *Polymer Bulletin*, **1987**, *17*, 1-6.

[91] Brooke, M. A. *Silicon in Organic, Organomettallic, and Polymer Chemistry,* John Wiley and Sons: USA, 2001.

[92] MacDonald, S. A.; Schlosser, H.; Clecak, N. J.; Willson, C. G. *Chem. Mater.* **1992**, *4*, 1364-1368.

Chapter 5 - Experimental Section

Materials Nitrogen was purified by passage through Sicapent® and then KOH. All solvents were dried by the standard methods. All manipulations and polymerizations with air-sensitive materials were performed in a helium-filled drybox or using standard Schlenk vacuum line techniques under argon. All starting materials were procured from Aldrich or Acros.

Instruments and Equipment Nuclear magnetic resonance (NMR) spectra were obtained using either a varian *Unity Plus 300* spectrometer (^{1}H: 300 MHz, ^{13}C: 75 MHz, ^{19}F: 282 MHz) or *varian Unity Plus 400* (^{1}H: 400 MHz, ^{13}C: 100 MHz). Shifts for NMR spectra are reported in ppm and refernced to the corresponding NMR solvent (for ^{19}F, $CFCl_3$. Infrared spectra were recorded on a Nicolet *Avatar 360* IR spectrometer. Melting points are uncorrected. Mass spectra were measured on a Finnigan *MAT TSQ-700* spectrometer. Molecular weights (M_w) and polydispersity indices (PDI) were measured from THF solutions using a Viscotek GPC equipped with a set of two 5 mm crosslinked polystyrene columns (linear mix and 100 Å) from American Polymer Standards and are reported relative to polystyrene standards. Polymers containing acidic functional groups were pretreated with TMS-diazomethane. Differential scanning calorimetry (DSC) measurements and thermal gravimetric analysis (TGA) were performed on a Perkin Elmer *Series-7* thermal analysis system. Gas chromatographs

were recorded on a Hewlett Packard *5890 Series II* with an *HP-5* (crosslinked 5% PH ME siloxane) capillary column and flame ionization detector (FID).

5,5-Dimethyl-4,10-dioxa-tricyclo[5.2.1.0]dec-8-en-3-one (2.6)

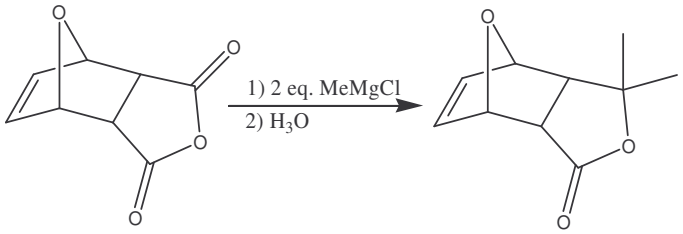

To a round bottom flask (250 mL) was added a solution of 7-oxabicyclo[2.2.1]hept-5-ene-2,3-dicarboxylic anhydride (4.00g, 0.0260 moles) in dry THF (125 mL). To this solution was added via syring 22% by weight methyl magnesium chloride (25.7 mL, 26.47g 0.0779 moles) at 0^{O}C. The solution was stirred for 4 hrs at 0^{O}C. The excess Grignard reagent was quenched with the addition 3M HCl. To the solution was added water (150 mL) and ether (300 mL) followed by acidification with 3 M HCl to Ph < 4. The layers were separated and the aqeous fraction was extracted with ether (300 mL). The organic layers were combined and washed with saturated aqeaous sodium bicarbonate (100 mL) and brine (100 mL). The organic layer was dried with anhydrous magnesium sulfate, filtered and the solvent removed via rotarty evaporation to yield a tan solid (3.273g). The crude solid was chromatographed on silica (hex:EtOAc 3:2) collecting first fraction yield **2.6** (2.888g, 0.0160 moles, 62%%) as a white solid**:** mp = 80-80.5^{O}C; ^{1}H NMR ($CDCl_3$, 300 MHz) 1.427 (s, 3H), 1.505 (s, 3H), 2.258 (d, *J* = 7.8 Hz, 1H), 2.971 (d, *J* = 7.5 Hz, 1H), 5.127 (s, 1H), 5.256 (s, 1H), 6.438 (dq, *J* = 1.7 Hz,

5.9 Hz); ^{13}C NMR ($CDCl_3$, 300 MHz) 23.493, 31.548, 49.828, 50.753, 80.416, 81.464, 84.021, 136.945, 137.295, 74.787; IR (DCM, NaCl) 3056, 2979, 1759; HRMS (CI, CH_4) M+1 Calc. 181.0865, Found 181.0868;

5,5-Dimethyl-5*H*-furan-2-one (2.7)

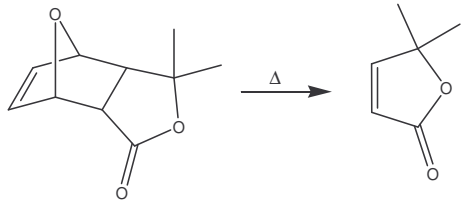

In a round bottom flask (25 mL) was added **2.6** (2.695g, 0.0160 moles) and heated at 130^{O}C under reflux for two hours. The resulting oil was distilled to yield **2.7** (1.395g, 0.0124 moles, 78%) as a clear oil: bp 45^{O}C @ 1.5 torr; ^{1}H NMR ($CDCl_3$, 300 MHz) 1.432 (s, 6H), 5.923 (d, *J* = 5.7 Hz, 1H), 7.369 (d, *J* = 5.7 Hz, 1H); ^{13}C NMR ($CDCl_3$, 300 MHz) 25.234, 86.541, 119.714, 161.306, 172.398; IR (neat, NaCl) 3084, 2979, 2932, 2866, 1748; HRMS (CI, CH_4) M+1 calc. = 113.0603, found 113.0600;

5,5-Dimethyl-dihydro-furan-2-one (2.1)

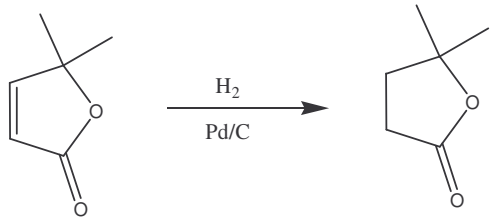

In a Parr high pressure apparatus was added **2.7** (1.00g, 0.00892 moles), Pd/C (100 mg) and ethyl acetate 20 ml. The bomb was pressurized to 65 psig and was stirred over night. The Pd was filtered out with a celite plug and the solvent removed by rotary evaporation

to yield **2.1** (927 mg, 0.008126 moles, 91%) as a clear oil: ^{1}H NMR (DMSO-d_6, 300 MHz) 1.335 (s, 6H), 1.981 (t, *J* = 8.1 Hz, 2H), 2.580 (t, *J* = 8.7 Hz, 2H); ^{13}C NMR (DMSO-d_6, 300 MHz) 27.338, 28.867, 33.900, 84.173, 176.475; IR (neat, NaCl) 2971, 2932, 2874, 1767; HRMS (CI, CH_4) M+1 calc = 115.-759 found 115.0763;

6,6-Dimethyl-tetrahydro-pyran-2-one (2.2)

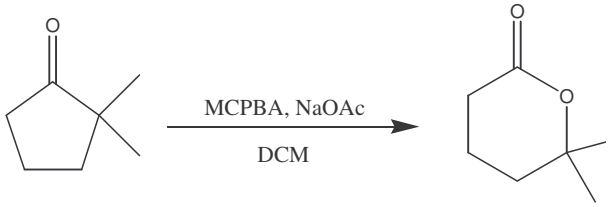

To a round bottom flask (25 mL) was added 2,2-dimethycyclopentanone (0.200g, 0.00178 moles), MCPBA (~77% pure, 0.559g, 0.00250 moles), sodium acetate (0.2457 g, 0.00300 moles) in DCM (20 mL). The reaction was heated at 42^{O}C overnight. The reaction solution was stirred with an aqeous sodium thiosulfate solution (10% by weight, 50 mL) until the DCM layer turned from cloudy to clear. The DCM layer was separated and washed with saturated sodium bicarbonate (3x100 mL), dried with magnesium sulfate, filtered and the solvent removed by rotary evaporation to yield a clear liquid **2.2** (0.183g, 0.00143 moles, 80%): ^{1}H NMR ($CDCl_3$) 1.329 (s, 6H), 1.685 (m, 2H), 1.811 (m, 2H), 2.402 (t, *J* = 6.9 Hz, 2H); ^{13}C NMR ($CDCl_3$) 16.63, 28.54, 28.93, 33.67, 82.08, 171.20; IR (neat, NaCl) 2971, 2889, 1728; HRMS (CI) M+1 calc = 129.0916 found 129.0920.

7,7-Dimethyl-oxepan-2-one (2.5)

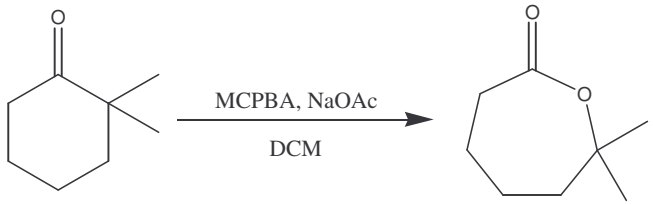

In a round bottom flask (25 mL) was added 2,2-dimethylcyclohexanone (0.100g, 7.90×10^{-4} moles), MCPBA (77% pure, 0.248g, 0.00144 moles), sodium acetate (0.1093g, 0.00133 moles) in DCM (10 mL). The reaction was heated at $42^{O}C$ overnight. The reaction was allowed to cool to r.t. and then stirred with aqeous sodium thiosulfate (10% by weight, 20 mL) until the DCM layer turned from cloudy to clear. The DCM layer was seperated and washed with saturated sodium bicarbonate (3x50 mL), dried with magnesium sulfate and the solvent removed via rotary evaporation to yield **2.5** (0.096g, 6.75×10^{-4} moles, 85%) as a clear liquid: ^{1}H NMR (DMSO-d_6) 1.369 (s, 6H), 1.564 (m, 2H), 1.707 (m, 2H), 1.776 (m, 2H), 2.598 (m, 2H); ^{13}C NMR ($CDCl_3$, 75 MHz) 23.10, 23.94, 28.20, 36.88, 39.95, 81.05, 174.58; IR (neat, NaCl) 2975, 2928, 2862, 1713; HRMS (CI) M+1 calc. = 143.1072 found 143.1073

3-hydroxy-3-methyl-2-phenylbutyric acid (2.8)

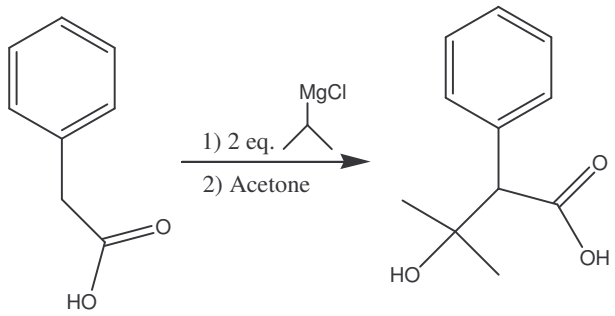

In a three necked round bottom flask (500 mL) fitted with a condenser under nitrogen atmosphere was added phenyl acetic acid (10.00 g, 0.0734 moles) and dry THF (50 mL). The solution was stirred at 0 °C while a freshly prepared solution of isopropylmagnesium chloride (12.98 g, 0.165 moles, 14.55 mL isopropyl chloride; 4.103 g, 0.169 moles magnesium, 200 mL dry THF) was added via canula. The reaction mixture was warmed to room temperature and stirred for 12 hrs. Dry acetone (8.53 g, 0.147 moles, 10.78 mL) was added via syringe and the reaction mixture was heated to 70 °C for 2 hrs. The reaction mixture was cooled to r.t., poured into ice and acidified to pH<4 with 3M HCl. The solution was extracted with ether (2 x 250 mL), the organic layer was washed with brine and dried with magnesium sulfate. The volatiles were removed via rotary evaporation and the residue was dried under high vacuum at 60 °C for 2 hrs to produce **2.8** (14.30 g, 0.0736 moles, 100%) as a yellow oil: ^{1}H NMR ($CDCl_3$, 400 MHz) 1.089 (s, 3H), 1.369 (s, 3H), 3.625 (s, 1H), 7.35 (m, 5H); ^{13}C NMR ($CDCl_3$, 400 MHz) 26.54, 29.39, 60.45, 72.07, 127.84, 128.40, 129.59, 134.77, 178.324; HRMS (CI, CH_4) M^{+1} = 195.1027, calculated = 195.1021.

4,4-dimethyl-3-phenyl-oxetan-2-one (2.4)

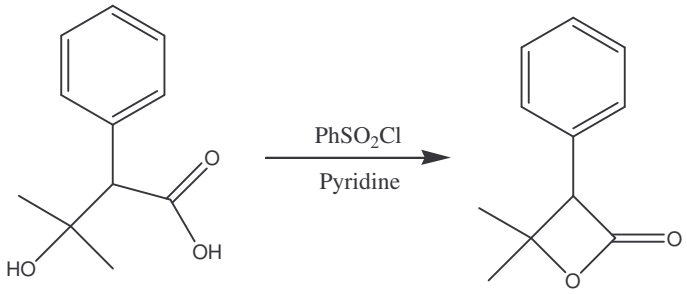

To a round bottom flask (250 mL) was added **2.8** (14.30 g, 0.0736 moles) and dry pyridine (100 mL). The solution was stirred at 0 °C and phenylsulfonyl chloride (15.15 g, 0.0883 moles, 10.95 mL) was added via syringe over 10 min. The reaction was stirred at 0 °C for 30 min and then stored in the freezer for 12 hrs. The solidified reaction mixture was dissolved in ether (350 mL) and extracted with aqueous saturated copper sulfate until no color change in the copper sulfate solution was observed. The ether was washed with brine and dried with magnesium sulfate, filtered and rotovaped. Chromatography (9:1, Hex:EtOAc; silica) yielded **2.4** (9.293 g, 0.0527 moles, 72%) as a white solid: mp = 56-57 °C; ^{1}H NMR ($CDCl_3$, 400 MHz) 1.195 (s, 3H), 1.750 (s, 3H), 4.607 (s, 1H), 7.183 (m, 2H), 7.340 (m, 3H); ^{13}C NMR ($CDCl_3$, 400 MHz) 23.18, 27.91, 63.82, 81.67, 128.00, 128.10, 128.91, 131.56, 169.03.

Fittig Bis-lactone (2.3)

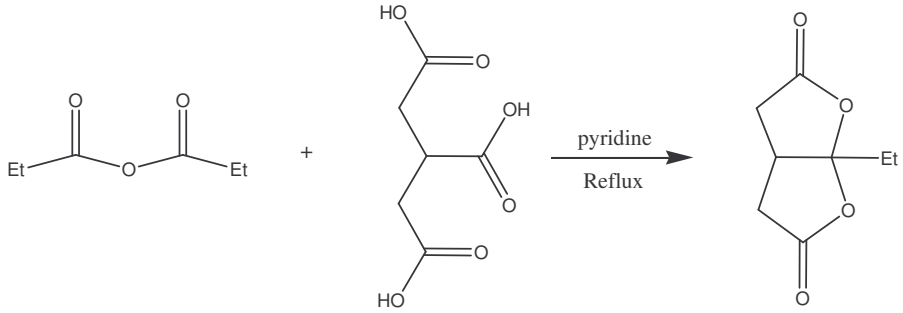

In a round bottom flask (250 mL) with a condenser was added tricarballyic acid (6.0 g, 0.0341 moles), pyridine (0.6 mL) and acetic anhydride (49 mL). The reaction mixture was heated under nitrogen to 160 °C for 6.5 hrs. The volatiles were distilled off and acetone (300 mL) and activated charcoal were added. The solution was stirred for 30 min, the charcoal removed by filtration and the volatiles removed by rotary evaporation. Recrystallization three times from toluene afforded **2.3** (0.454 g, 0.00289 moles, 9%) as white crystals: ^{1}H NMR (CD_3CN, 400 MHz) 1.766 (s, 3H), 2.53 (m, 2H), 3.00 (m, 3H); ^{13}C NMR (CD_3CN, 400 MHz) 23.81, 35.36, 38.94, 113.02, 172.35.

(4-Vinylphenyl)-acetic acid (2.13)

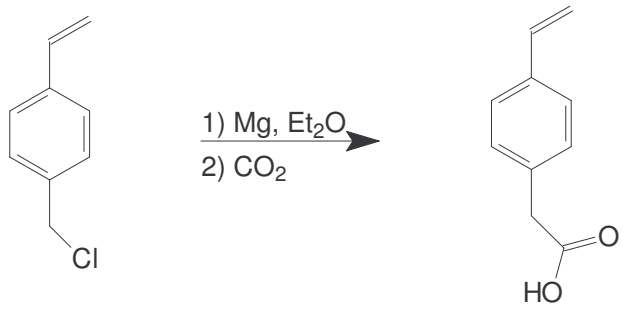

In a round bottom flask (1000 mL) fitted with a dropping funnel and condenser was added magnesium (5.28g, 0.220 moles), diethyl ether (400 mL) and the flask was purged with nitrogen. A solution of 1-chloromethyl-4-vinyl-benzene (30.5 g, 0.200 moles) in diethyl ether (100 mL) was added dropwise to the magnesium. After the Grignard reagent began forming the rest of the halide solution was added dropwise. The reaction mixture was then heated at reflux for 2½ hours. After cooling to room temperature carbon dioxide was bubbled through the solution. This was done for about 1 hour to insure excess carbon dioxide. The reaction mixture was then extracted with water (3X300 mL). The combined aqueous layers were acidified with 1 M HCl to pH = 1. The acidified aqueous fraction was extracted with ether (3X300 mL). The combined ether fractions were washed with brine (200 mL), dried with magnesium sulfate, filtered and the ether removed via rotary evaporation to yield crude **1** as a tan solid. The crude material was dissolved in ether (200 mL) and extracted with 1 N Sodium Hydroxide (3X200 mL). The combined aqueous fractions where acidified with 1 M HCl to pH = 1. The resulting precipitate was filtered and dried to yield **2.13** (16.393g, 0.1011 moles,

51%) as a white solid: ^{1}H NMR (DMSO-d_6) 3.546 (s, 2H), 5.223 (d, *J* = 5.4 Hz, 1H), 5.792 (d, *J* = 17.7 Hz, 1H), 6.69 (dd, *J* = 10.8, 17.7 Hz), 7.221 (d, *J* = 8.1 Hz, 2H), 7.401 (d, *J* = 8.1 Hz, 2H), 12.37 (s, 1H); ^{13}C NMR (DMSO-d_6) 40.381, 113.886, 126.012, 129.012, 134.759, 135.524, 136.376, 172.622; IR (KBr), 3448, 3083, 3029, 2970, 2924, 3300-2500, 1697; HRMS (CI, CH_4) calc. M+ = 162.0681 found 162.0686.

3-hydroxy-3-methyl-2-(4-vinylphenyl) butyric acid (2.14)

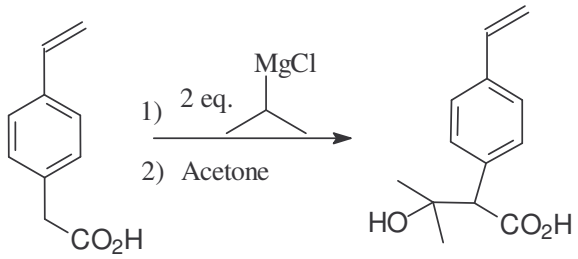

In a round bottom flask (250 mL) was added (4-Vinylphenyl)-acetic acid (5.00g, 0.0308 moles) and dry THF (50 mL). This solution was cooled in an ice bath and isopropyl magnesium chloride (2M in THF, 32.3 mL, 0.0646 moles) was added dropwise. The resulting mixture was stirred at 0^{O}C for 2 hrs. The reaction was warmed to rt and freshly distilled acetone (5 mL, excess) was added via syringe. The solution was then heated at 65^{O}C for 45 min. The reaction was cooled by addition of ice (~100 mL) and then acidified with HCl (3M) until pH 4. It was then extracted with ether (3 X 200 mL). The combined ether layers were washed with brine (200 mL) and dried over anhydrous magnesium sulfate. The solvent was removed via rotary evaporation and then dried under high vacuum to yield **2.14** (4.83g, 0.0219 moles, 71%) as a red oil: ^{1}H NMR ($CDCl_3$) 1.067 (s, 3H), 1.351 (s, 3H), 3.582 (s, 1H), 5.221 (dd, *J* = 0.9 Hz, 11.1 Hz, 1H),

5.713 (dd, *J* = 0.8 Hz, 17.6 Hz, 1H), 6.672 (dd, *J* = 11.0 Hz, 17.4 Hz, 1H), 7.331 (s, 4H); ^{13}C NMR ($CDCl_3$) 26.566, 29.480, 60.082, 71.960, 114.113, 126.145, 129.771, 134.644, 134.644, 136.260, 137.040, 177.088; IR (neat, NaCl) 3363, 2974, 2878, 2936, 2714, 2602, 1701; HRMS (CI, CH_4) calc. M+1 = 221.1178 found 221.1181.

4,4-dimethyl-3-(4-vinylphenyl)-oxetan-2-one (2.12)

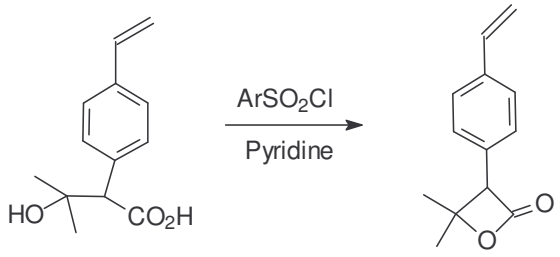

3-hydroxy-3-methyl-(4-vinylphenyl) butyric acid (4.83g, 0.0219 moles) was dissolved in dry pyridine (30 mL). This solution was cooled to $0^{O}C$ and phenyl sulfonyl chloride (5.60 mL, 0.0439 moles) was added dropwise. The reaction was stirred at $0^{O}C$ for 30 minutes and placed in the freezer overnight. The reaction mixture was then diluted with ether (~75 mL) and then extracted with a saturated aqeous copper sulfate solution until the copper sulfate solution didn't turn dark blue. The ether was then dried with anhydrous magnesium sulfate, filtered and the volatiles removed by rotary evaporation. The resulting oil was run through a polar plug (silica, Hex: EtOAc, 9:1). After removal of the solvent by rotary evaporation the oil was then chromatographed (basic alumina, Hex:EtOAc, 9:1) to yield **3** (0.871g, 0.00431 moles, 20%) as a yellow oil: ^{1}H NMR ($CDCl_3$) 1.199 (s, 3H), 1.744 (s, 3H), 4.588 (s, 1H), 5.261 (dd, *J* = 0.9 Hz, 10.8 Hz, 1H),

5.746 (dd, *J* = 0.8 Hz, 17.7 Hz, 1H), 6.684 (dd, *J* = 10.5 Hz, 17.7 Hz, 1H), 7.150 (d, *J* = 8.1 Hz, 2H), 7.395 (d, *J* = 8.1 Hz, 2H); ^{13}C NMR (CDCl3) 23.143, 27.855, 63.563, 81.676, 114.572, 126.699, 128.191, 130.937, 136.020, 137.382, 168.975; IR (neat, NaCl)3616, 3086, 2981, 2927, 2865, 1810; HRMS (CI, CH_4) calc M+ = 202.0994 found 202.0999.

4-tert Butyldimethylsiloxybenzaldehyde (2.16)

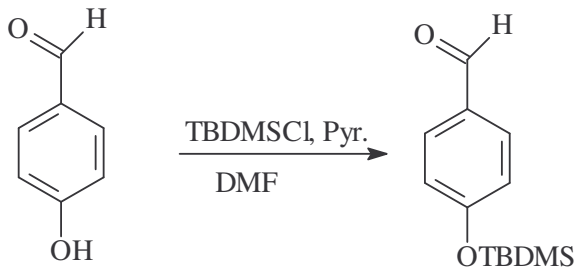

In a round bottom flask (100 mL) was added a solution of 4-hydroxybenzaldehyde (5.34 g, 0.031 mol) in DMF (50 mL). To this solution was added dropwise a solution of imidazole (5.297 g, 0.0777 mol) in dimethylformamide. This solution was stirred for 5 min. and a solution of tert-butyldimethylsilyl chloride (6.0 g, 0.039 mol) in DMF was added dropwise at room temperature. The reaction was stirred at rt. under an argon atmosphere for two days. The reaction mixture was diluted with ether (100 mL) and washed with DI water (3X100 mL). The organic layer was dried with anhydrous magnesium sulfate, filtered and the solvent removed with rotary evaporation to yield **2.16** (5.5 g, 0.0233 moles, 75 %) as pale yellow oil: ^{1}H NMR (DMSO-d_6) 0.222 (s, 6H), 0.936 (s, 9H), 7.022 (d, *J* = 8.4 Hz, 2H), 7.823 (d, *J* = 8.7 Hz, 2H), 9.865 (s, 1H); ^{13}C

NMR (DMSO-d_6) -4.641, 17.928, 25.386, 120.354, 130.309, 131.795, 160.657, 191.317; IR (neat, NaCl) 2957, 2931, 2859, 1700, 1596; MS (CI, CH_4) M+1 = 236.

4-tert Butyldimethylsiloxystyrene (2.17)

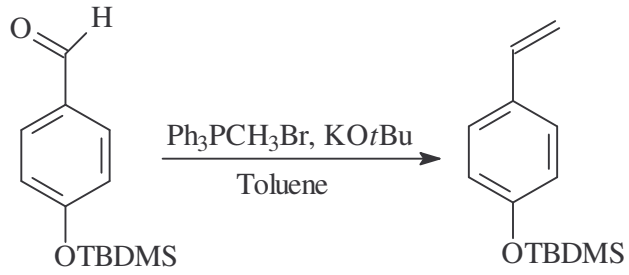

In a round bottom flask (250 mL) purged with argon was added methyl triphenylphosphonium bromide (8.310g, 0.0233 moles) and dry toluene (100 mL). To this stirred solution was added dropwise potassium *t*-butoxide (1M in THF, 23.3 mL, 0.0233 moles) at rt. The reaction mixture was stirred at rt. for 45 min. and a solution of 4-tert Butyldimethylsiloxybenzaldehyde (5.00g, 0.0211 moles) in dry toluene (30 mL) was added dropwise. The reaction solution was stirred at rt. for 1½ days and vacuum filtered. The mother liquor was concentrated by rotary evaporation and the resulting oil was chromatographed (silica, Hexanes) to yield **2.17** (4.138g, 0.0211 moles, 84%) as a clear oil: ^{1}H NMR (DMSO-d_6) 0.155 (s, 6H), 0.923 (s, 9H), 5.102 (dd, *J* = 0.8 Hz, 11.1 Hz, 1H), 5.634 (dd, *J* = 1.2 Hz, 17.7 Hz, 1H), 6.633 (dd, *J* = 10.7 Hz, 17.7 Hz, 1H), 6.793 (d, *J* = 8.4 Hz, 2H), 7.326 (d, *J* = 8.7 Hz, 2H); ^{13}C NMR (DMSO-d_6) -4.670, 17.841, 25.437, 111.949, 119.829, 127.360, 130.600, 136.033, 154.910; IR (neat, NaCl) 3080, 3062, 3033, 3003, 2956, 2930, 2883, 2854, 1627,1602; MS (CI, CH_4) M+1 = 235.

Poly-4-tert Butyldimethylsiloxystyrene (2.18)

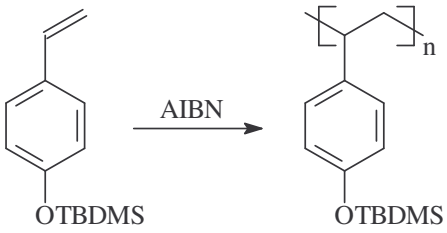

To a round bottom flask (25 mL) was added AIBN (0.049g, 0.299 mmol) and a solution of 4-tert Butyldimethylsiloxystyrene (0.710g, 0.00299 mol) in tetrahydrofuran (1 mL). This mixture freeze-pump-thawed three times and back filled with argon. The mixture was then heated at 65 degrees C for 15 hours. The polymer was precipitated into 300 mL of methanol. The precipitate was dried under vacuum to yield 11 (0.460 g, 65%) as a white powder: ^{1}H NMR ($CDCl_3$) 0.0-0.2, 0.8-1.0, 1.0-1.8; GPC (polystyrene standard) Mn = 4690, Mw = 11100, Pd = 2.367; IR (KBr) 3428, 2957, 2929, 28571607,1509.

4-Benzyloxybenzaldehyde (2.19)

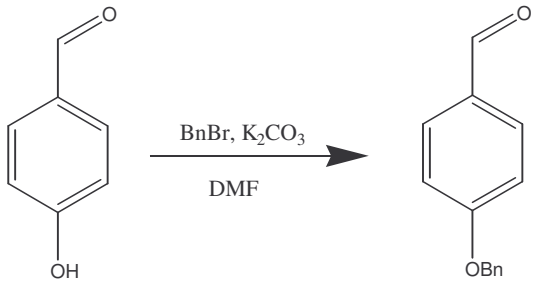

In a round bottom flask (500 mL) was added 4-hydroxybenz aldehyde (15.00g, 0.123 moles), sodium carbonate (15.62g, 0.1474 moles), benzyl bromide (25.21g, 17.5 mL, 0.1474 moles) and dry DMF (250 mL). The reaction mixture was allowed to stir at r.t. overnight. TLC (Hex: EtOAc 3:1, silica) showed some residual starting material. The

reaction was diluted with ether (500 mL) and then washed with water (5 X 600 mL), 1 N sodium hydroxide (3 X 300 mL), water (1 X 400 mL) and brine (1 X 400 mL). The ether layer was dried over magnesium sulfate, filtered and the ether was removed by rotary evaporation to yield **2.19** (16.556g, 0.0780 moles, 63%) as a tan solid: ^{1}H NMR (DMSO-d_6) 5.210 (s, 2H), 7.192 (d, *J* = 8.7 Hz, 2H), 7.393 (m, 5H), 7.864 (d, *J* = 8.7 Hz, 2H), 9.865 (s, 2H); ^{13}C NMR (DMSO-d_6) 69.64, 115.23, 127.82, 128.05, 128.48, 129.77, 131.77, 136.28, 163.28, 191.22; MS (EI) M^+ = 212.

4-Benzyloxystyrene (2.20)

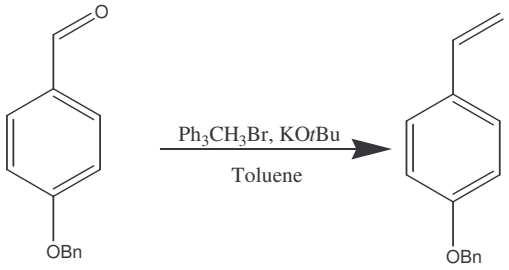

In a round bottom flask (250 mL) was added methyltriphenylphosphonium bromide (4.376g, 0.0123 moles) in dry toluene (50 mL). To this mixture was added potassium *t*-butoxide (1M in THF, 13.5 mL, 0.0135 moles) via syringe. This solution was allowed to stir at r.t. for 5 hours. A solution of 4-benzyloxy benzaldehyde (2.00g, 0.004942 moles) in toluene (15 mL) was added by syringe and the reaction solution was stirred at r.t. overnight (the reaction flask was wrapped in foil to minimize exposure to light). The reaction was then filtered and the volatiles were removed via rotary evaporation. The resulting residue was chromatographed (Hex: EtOAc, 3:1, Silica) to yield **2.20** (1.736g, 0.00858 moles, 91%) as a white solid: ^{1}H NMR (DMSO-d_6) 5.095 (s, 2H), 5.105 (dd, *J* = 0.6 Hz, 11.1 Hz, 1H), 5.660 (dd, *J* = 0.6 Hz, 17.7 Hz, 1H), 6.652 (dd, *J* = 11.1 Hz, 17.7

Hz, 1H), 6.979 (d, *J* = 8.7 Hz, 2H), 7.378 (m, 7H); ^{13}C NMR (DMSO-d_6) 69.18, 11.86, 114.84, 127.37, 127.65, 127.80, 128.40, 130.00, 136.05, 136.98;

Poly co-4,4-Dimethyl-3-(4-vinyl-phenyl)-oxetan-2-one 4-Benzyloxystyrene (2.21)

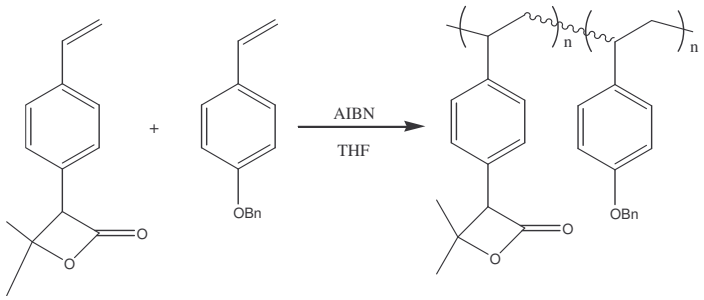

In a round bottom flask (25 mL) was added 4-Benzyloxystyrene (1.00g, 0.0051 moles), 4,4-Dimethyl-3-(4-vinyl-phenyl)-oxetan-2-one (0.257g, 0.00127 moles) and AIBN (0.105g, 6.37x10^{-4} moles) and THF (2 mL). The reaction was subjected to three freeze, pump, thaw cycles and then heated at 65^{O}C overnight. The polymer was precipitated from THF into hexanes and dried overnight under vacuum at r.t. to yield **2.21** (1.257g, 91%) as a light yellow solid: ^{1}H NMR (DMSO-d_6) 0.8-2.0, 4.6-5.2, 6.2-7.5; GPC (poly styrene standard) Mn = 3,310 Mw = 7,870 PDI = 2.378

1,1,1,3,3,3-Hexafluoro-2-(4-vinylphenyl)-propan-2-ol (2.22)

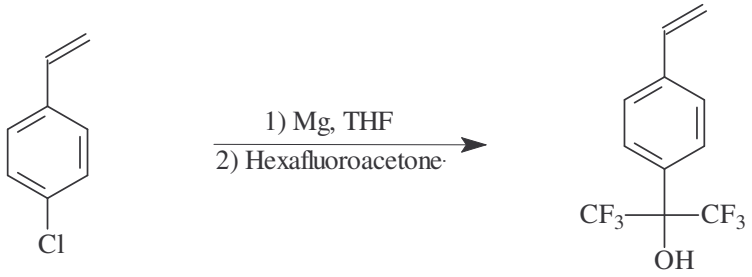

A three necked round bottom flask (250 mL) was fitted with a jacketed addition funnel with a dry ice acetone condenser on top of the addition funnel. One of the other necks was fitted with a dropping funnel, filled with THF (50 mL), and the last neck was plug with a rubber septum. The whole apparatus was evacuated, flamed dried and back filled with argon. To the round bottom flask were added magnesium (2.105g, 0.0866 moles), THF (5 mL) and a crystal of iodine. This was stirred as 0.8 mL of 4-chlorostyrene (8.66 mL, 0.0722 moles total) was added via syringe and then heated at 35^{O}C. Once the Grignard reaction initiated the remaining THF and remaining 4-chlorostyrene were added dropwise to maintain a gentle reflux. Following addition of all the reagents the Grignard was heated at 40^{O}C for 30 min. It was then cooled to rt. for 15 min. while the hexafluoro acetone (Excess) was condensed into the dry ice/acetone jacketed addition funnel. The Grignard was then cooled to -78^{O}C and the hexafluoroacetone was added dropwise. This solution was stirred at -78^{O}C for 1 hr. It was then warmed up to rt. and some excess hexafluoroacetone is released. The mixture was cooled in an ice bath and acidified with HCl (3M). The solution was diluted with ether (150 mL) and extracted with water (3X300 mL), washed with brine (300 mL), dried with anhydrous magnesium sulfate, filtered and the volatiles removed by rotary evaporation. The remaining oil was distilled

at 10 Torr and three fractions were collected; 1) bp. 35-40^{O}C 2) bp. 48-70^{O}C 3) bp. 70-85^{O}C. fractions 2 and 3 were combined and redistilled at 10 Torr to yield two fractions; 1) bp. 40-74^{O}C 2) bp. 74-84^{O}C, 17.206g. Fraction 2 contained both **2.23** and THF. The solution was 91.3% (determined by NMR) by weight **2.23** (15.709g, 0.0581 moles, 81%) as a clear liquid: ^{1}H NMR (DMSO-d_6) 5.357 (d, *J* = 11.1 Hz, 1H), 5.916 (d, *J* = 17.4 Hz, 1H), 6.769 (dd, *J* = 11.1 Hz, 17.7 Hz, 1H), 7.595 (d, *J* = 8.7 Hz, 2H), 7.653 (d, *J* = 8.4 Hz, 2H), 8.697 (s, 1H); ^{13}C NMR (DMSO-d_6) 76.810 (septuplet, *J* = 29.1 Hz), 116.232, 122.943 (q, *J* = 286 Hz), 126.253, 127.068, 130.069, 135.604, 138.830; ^{19}F NMR (DMSO-d_6) -73.589; IR (neat, NaCl) 3606, 3547, 3091, 3051, 2981, 2883; HRMS (CI, CH_4) M+1 calc. = 271.0558 found 271.0556.

Copolymer of 1,1,1,3,3,3-Hexafluoro-2-(4-vinylphenyl)-propan-2-ol and 4,4-dimethyl-3-(4-vinylphenyl)-oxetan-2-one (2.23)

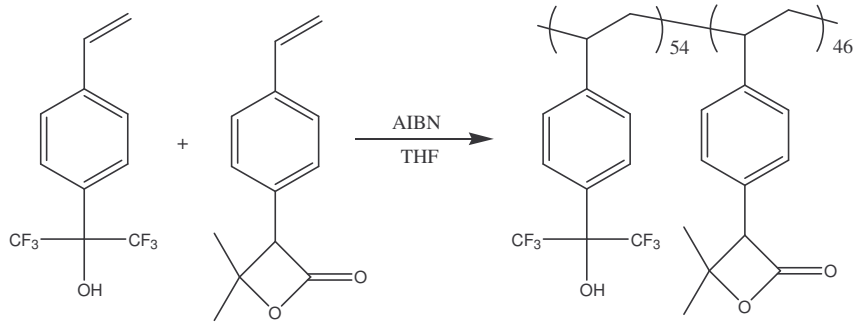

In a round bottom flask (25 mL) was added **2.12** (0.510 g, 2.5 mmol), **2.22** (0.980 g, 3.86 mmol), AIBN (0.092 g, 0.56 mmol) and THF (3 mL). The reaction solution was freeze, pumped, thawed three times and back filled with nitrogen. The reaction vessel was heated at 70° C fro 18 hrs. THF (4 mL) was added and the solution was precipitated into

hexanes (1 L), filtered and dried under high vacuum overnight at 40° C to give XX as a white solid (1.216 g, 82%): ^{1}H NMR (300 MHz, $CDCl_3$) 8.5 (alcohol), 6.0-7.2 (aromatic), 4.8 (olefin), 0.8-2.1 (aliphatic); ^{19}F NMR ($CDCl_3$) -73.786; IR (KBr) 3379, 2975, 2924, 2858, 1802; TGA decomposition onset 103° C, 5.381%; GPC (polystyrene standard) M_w=14,870 M_n=8,648 (PDI = 1.72); DSC T_g above decomposition temperature.

1-Methyl-2-oxo-cyclopentanecarboxylic acid ethyl ester (3.4)

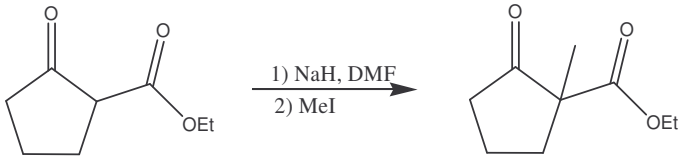

To a round bottom flask (2 L) was added dry THF (1500 mL) and sodium hydride (95%, 17.51g, 0.6931 moles). To this solution was added a solution of 2-Oxo-cyclopentanecarboxylic acid ethyl ester (100g, 0.640 moles) in dry THF (150 mL) dropwise with stirring while under nitrogen. The reaction solution was stirred overnight at room temperature and then methyl iodide (60.0 mL, 0.963 moles) was added via syringe while cooling the reaction in an ice bath. The solution was stirred overnight and the volatiles removed via rotary evaporation. The residue was taken up in ether (600 mL) and washed with water (200 mL), brine (100 mL) and then dried with magnesium sulfate. The ether was removed via rotary evaporation and the residue distilled to yield **3.4** (99.695 g, 0.586 moles, 92 %) as a clear oil: bp 72-82^{O}C @ 5 torr; ^{1}H NMR ($CDCl_3$, 300 MHz) 1.165 (t, *J* = 7.2 Hz, 3H), 1.223 (s, 3H), 1.847 (m, 3H), 2.335 (m, 3H), 4.074 (dq, *J*

= 1.2 Hz, 6.9 Hz; ^{13}C NMR ($CDCl_3$, 400 MHz) 13.917, 19.226, 19.447, 36.052, 37.527, 55.751, 61.166, 172. 254, 215.852; MS (CI, CH_4) M+1 = 171.

1,4-Dioxa-spiro[4.4]nonane-6-carboxylic acid ethyl ester (3.5)

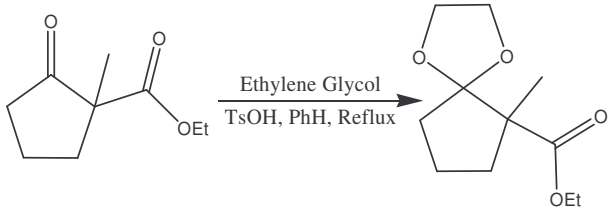

To a one necked round bottom flask fitted with a dean stark trap was added **3.4** (40.00 g, 0.235 moles), ethylene glycol (15.53 g, 0.285 moles), benzene (70 mL) and tosic acid (125 mg). The solution was heated at reflux overnight and collected aprox. 5 mL of water. The solution was cooled to room temperature and was washed with water (125 mL), sodium bicarb (sat., 125 mL), water (2 x 175 mL) and brine (125 mL). The organic layer was then dried with magnesium sulfate, filtered, the volatiles removed by rotary evaporation. The resulting residue was distilled to give **3.5** (44.278g, 0.207 moles, 95%) as a clear oil: bp 70-80^{O}C @ 1.5 torr; ^{1}H NMR ($CDCl_3$, 300 MHz) 1.183 (m, 6H), 1.42-2.48 (m, 6H), 3.7-4.1 (m, 4H); MS (CI, CH_4) M+1 = 215.

(6-Methyl-1,4-dioxa-spiro[4.4]non-6-yl)-methanol (3.7)

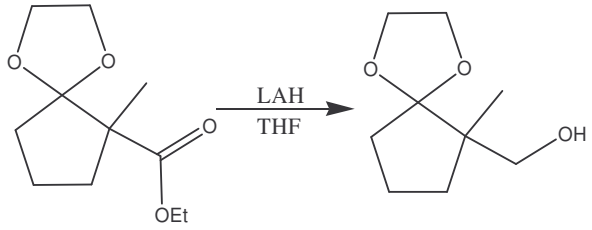

In a round bottom flask (1000 mL) was added LAH (7.44g, 0.196 moles) in dry THF (500 mL). To this solution was added a solution of **3.5** (30.00g, 0.140 moles) in dry THF (150 mL) dropwise. The reaction solution was allowed to stir at room temperature overnight. Excess LAH was quenched with water and the solution acidified to ph=4. This was then immediately extracted with ether (3 x 500 mL). The combined ether fractions were then washed with bicarb (sat., 350 mL), brine (200 mL) and the ether was removed by rotary evaporation. The residue was distilled to yield **3.7** (19.753g, 0.115 moles, 82%) as a colorless oil: bp 70-72^{O}C @ 1 torr; ^{1}H NMR ($CDCl_3$, 300 MHz) MS (CI, CH_4) M+1 = 173.

2-Hydroxymethyl-2-methyl-cyclopentanone (3.8)

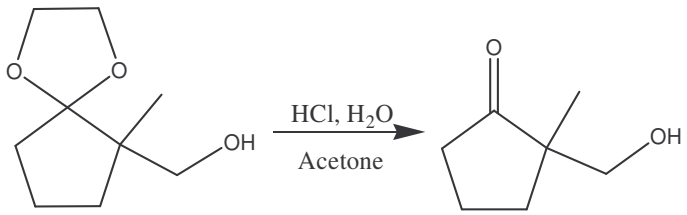

To a round bottom flask (500 mL) was added **3.7** (18.500g, 0.1074 moles) in acetone (250 mL) and tosic acid (25 mg). The solution was stirred overnight. Ether (240 mL) and water (150 mL) was then added and the organic layer separated. It was washed with

bicarb (sat., 150 mL) and brine (50 mL). The volatiles were removed by rotary evaporation and the residue distilled to yield **3.8** (6.175g, 0.0482 moles, 45%) as a clear oil: bp 56-60^{O}C @ 250 mtorr; ^{1}H NMR ($CDCl_3$, 300 MHz) 0.897 (s, 3H), 1.622 (m, 1H), 1.826 (m, 2H), 2.110 (m, 3H), 3.057 (s, 1H), 3.330 (d, *J* = 10.8 Hz, 1H), 3.521 (d, *J* = 3.521 (d, *J* = 10.8 Hz, 1H); ^{13}C NMR ($CDCl_3$, 300 MHz) 18.621, 19.101, 32.815, 38.270, 50.287, 66.578, 224.390; MS (CI, CH_4) M+1 = 129.

Toluene-4-sulfonic acid 1-methyl-2-oxo-cyclopentylmethyl ester (3.9)

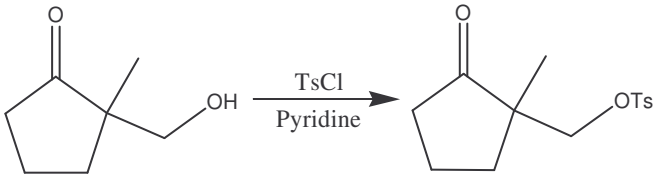

In a round bottom flask (500 mL) was added dry DCM (150 mL) and tosyl chloride (48.27g, 0.253 moles). To this solution was added dropwise a solution of dry DCM (150 mL), **3.8** (27.00g, 0.211 moles) and dry pyridine (34.13 mL, 33.38g, 0.422 moles). The solution was stirred overnight and then extracted with 3M HCl (150 mL), bicarb (sat., 150 mL) and brine (150 mL). The DCM was dried over magnesium sulfate, filtered and removed by rotary evaporation. The oil slowly crystallized to an oily solid which was titerated with hexanes to yield **3.9** (53.745g, 0.1903 moles, 90%) as a white solid: ^{1}H NMR ($CDCl_3$, 400 MHz) 0.918 (s, 3H), 1.829 (m, 3H), 2.163 (m, 3H), 2.410 (s, 3H), 3.825 (d, *J* = 9.6 Hz, 1H), 3.900 (d, *J* = 9.2 Hz, 1H), 7.311 (d, *J* = 7.6 Hz, 2H), 7.703 (d,

J = 8 Hz, 2H); ^{13}C NMR ($CDCl_3$, 400 MHz) 18.508, 19.195, 21.578, 32.684, 37.702, 48.395, 73.112, 127.84, 129.825, 132.315, 144.918, 219.312; MS (CI, CH_4) M+1 = 283.

5-Methyl-hex-5-enoic acid (3.2)

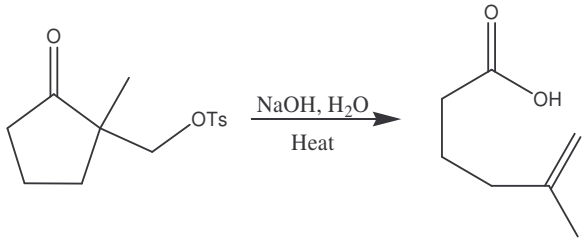

In a round bottom flask (500 mL) was added **3.9** (30.00g, 0.106 moles) and 40% w/v KOH (60 mL). This solution was heated for 40 min at 125^{O}C. Additional water (300 mL) was added and the solution was heated for another 3.5 hours. The solution was cooled and poured into ice and acidified to ph~4. The solution was extracted with ether (3 x 600 mL) and the ether was then washed with brine (150 mL) and dried over magnesium sulfate, filtered and rotovaped. The residue was distilled to yield **3.2** (8.726g, 0.0681 moles, 64%) as light yellow oil: bp 76-80^{O}C @ 400 mtorr; ^{1}H NMR ($CDCl_3$, 400 MHz) 1.717 (s, 3H), 1.785 (pentet, J = 7.2 Hz, 2H), 2.066 (t, *J* = 7.6 Hz, 2H), 2.352 (t, *J* = 7,2 Hz, 2H), 4.682 (d, *J* = 1.2 Hz, 1H), 4.731 (d, *J* = 1.6 Hz, 1H); MS (CI, CH_4) M+1 = 129.

5-Methyl-hex-5-enoic acid (3.2)

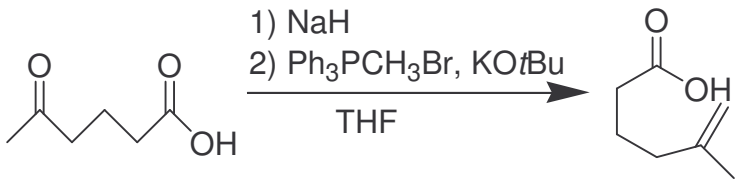

In a round bottom flask (1000mL) was added methyltriphenylphosphonium bromide (15.10g, 0.0423 moles) and dry THF (400 mL), plugged with a rubber septum, and purged under nitrogen. At room temperature Potassium tert-butoxide (5.22g, 0.0465 moles) in dry THF (80 mL) was added dropwise to the wittig salt over 15 minutes. In another round bottom flask (100 mL) sodium hydride (1.01g, 0.0421 moles) was added with dry THF (80 mL) and cooled to 0^{O}C under nitrogen. 4-acetylbutyric acid (5.00g, 0.0312 moles) is syringed slowly into the cooled NaH over 15 minutes, then allowed to warm to room temperature. The sodium salt was added dropwise to the ylide at room temperature and allowed to stir overnight (~12 hours). The reaction was acidified with HCl (3M) until pH 2 then extracted with diethyl ether (2 x 300mL). The combined ether layers were washed with brine (200 mL) and dried over anhydrous magnesium sulfate. The solvent was removed via rotary evaporation and then distilled at 180 mtorr, which provided a single fraction at 56-59^{O} C, yielding **3.2** (2.113g, 0.01645 moles, 53%) as a clear oil: ^{1}H NMR ($CDCl_3$) 1.690 (s, 3H), 1.759 (quint, *J* = 7.5 Hz, 2H), 2.040 (t, *J* = 7.5 Hz, 2H), 2.329 (t, *J* = 7.35 Hz, 2H), 4.691 (d, *J* = 15 Hz, 2H), 11.646 (s, broad OH); ^{13}C NMR ($CDCl_3$) 22.109, 22.342, 33.398, 36.842, 110.749, 114.497, 180.365; IR (neat, NaCl) 3076, 2971, 2932, 2668, 1709, 1647; HRMS (CI, CH_4) M+ = calc. 129.0916, actual 129.0916.

4-Methyl-pent-4-enoic acid (3.1)

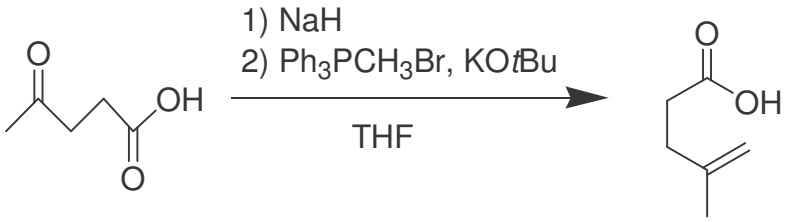

In a round bottom flask (1000mL) was added methyltriphenylphosphonium bromide (16.94g, 0.0474 moles) and dry THF (400 mL), plugged with a rubber septum, and purged under nitrogen. At room temperature potassium tert-butoxide (5.88g, 0.0524 moles) in dry THF (80 mL) was added dropwise to the wittig salt over 15 minutes. In another round bottom flask (100 mL) sodium hydride (1.14g, 0.0475 moles) was added with dry THF (80 mL) and cooled to 0^{O}C under nitrogen. Levulinic acid (5.00g, 0.0431 moles) is syringed slowly into the cooled NaH over 15 minutes, then allowed to warm to room temperature. The sodium salt was added dropwise to the ylide at room temperature and allowed to stir overnight (~12 hours). The reaction was acidified with HCl (3M) until pH 2 then extracted with diethyl ether (2 x 300mL). The combined ether layers were washed with brine (200 mL) and dried over anhydrous magnesium sulfate. The solvent was removed via rotary evaporation and then distilled at 180 mtorr, which provided a single fraction at 47-49^{O} C, yielding **3.1** (2.395g, 0.0210 moles, 49%) as a clear oil: ^{1}H NMR ($CDCl_3$) 1.727 (s, 3H), 2.320 (t, *J* = 5.7 Hz, 2H), 2.495 (t, *J* = 5.7 Hz, 2H), 4.716 (d, *J* = 17.1 Hz, 2H); IR (neat, NaCl) 3079, 2980, 2918, 2665, 1715, 1649; HRMS (CI, CH_4) M+ = calc. 115.076, actual 115.076.

5-Methyl-2-(4-vinyl-benzyl)-hex-5-enoic acid (3.11)

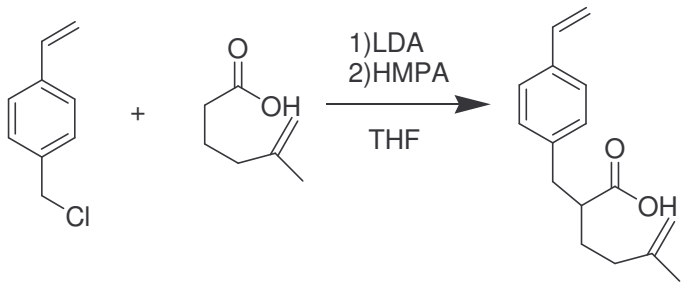

In a round bottom flask (250 mL) was added Diisopropyl amine (4.59 mL, 0.0328 moles) with dry THF (10 mL), under a nitrogen atmosphere, and cooled to -78^{O} C. N-Butyllithium (2.20M, 14.54 mL, 0.0320 moles) was slowly added to the round bottom flask over 15 minutes, then warmed to 0^{O} C. **(3.2)** (2.00g 0.0156 moles) was syringed slowly into the LDA over 15 minutes at 0^{O} C, allowed to warm to room temperature and stirred for an additional 30 minutes. The reaction flask is cooled to 0^{O} C, then HMPA (2.99 mL, 0.0172 moles) is added dropwise; allowing the flask to stir for 15 minutes at 0^{O} C after addition. With the flask maintained at 0^{O} C Vinylbenzyl Chloride (2.44 mL, 0.0172 moles) is delivered, stirred for 30 minutes at 0^{O} C, then allowed to warm to room temperature, covered with foil, allowed to react for 6-8 hours. To the reaction was added diethyl ether (250 mL), then extract with deionized water (2 x 250 mL). Acidify aqueous layer to pH 2, extract with diethyl ether (2 X 300 mL). The combined ether layers were washed with brine (100 mL) and dried over anhydrous magnesium sulfate. The solvent was removed via rotary evaporation, the oil was then chromatographed (basic alumina, Hex:EtOAc, 3:2) yielding **3.11** (1.244g, 0.0051 moles, 38%) as a pale yellow oil: ^{1}H

NMR; ^{13}C NMR ($CDCl_3$) 17.805, 25.794, 30.208, 36.988, 47.446, 113.276, 120.384, 126.247, 129.050, 134.469, 135.729, 136.537, 138.817, 181.195; IR (neat, NaCl) 3083, 2962, 2899, 1748, 1704; HRMS (CI, CH_4) M+ = calc. 244.146, actual 244.146.

4-Methyl-2-(4-vinyl-benzyl)-pent-4-enoic acid (3.10)

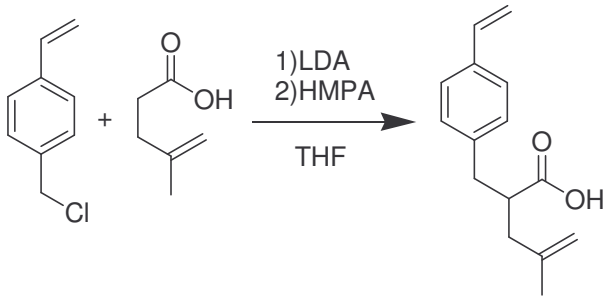

In a round bottom flask (250 mL) was added Diisopropyl amine (5.15 mL, 0.03675 moles) with dry THF (10 mL), under a nitrogen atmosphere, and cooled to -78^{O} C. N-Butyllithium (2.20M, 16.76 mL, 0.0359 moles) was slowly added to the round bottom flask over 15 minutes, then warmed to 0^{O} C. **(3.1)** (2.00g 0.0156 moles) was syringed slowly into the LDA over 15 minutes at 0^{O} C, allowed to warm to room temperature and stirred for an additional 30 minutes. The reaction flask is cooled to 0^{O} C, and then HMPA (3.35 mL, 0.0193 moles) is added dropwise; allowing the flask to stir for 15 minutes at 0^{O} C after addition. With the flask maintained at 0^{O} C Vinylbenzyl Chloride (2.74 mL, 0.0193 moles) is delivered, stirred for 30 minutes at 0^{O} C, then allowed to warm to room temperature, covered with foil, allowed to react for 6-8 hours. To the reaction was added diethyl ether (250 mL), then extract with deionized water (2 x 250 mL). Acidify aqueous

layer to pH 2, extract with diethyl ether (2 X 300 mL). The combined ether layers were washed with brine (100 mL) and dried over anhydrous magnesium sulfate. The solvent was removed via rotary evaporation, the oil was then chromatographed (basic alumina, Hex:EtOAc, 3:2) to yield **3.10** (1.354g, 0.0059 moles, 38%) as a white crystalline solid: ^{1}H NMR ($CDCl_3$) 1.705 (s, 3H), 2.178 (dd, *J* = 4.8 Hz, 10.8 Hz, 1H), 2.379 (dd, *J* = 6 Hz, 10.6 Hz, 1H), 2.745 (dd, *J* = 4.2 Hz, 9.6 Hz, 1H), 2.871 (multiplet, 2H) 4.765 (d, *J* = 6.7 Hz, 2H), 5.193 (d, *J* = 8.1 Hz, 1H), 5.692 (d, *J* = 14.1 Hz, 1H), 6.666 (dd, *J* = 8.1 Hz, 12.9 Hz, 1H), 7.121 (d, *J* = 6.3 Hz, 2H), 7.305 (d, *J* = 6 Hz, 2H); IR (neat, NaCl) 3079, 2969, 2676, 1740, 1707; HRMS (CI, CH_4) M+ = calc. 231.139, actual 231.139.

Ter-polymer of – Styrene / 1,1,1,3,3,3-Hexafluoro-2-(4-vinylphenyl)-propan-2-ol / 5-Methyl-2-(4-vinyl-benzyl)-hex-5-enoic acid (3.14)

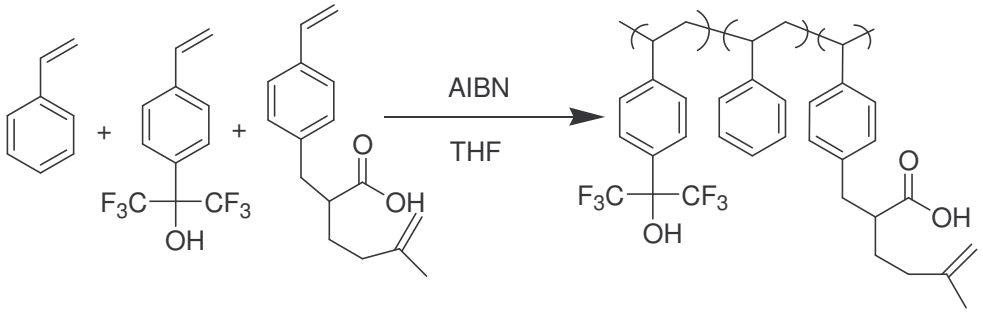

In a dry round bottom flask (25 mL) was added dry THF (4 mL), **3.2** (.400g, .00165 moles), styrene (.171g, .00165 moles), and 1,1,1,3,3,3-Hexafluoro-2-(4-vinylphenyl)-propan-2-ol (.892g, .0033 moles). AIBN mass is calculated at 10 mole% of combined monomer total (.108g, .00066 moles), then added to flask. Three freeze-pump-thaw cycles are conducted and then the polymerization is heated to 70^{O} C and maintained

overnight (~12-18 hours). Precipitation of polymer is conducted in 500 mL Hexanes at 0^{O} C, filtrated, and then dried on high vacuum approximately 12 hours to remove all solvent to give **3.14**. ^{1}H NMR (DMSO-D_6) 0.7-2.3, 2.760, 3.729, 4.745, 6.1-7.6; IR (KBr) 3596, 3376, 3024, 2921, 2852, 1704, 1649, 1509; TGA decomposition onset 382 ^{O} C, 94.4%; GPC (polystyrene standard) M_w=17,290 M_n=9,076 (PDI = 1.91).

Ter-polymer of – Styrene / 1,1,1,3,3,3-Hexafluoro-2-(4-vinylphenyl)-propan-2-ol / 5-Methyl-2-(4-vinyl-benzyl)-hex-5-enoic acid (3.15)

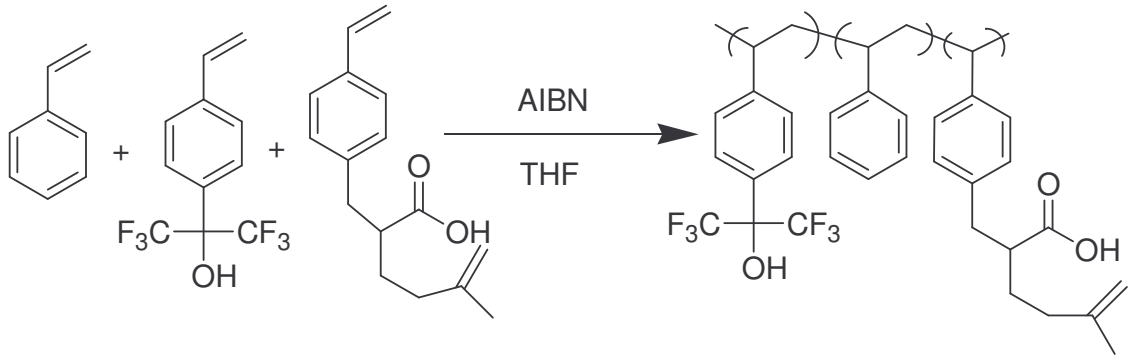

In a dry round bottom flask (25 mL) was added dry THF (4 mL), **3.2** (.300g, .00124 moles), styrene (.193g, .00186 moles), and 1,1,1,3,3,3-Hexafluoro-2-(4-vinylphenyl)-propan-2-ol (838g, .0031 moles). AIBN mass is calculated at 10 mole% of combined monomer total (.102g, .00062 moles), then added to flask. Three freeze-pump-thaw cycles are conducted on the flask and then the polymerization is heated to 70^{O} C and maintained overnight (~12-18 hours). Precipitation of polymer is conducted in 500 mL Hexanes at 0^{O} C, filtrated, and then dried on high vacuum approximately 12 hours to remove all solvent to give **3.15**. ^{1}H NMR (DMSO-D_6) 0.6-2.9, 3.328, 4.553, 6.0-7.7,

8.477, 12.139; IR (KBr) 3600, 3395, 3028, 2921, 2848, 171; TGA decomposition onset 385 ^{O} C, 92.7%; GPC (polystyrene standard) M_w=12,159 M_n=7,748 (PDI = 1.57).

***Endo*-5-Norbornene-2,3-Dicarboxylic Anhydride (4.12)**

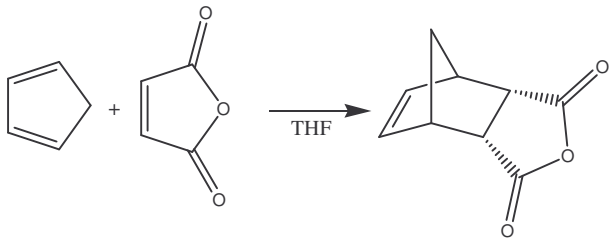

Maleic anhydride (20.031 g, 204.4 mmol) in THF (100 mL) was added dropwise to dicyclopentadiene (27.023 g, 204.4 mmol) in THF (100 mL), and the mixture was stirred overnight in an ice bath. The mixture was evaporated and dried under vacuum to yield **4.12** (33.439 g, 71%) as a white solid: ^{1}H NMR ($CDCl_3$, 400 MHz), 1.540 (d, *J* = 8,8 Hz, 1H), 1.739 (d, *J* = 8.8 Hz, 1H), 3.465 (m, 2H), 3.553 (q, *J* = 1.2 Hz, 2H), 6.267 (t, *J* = 2 Hz, 2H); MS (CI, CH_4) M+1 = 165; IR (KBr) 3569, 2979, 2878, 1868.

***Endo*-5-Norbornene-2,3-Bis(Hydroxymethyl) (4.16)**

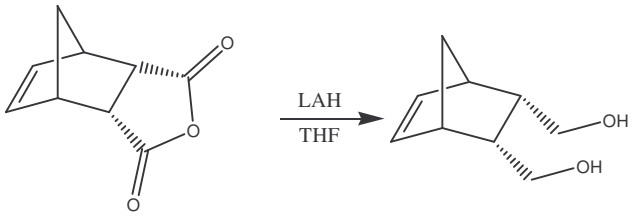

4.12 (88.618 g, 540.4 mmol) in dry THF (150 mL) was added dropwise to LAH (29.672 g, 756.5 mmol) in dry THF (100 mL), and the mixture was stirred overnight in an ice bath under nitrogen. To the mixture was added DI water to quench the unreacted

LAH. To the mixture was added 3M HCl until the pH was about 4. The mixture was extracted with ethyl ether three times, and the organic layer was recovered. The organic layer was then washed with saturated $NaHCO_3$ followed by brine. The recovered organic layer was dried over $MgSO_4$ for 1 hour. The insoluble materials were filtered off, and the filtrate was evaporated. The product was then distilled under vacuum (250 mTorr, 106-120 °C) to yield **4.16** (7.863 g, 9%) as clear oil: ^{1}H NMR ($CDCl_3$, 400 MHz), 1.361 (m, 2H), 2.481 (m, 2H), 2.753 (s, 2H), 3.319 (t, J = 10.8 Hz, 2H), 3.572 (m, 2H), 4.201 (s, 2H), 5.990 (t, J = 1.8, 2H); IR (Neat/NaCl) 3313, 2928.

***Endo*-5-Norbornene-2,3-Bis(*t*-Butoxycarbonyloxymethyl) (4.17)**

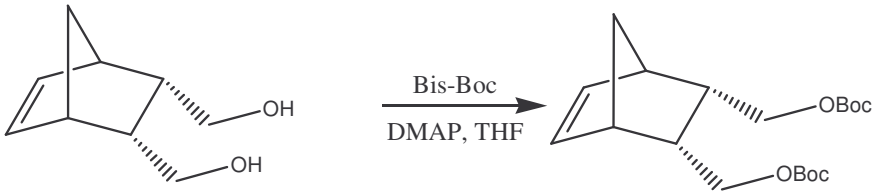

4.16 (2.973 g, 19.3 mmol) in dry THF (20 mL) was added to di-*t*-butyl di-carbonate (7.050 g, 32.3 mmol) and a catalytic amount of *p*-dimethylaminopyridine in dry THF (50 mL), and the mixture was stirred overnight at room temperature under nitrogen. The mixture was then evaporated to yield a yellow oil. The oil was purified using column chromatography (6:1 volume hexane:AcOEt) on silica gel to yield **4.17** (4.760 g, 69%) as a clear oil: ^{1}H NMR ($CDCl_3$, 400 MHz), 0.859 (t, J = 6.8 Hz, 2H), 1.462 (m, 18H), 2.555 (s, 2H), 2.939 (s, 2H), 6.174 (s, 2H);; IR (Neat/NaCl) 2979, 1748.

Exo-5-Norbornene-2,3-Dicarboxylic Anhydride (4.13)

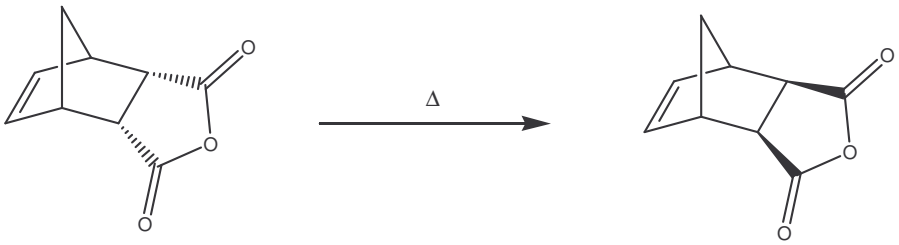

4.12 (11.415 g, 69.6 mmol) was added to a flask and heated to 190 °C with stirring for 1 hour. The liquid was allowed to cool room temperature, and the resulting solid was recrystallized from benzene. The first recrystallization fraction was 8:1 molar exo to endo. The second fraction was 9:1 molar exo to endo. The mixture was filtered out to recover a white, solid product in each case. The filtrate was then taken and isomerized using the procedure outlined above. Two recyrstallization steps were performed on the product, and the combined fractions yielded **4.13** (8.064 g, 71%) as a white solid: Characterization of the first fraction is as follows: ^{1}H NMR ($CDCl_3$, 400 MHz), 1.424 (d, *J* = 10 Hz, 2H), 1.648 (dt, J = 1.6 Hz, 10 Hz, 2H), 2.979 (d, *J* = 1.2 Hz, 1H), 3.434 (t, *J* = 1.2 Hz, 1H), 6.310 (t, *J* = 2 Hz, 2H); MS (CI, CH_4) M+1 = 165; IR (KBr) 3588, 2998, 2882, 1872.

Exo-5-Norbornene-2,3- Bis(Hydroxymethyl) (4.14)

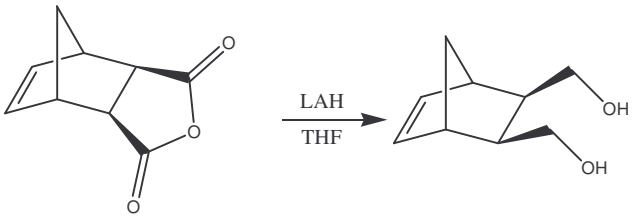

4.13 (8.064 g, 49.2 mmol) in dry THF (50 mL) was added dropwise to LAH (2.590 g , 68.3 mmol) in dry THF (230 mL), and the mixture was stirred overnight in an ice bath under nitrogen. To the mixture was added DI water to quench the unreacted LAH. To the mixture was added 3M HCl until the pH was about 4. The mixture was extracted with ethyl ether three times, and the organic layer was recovered. The organic layer was then washed with saturated $NaHCO_3$ followed by brine. The recovered organic layer was dried over $MgSO_4$ for 1 hour. The insoluble materials were filtered off, and the filtrate was evaporated. The product was then distilled under vacuum (250 mTorr, 110-120 °C) to yield **4.14** (3.416 g, 45%) as clear oil: ^{1}H NMR ($CDCl_3$, 400 MHz), 1.226 (d, *J* = 9.2 Hz, 1H), 1.326 (d, *J* = 8.8 Hz, 1H), 1.813 (m, 2H), 2.499 (t, *J* = 1.6 Hz, 2H), 3.718 (m, 6H), 6.160 (t, *J* = 1.6 Hz, 2H); MS (CI, CH_4) M+1 = 155; IR (Neat/NaCl) 3293, 2901.

Exo-5-Norbornene-2,3-Bis(t-Butoxycarbonyloxymethyl) (4.15)

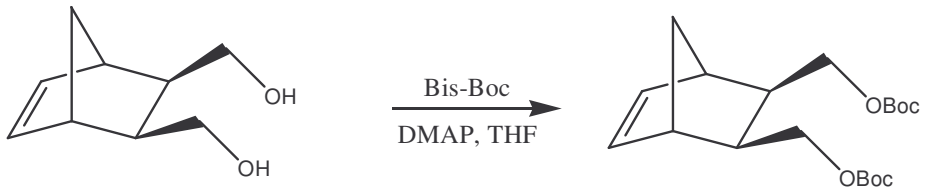

4.14 (15.000 g, 97.7 mmol) was added to di-*t*-butyl carbonate (53.090 g, 243.5 mmol) and a catalytic amount of *p*-dimethylaminopyridine in dry THF (350 mL), and the mixture was stirred overnight at room temperature under nitrogen. The mixture was then evaporated to yield a yellow oil. The oil was purified using column chromatography (5:1 volume hexane:AcOEt) on silica gel to yield **4.15** (31.372 g, 91%) as a clear oily solid: ^{1}H NMR ($CDCl_3$, 300 MHz), 0.846 (t, J = 6.8 Hz, 2H), 1.310 (m, 4H), 1.456 (m, 18H), 1.875 (s, 2H), 2.749 (s, 2H), 2.958 (m, 2H), 4.185 (m, 2H); MS (CI, CH_4) M+1 = 355; (KBr) 3056, 2971, 2928, 2866, 1744.

Poly-5-Norbornene-2,3-Bis(t-Butoxycarbonyloxymethyl)

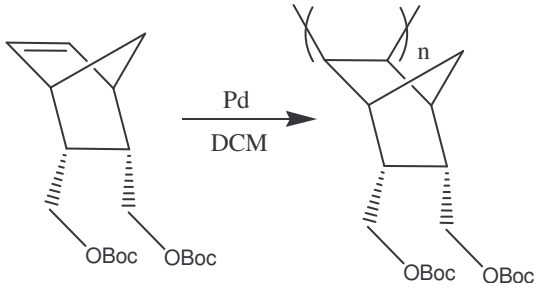

$AgSbF_6$ (0.669 g, 1.9 mmol) and allylpalladium chloride dimer (0.356 g, 0.9 mmol) were added to a flask in a dry box and were dissolved in dry, degassed DCM (11 mL). **4** (2.003 g, 5.6 mmol) was added to a separate flask and dissolved in dry, degassed DCM (7 mL). Palladium catalyst **A** and polymer-bound 2,6-di-*t*-butylpyridine (0.447 g) were added to **4** while under nitrogen, and the mixture was stirred at room temperature for 4 days. The product was evaporated and re-dissolved in dry THF. H_2 was bubbled in the mixture for 1 hour to precipitate the palladium. The product was filtered through celite to remove the palladium, re-dissolved in THF, and precipitated into hexanes. The product was filtered and dried to yield **1** (0.365 g, 18%): H^1 NMR ($CDCl_3$, 400 MHz) 1.443 (s), 1.8-3.0, 3.2-4.6; IR (KBr) 3452, 2975, 1740.

Isocyanatomethyl-trimethyl-silane (4.11)

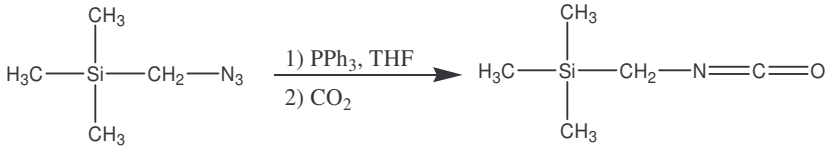

To a round bottom flask (250 mL) was added **4.10** (10.00g, 0.0774 moles) and dry THF (100 mL). To this solution under nitrogen was added triphenylphosphine (22.33g, 0.0851 moles) in bulk. The reaction solution was heated at reflux for 1.5 hours which produced a canary yellow solution. The yellow solution was then cooled in a dry ice acetone bath and carbon dioxide from a lecture bottle was bubbled through the solution for 25 minutes producing a white precipitate. The THF was removed by rotary evaporation and the resulting white solid was extracted with pet ether several times. The combined pet ether fractions were rotovaped and the resulting residue was distilled to give **4.11** (3.567g, 0.0276 moles, 36%) as a clear oil: bp matched the literature; ^{1}H NMR ($CDCl_3$, 400 MHz) 0.101 (s, 9H), 2.694 (s, 2H); ^{13}C NMR ($CDCl_3$, 400 MHz) -3.222, 31.997; MS (CI, CH_4) M+1 = 130.

Azidomethyl-trimethyl-silane (4.10)

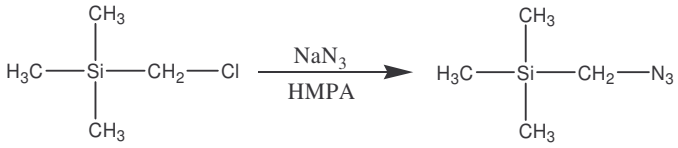

In a round bottom flask (250 mL) was added chloromethyl trimethylsilane (60.00 mL, 52.47g, 0.430 moles), sodium azide (33.54g, 0.516 moles) and HMPA (130 mL). The reaction solution was heated for 12 hours at 80^{O}C behind a blast shield. The product was distilled from the reaction solution to give **4.10** (41.403g, 0.320 moles, 74%) as a light yellow oil: bp 40-42^{O}C @ 40 torr; ^{1}H NMR ($CDCl_3$, 300 MHz) 0.093 (s, 9H), 2.733 (s, 2H); ^{13}C NMR ($CDCl_3$, 300 MHz) -2.665, 42.003; MS (CI, CH_4) M+1 = 130.

Azidopropyl-3-trimethyl-silane (4.23)

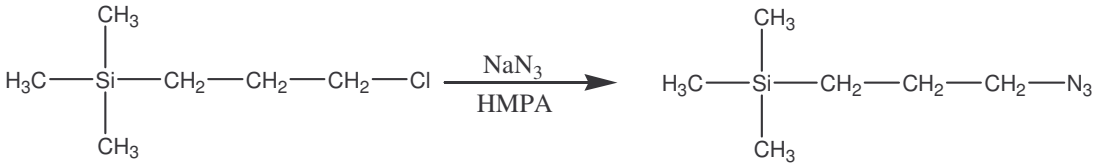

To a three necked round bottom flask (250 mL) fitted with a condenser under nitrogen was added 3-trimethylsilyl-1-chloropropane (25.00g, 0.166 moles, 28.44 mL), dry HMPA (50 mL) and sodium azide (11.86g, 0.182 moles). The reaction mixture was heated at 80°C for 22 hrs. The product was distilled from the reaction mixture to yield product and HMPA. This solution was redistilled through a two inch vigreux column to yield pure **4.23** (14.599g, 0.0928 moles, 56%) as a clear liquid: bp 54-56°C (13 Torr); ^{1}H

NMR ($CDCl_3$, 400 MHz) -0.017 (s, 9H), 0.511 (m, 2H), 1.58 (m, 2H), 3.21 (t, *J* = 6.8 Hz, 2H); ^{13}C NMR ($CDCl_3$, 400 MHz) -1.83, 13.76, 23.66, 54.50..

Isocyanatopropyl-3-trimethyl-silane (4.24)

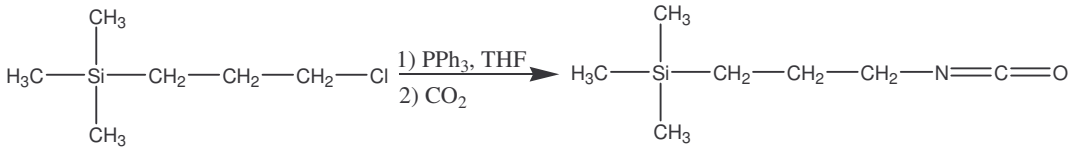

In a three neck round bottom flask (250ml) fitted with a condenser under nitrogen was added dry THF (60 ml) and triphenylphosphine (7.328g, 0.0279 moles). At room temperature was added via syringe neat Azide **4.23** (4.00g, 0.0254 moles). The solution was stirred at room temperature and then heated at reflux for 1 hr. The reaction mixture was cooled in an ice bath and dry ice was added to the reaction mixture with stirring for 30 min. The solvent was removed via rotary evaporation till about 10 ml of solution was remaining. Pentane (150 mL) was added and the precipitate was filtered by vacuum filtration. The Precipitate was rinsed with pentane (150 mL). The pentane fractions were collected and the solvent removed via rotary evaporation. The resulting liquid was distilled to give **4.24** (2.526g, 0.0161 moles, 63%) as a clear oil: bp 45-45°C (6 Torr); ^1H NMR ($CDCl_3$, 400 MHz) -0.005 (s, 9H), 0.517 (m, 2H), 1.58 (m, 2H), 3.23 (t, *J* = 6.4 Hz, 2H); ^{13}C NMR ($CDCl_3$, 400 MHz) -1.85, 13.66, 26.25, 46.03; HRMS (EI) M^+ = 158.100079 found, calc. = 158.100012.

Neopentyl Azide (4.21)

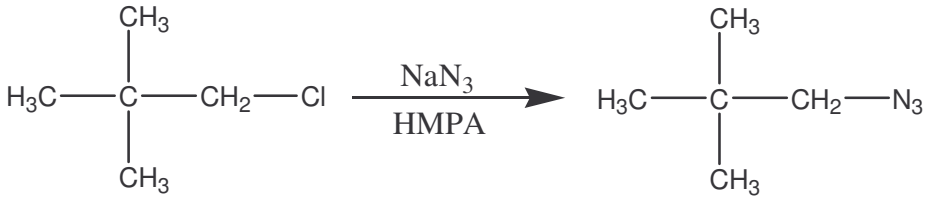

In a round bottom flask (250 mL) fitted with a condenser under a nitrogen atmosphere was added neopentyl iodide (12.00 g, 0.0606 moles, 8.06 mL), sodium azide (13.23g, 0.204 moles) and dry HMPA (40 mL). The reaction mixture was heated at 80° C for 24 hrs. Distillation from the reaction mixture yielded **4.21** (4.672 g, 0.0413 moles, 68%) as a clear liquid: bp = 30-32° C (45 torr); ^{1}H NMR ($CDCl_3$, 400 MHz) 0.892 (s, 9H), 3.136 (s, 2H); ^{13}C NMR ($CDCl_3$, 400 MHz) 26.70, 32.58, 62.83.

Neopentyl Isocyanate (4.22)

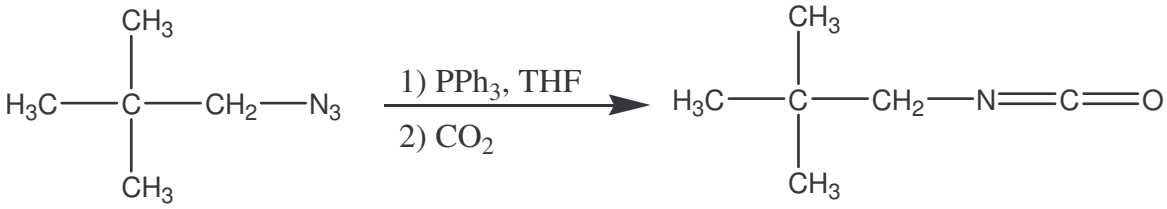

In a three necked round bottom flask (250 mL) fitted with a condenser under nitrogen atmosphere was added Azide **4.21** (4.00 g, 0.0353 moles) in dry THF (150 mL).

To the reaction solution was added via syringe a solution of triphenylphosphine (9.73g, 0.0371 moles) in dry THF (75 mL). The reaction mixture was stirred at room temperature for 30 min. and then heated to reflux for 5 hrs. The resulting clear ylide was cooled to 0° C and dry ice was added for 30 min. The volatiles were removed via rotary evaporation to yield an oily solid. Pentane was added and the precipitate was removed by vacuum filtration. The pentane was removed via rotary evaporation and subsequent distillation (bp = 30-32° C, 42 torr) produced crude XX (1.772 g). Distillation at atmospheric pressure yielded pure **4.22** (0.666 g, 0.00589 moles, 17%) as a clear liquid: bp = 120 °C; ^{1}H NMR ($CDCl_3$, 400 MHz) 0.930 (s, 9H), 3.032 (s, 2H); ^{13}C NMR ($CDCl_3$, 400 MHz) 26.75, 32.56, 55.05.

Bibliography

Adam, W.; Baeza, J. ; Liu, J. C. *J. Amer. Chem. Soc.,* **94**, 2000 (1972)

Bae, C. Y.; Douki, K.; Yu, T.; Dai, J.; Schmaljohann, D.; Koerner, H.; Ober, C. K. *Chem. Mater.* **2002**, *14*, 1306-1313.

Baik, K.; Van den hove, L.; Roland, B. *J. Vac. Sci. Technol. B.* **1991**, 3399-3405.

Brooke, M. A. *Silicon in Organic, Organomettallic, and Polymer Chemistry,* John Wiley and Sons: USA, 2001.

Brunner, T. A.; Fonseca, C. *Proc. SPIE-Int. Soc. Opt. Eng.* **2001**, *4690*, 76-83.

Chang, S. J.; McNally, D.; Shary-Tehrany, S.; Hickey, S. M. J.; Boyd, R. H. *J. Amer. Chem. Soc.* **1970**, *92*, 3109-3118.

Cho, S.; Vander Heyden, A.; Byers, J.; Willson, C. G. *Proc. SPIE-Int. Soc. Opt. Eng.* **2000**, *3999*, 62.

Chung, K., Takata, T., Endo, T. *Macromolecules*, **1997**, *30*, 2532-2538.

Conley, W.; Brunsvold, W.; Ferguson, R.; Gelorme, J.; Holmes, S.; Martino, R.; Petryniak, M.; Rabidoux, P.; Sooriyakumaran, R.; Sturtevant, J. *Proc. SPIE-Int. Soc. Opt. Eng.* **1993**, *1925*, 120-126.

Coopmans, F., Roland, B., Lombaerts, R. *Microelectronic Engineering*, **1986**, *5*, 291-297.

Craig, D. *J. Am. Chem. Soc.* **1951**, *73*, 4889-4892.

Crawford, M. K.; Farnham, W. B.; Feiring, A. E.; Feldman, J.; French, R. H.; Leffew, K. W.; Petrov, V. A.; Qiu, W.; Schadt III, F. L.; Tran, H. V.; Wheland, R. C.; Zumsteg, F. C. *Proc. SPIE-Int. Soc. Opt. Eng.* **2003**, *5039*, 80-92.

Dektar, J. L.; Hacker, N. P. *J. Am. Chem. Soc.*, **1990**, *112*, 6004-6015.

Do, Y.; Kim, Y. *Macromol. Rapid Commun.* **2000**, *21*, 1148-1155.

Duda, A., Penczek, S. *Macromolecules*, **1995**, *28*, 5981-5992.

Eschenmoser, A.; Frey, A. *Helvetica Chimica Acta.*, **1952**, *35*, 1660-1666.

Fedynyshyn, T. H.; Mowers, W. A.; Kunz, R. R.; Sinta, R. F.; Sworin, M.; Cabral, A.; Curtin, J. *Polymeric Materials Science and Engineering*, **2002**, *87*, 398-399.

Fujigaya, T.; Sibasaki, Y.; Ando, S.; Kishimura, S.; Endo, M.; Sasago, M.; Ueda, M. *Chem. Mater*. **2003**, *15*, 1512-1517.

Garza, C. M., *Proc. SPIE-Int. Soc. Opt. Eng*. **1988**, *920*, 233-240.

Goodall, B. L. *et al*. *International patent,* WO 9733198 (1997)

Greene, T. W.; Wuts, P. G. M. *Protecting Groups in Organic Synthesis 2nd Ed.* John Wiley and Sons: USA, 1991.

Hall, D. S., Osborn, B., Patterson, K., Burns, S. D., Willson, C. G.; *Proc. SPIE-Int. Soc. Opt. Eng*. **2001**, *4345*, 1066-1072.

Hartney, M. A.; Kunz, R. R.; Eriksen, L. M.; LaTulip, D. C. *Optical Engineering* **1993**, 2382-2387.

Hein, S.; Angwood, S.; Ashworth, D.; Basset, S.; Bloomstein, T.; Dean, K.; Kunz, R. R.; Miller, D.; Patel, S.; Rich, G. *Proc. SPIE* **2001**, *4345,* 439-447.

Heinz, U.; Adams, E.; Klintz, R.; Welzel, P. *Tetrahedron*, **1990**, *46*, 4217-4230.

Hennis, A. D., Polley, J. D., Long, G. S., Sen, A. *Organomettallics*, **2001**, *20*, 2802-2812.

Ho, B.; Chang, J.; Liu, T.; Chen, J. *Proc. SPEI-Int. Soc. Opt. Eng*. **1998**, *3333*, 448-453.

Houlihan, F. M.; Rushkin, I. L.; Hutton, R. S.; Gabor, A. H.; Medina, A. N.; Malik, S.; Neiser, M.; Kunz, R. R.; Downs, D. K. *Proc. SPIE* **1999**, *3678,* 264-274.

Hung, R. J.; Tran, H. V.; Trinque, B. C.; Chiba, T.; Yamada, S.; Sanders, D. P.; Connor, E. F.; Grubbs, R. H.; klopp, J.; Frechet, J. M. J.; Thomas, B. H.; Shafer, G. J.; DesMarteau, D. D., Conley, W.; Willson, C. G. *Proc. SPIE-Int. Soc. Opt. Eng*. **2001**, *4345*, 385-395.

Jamieson, Andrew PhD Thesis, University of Texas at Austin, **2004**.

Jiang, Y., Frechet, J. M. J., Willson, C. G., *Polymer Bulletin*, **1987**, *17*, 1-6.

Kodama, S.; Kaneko, I.; Takebe, Y.; Okada, S.; Kawaguchi, Y.; Shida, N.; Ishikawa, S.; Toriumi, M.; Itani, T. *Proc. SPIE-Int. Soc. Opt. Eng*. **2002**, *4690*, 76-83.

http://public.itrs.net/Files/2003ITRS/Litho2003.pdf

http://www.intel.com/research/silicon/mooreslaw.htm

http://www.library.upenn.edu/exhibits/rbm/mauchly/jwmintro.html

http:// www.tsmc.com

Illumanti, G.; Mandolini, L. *Acc. Chem. Res.* **1981**, *14*, 95-102.

Ishikawa, T., Kodani, T., Yoshida, T., Moriya, T., Yamashita, T., Toriumi, M., Araki, T., Aoyama, H., Hagiwara, T., Furukawa, T., Itani, T., Fujii, K., *Journal of Fluorine Chemistry*, **2004**, *125*, 1791-1799.

Ito, H. *IBM J. Res & Dev.* **2001**, *45*, 683-695.

Ito, H. *J. Polym. Sci. Part A: Polym. Chem.* **2003**, *41*, 3863-3870.

Ito, H.; Hinsberg, W. D.; Rhodes, L. F.; Chang, C. *Proc. SPIE-Int. Soc. Opt. Eng.* **2003**, *5039*, 70-79.

Ito, H., Knebelkamp, A., Lundmark, S. B., Nguyen, C. V., Hinsberg, W. D. *J. Polym. Sci. Part A*, **2000**, *38*, 2415-2427.

Ito, H.; MacDonald, S. A.; Miller, R. D.; Willson, C. G. U.S. Patent 4,552,83, (1985).

Ito, H.; Wallraff, G. M.; Brock, P.; Fender, N.; Truong, H.; Breyta, G.; Miller, D. C.; Sherwood, M. H.; Allen, R. D. *Proc. SPIE-Int. Soc. Opt. Eng.* **2001**, *4345*, 273-284.

Kane, V. V.; Doyle, D. L.; Ostrowski, P. C. *Tetrahedron Letters*, **1980**, *21*, 2643-2646.

Kato, M. *J. Polym. Sci. Part A-1*. **1969**, *7*, 2415-2427.

Kim, J. B. and Lee, J. J. *Polymer,* **43**, 2002,1963-1967

Kim, K. H.; Jo, W. H.; Kwak, S.; Kim, K. U.; Hwang, S. S.; Kim, J. *Macromolecules*, **1999**, *32*, 8703-8710.

Kunz, R.R. *et al*., Proc. SPIE 3678, 13 (1999).

Kunz, R. R.; Downs, D. K. *J. Vac. Sci. Technol. B*, **1999**, *17*, 3330-3334.

Leebrick, J. R. and Ramsden, H. E. *J. Org. Chem.*, **23**, 953 (1958)

Li, W., Varanasi, P. R.; Lawson, M. C.; Kwong, R. W.; Chen, K.; Ito, H.; Truong, H.; Allen, R. D.; Yamamoto, M.; Kobayashi, E.; Slezak, M. *Proc. SPIE-Int. Soc. Opt. Eng.* **2003**, *5039*, 61-69.

Lightstone, F. C.; Bruice, T. C. *Bioorganic Chemistry*, **1998**, *26*, 193-199.

Liu, X.; Wang, M.; Li, Z.; Li, F. *Macromol. Chem. Phys.* **1999**, *200*, 468-473.

MacDonald, S. A.; Schlosser, H.; Clecak, N. J.; Willson, C. G. *Chem. Mater.* **1992**, *4*, 1364-1368.

MacDonald, S. A.; Willson, C. G.; Frechet, J. M. J. *Acc. Chem. Res.,* **1994**, *27*, 151-158.

Mathew, J. P., Reinmuth, A., Melia, J., Swords, N., Risse, W. *Macromolecules*, **1996**, *29*, 2755-2763.

Odian G., . *Principles of polymer Chemistry,* John Wiley and Sons: USA, 1991.

Okoroanyanwu, U. Ph.D. Dissertation, The University of Texas at Austin, **1997**.

Osborn, Brian PhD Thesis, University of Texas at Austin, **2004**.

Patterson, K.; Okoroanyanwu, U.; Shimokawa, T.; Cho, S.; Byers, J.; Willson, C. G. *Proc. SPEI-Int. Soc. Opt. Eng.* **1998**, *3333*, 425-437.

Patterson, K.; Yamachika, M.; Hung, R.; Brodsky, C.; Yamada, S.; Somervell, M.; Osborn, B.; Hall, D.; Dukovic, G.; Byers, J.; Conley, W.; Willson, C. G. *Proc. SPIE-Int. Soc. Opt. Eng.* **2000**, *3999*, 365-374.

Pfeffer, P. E.; Silbert, L. S.; Chirinko Jr., J. M. *J. Org. Chem.*, **1972**, *37*, 451-458.

Pike, R. M. *J. Polymer Sci.,* **40**, 577 (1959)

Pinnow, M. J., *et. al., Polymeric Materials Science and Engineering*. **2002**, *87*, 403-404

Pinnow, M. J., *et. al., Design and Synthesis of Mass Persistent Photoresists.* Poster Presentation. **2nd International Symposium on 157nm Lithography**, Dana Point, CA, May 16, 2001.)

Risse *et al, Makromol. Chem., Rapid Commun*., **1991**, 12, 255

Roland, B., Lambaerts, R., Jakus, C., Coopmans, F., *Proc. SPIE-Int. Soc. Opt. Eng.* **1987**, *771*, 69-76.

Schleyer, P. V. R.; Williams, J. E.; Blanchard, K. R. *J. Amer. Chem. Soc.* **1970**, *92*, 2377-2386.

Schmittling, E. A., *Et. Al.*, *Tetrahedron Lett.* **1991**, 7207-7210.

Sebald, M.; Sezi, R.; Leuschner, R.; Ahne, H.; Birkle, S. *Microelectr. Eng.* **1990**, *11*, 531-534.

Shaw, J. M.; Hatzakis, M.; Babich, E. D.; Paraszczak, J. R.; Whitman, D. F.; Stewart, K. J. *J. Vac. Sci. Technol. B.* 1989, *7*, 1709-1716.

Sommerville, Mark PhD Thesis, University of Texas, **2000**.

Sooriyakumaran, B.; Davis, C. E.; Larson, P. J.; Brock, R. A.; DiPietro, R. A.; Wallow, T. I.; Connor, E. F.; Sundberg, L.; Breyta, G.; Allen, R. D. *Proc. SPIE-Int. Soc. Opt. Eng.* **2004**, *5376*, 71-78.

Sreekumar, C.; Darst, K. P.; Still, W. C. *J. Org. Chem.*, **1980**, *45*, 4264-4263.

Strunz, G. M.; Lal, G. S. *Can. J. Chem.* **1982**, *60*, 2528-2530.

Strunz, G. M., Lal, G. L. *Can. J. Chem.* **1982**, *60*, 2528-2530.

Tran, Hoang Vi PhD Thesis, University of Texas at Austin, **2002**.

Tran, H. V.; Hung, R. J.; Chiba, T.; Yamada, S.; Mrozek, T.; Hsieh, Y.-T.; Chambers, C. R.; Osborn, B. P.; Trinique, B. C.; Pinnow, M. J.; MacDonald, S. A.; and Willson, C. G. *Macromolecules*, **2002**, *35*, 6539-6549.

Trinque, Brian PhD Thesis, University of Texas at Austin, **2003**.

Trinque, B. C., Chiba, T., Hung, R. J., Chambers, C. R., Pinnow, M. J., Osburn, B. P., Tran, H. V., Wunderlich, J., Hsieh, Y., Thomas, B. H., Shafer, G., DesMarteau, D. D., Conley, W., Willson, C. G. *J. Vac. Sci. Technol. B*, **2002**, *20*, 531-536.

Trinque, B. T.; *et. al. J. Vac. Sci. Technol. B.* **2002**, *20*, 531-536.

Tsuge, O., Kanemasa, S., Matsuda, K., *J. Org. Chem.*, **1984**, *49*, 2688-2691.

Tsuge, O., Kanemasa, S., Matsuda, K., *Chemistry Letters*, **1983**, 1131-1134.

Turner, S. R., Arcus, R. A., Houle, C. G., Schleigh, W. R. *Polymer Engineering and Science*, **1986**, *26*, 1096-110.

Wallraff, G. M; Hinsberg, W. D. *Chem. Rev.* **1999**, *99*, 1801-1821.

Weston, A. W.; DeNet, R. W. *J. Amer. Chem. Soc.,* **73**, 4221 (1951)

Wheeler, D., Hutton, R., Boyce, C., Stein, S., Cirelli, R., Taylor, G., *Proc. SPIE-Int. Soc. Opt. Eng.* **1995**, *2438*, 762-774.

Willson, C.G.; Bowden, M. J., Eds. "Introduction to Microlithography," 2nd Edition, American Chemical Society, Washington, D.C., **1994**, Chapter 3.

Venuti, M. C.; Loe, B. E.; Jones, G. H.; Young, J. M. *J. Med. Chem.* **1988**, *31*, 2132-2136.

Yokoyama, Y.; Hattori, T.; Kimura, K.; Tanaka, T.; Shiraishi, H. *Proc. SPIE-Int. Soc. Opt. Eng.* **2001**, *4345*, 58

Vita

Matthew James Pinnow the son of Nancy and Kory Pinnow was born on July, 29th 1977 in Green Bay, Wisconsin. He graduated from Northland Pines High School in Eagle River, Wisconsin in 1995 and enrolled at University of Minnesota, Duluth that fall. In the fall of 1996 he transferred to the University of Minnesota, Twin Cities Campus starting where he changed his major from chemical engineering to chemistry. Upon earning a B.S. in Chemistry in December 1999 he moved to Austin, Texas in May of 2000 to begin work in Professor C. Grant Willson's laboratories. He officially entered the graduate school at the University of Texas at Austin in the fall of 2000 working in the Organic Division of the Department of Chemistry in the labs of C. Grant Willson.

Permamnent address: 5358 Maple Leaf Rd. Land O' Lakes, WI 54540

This dissertation was typed by the author.